# Discontinuity Analysis for the Treatment of Lumped-Parameter Chemical Engineering Systems for Singular Inputs

*A Thesis submitted*
*in fulfillment of the requirements*
*for the award of the degree of*
*Doctor of Philosophy*

***by***

**Sanjeev Kumar Ahuja**

**(950901004)**

***Supervised by***

**Dr. P. K. Bajpai**

**Department of Chemical Engineering**
**Thapar University**
**Patiala-147004, Punjab, India**
**December 2012**

# CERTIFICATE

This is to certify that the thesis entitled "**Discontinuity analysis for the treatment of lumped-parameter chemical engineering systems for singular inputs**", being submitted by Mr. Sanjeev Kumar Ahuja to the Department of Chemical Engineering, Thapar University, Patiala for the award of degree of **DOCTOR OF PHILOSPHY**, is a record of bonafide research work carried out by him. Mr. Sanjeev Kumar Ahuja has worked under my guidance and supervision, and has fulfilled the requirements for the submission of this thesis, which to my knowledge has reached the requisite standard.

The results embodied in the thesis have not been submitted in part or full to any other University or institute for award of degree or diploma.

12.12.12

(Dr. P. K. Bajpai)
Distinguished Professor and Dean
Research and Sponsored Projects
Thapar University
Patiala

## List of Publications

### In SCI (International) Journals

Ahuja, S., 2010. Second-order numerator-dynamics systems: Effects of initial discontinuities. *Teoreticheskie Osnovy Khimicheskoi Tekhnologii* (Theor. Found. Chem. Eng.) 44, 300-308.

Ahuja, S., 2011. Effects of initial discontinuities on nonlinear systems represented by differential equations with terms containing differentials of the input function. Chem. Eng. Commun. 198, 760-782.

Ahuja, S., 2012. Initialization of lumped-parameter systems for singular inputs (communicated to Chem. Eng. Commun.).

## Acknowledgements

I'd like to thank my supervisor Dr. P. K. Bajpai, who has facilitated me right from the outset of my Ph. D. program, and with whose able guidance this thesis has been possible. His keen observations and valuable advice have been extremely useful. I'd also like to thank my family: mother, father, wife, and son, who have always been there whenever I've needed them. My special thanks have been long overdue to my friends Dr. Vineet Kumar, Dr. Rajeev Mehta, Dr. Satnam Singh and Dr. Jai Prakash Kushwaha, who have been a source of encouragement since this initiative was undertaken. I'd equally like to acknowledge my gratitude to Mr. Saurabh Srivastava, my ex-student and friend, who had been a constant companion through the crucial stages of this work. I sincerely acknowledge the support of all my colleagues.

I'd like to take this opportunity to pay my tributes to a great teacher, Late Prof. G. C. Mishra, who taught me at the Department of Chemical Engineering and Technology, Panjab University, Chandigarh. His excellent grasp of the subject combined with his untiring teaching efforts kindled my interest in Process Systems Engineering. He had always been extremely generous in offering guidance in professional matters. It is with a great sense of respect towards Prof. Mishra that I dedicate this piece of work to him.

Date: 12/12/12
Place: Patiala

(Sanjeev Ahuja)

## Contents

## List of Figures

## List of Tables

## Abstract

Chemical engineering presents unique and interesting cases consisting of chemical reactions, phase changes, and the interacting capacities of material, thermal and mechanical energy. Singular inputs cause initial discontinuities in the physical system and inconsistency in initial conditions. The mathematical problem of finding the dynamic response to these inputs arises in many fields of engineering and science. The literature studies on singularity deal mainly with electrical and mechanical engineering systems and pure mathematical systems that involve symbolically manipulated and transformed complicated models, and advocate either the use of approximate methods, or the demanding framework of generalized functions. The analysis of linear time-invariant systems in the Laplace domain, also, involves inconsistency.

Proposing a framework based on the direct, time domain approach of analysis, which aims to estimate reliably accurate initial conditions for the solution of the original un-manipulated models of chemical engineering for the singular inputs, and to reveal and resolve the inconsistencies, are the main objectives of the present study. Limitations of several transformed and approximated models are also indicated. The framework should also resolve the inconsistency in Laplace domain analysis. Analysis of initial discontinuities is carried out for the nonlinear, linearized and linear systems perturbed by the singular inputs.

Nonlinear lumped-parameter chemical engineering models, viz., non-isothermal CSTR, single component condenser, gravity-flow tank, interacting tanks, U-tube manometer, closed-loop stirred tank heater with dead time, etc. under singular inputs or initial conditions are considered. Upon linearization these are found to exhibit second-order numerator-dynamics behavior for some of the output variables that are represented by ODEs with terms containing differentials of the input function, and such systems have been the subject of extensive studies. These systems contain singular terms of differentials of the input function even for the step perturbation and, thus, exhibit initial discontinuities in the step and impulse responses. To explore the range of behavior of these systems in general, conditions are worked out for their assorted solution profiles to identify characteristic parameters, which unfold interesting cases of maximum, minimum,

inflection, input multiplicity, pole-zero cancellation, reduction to standard systems, etc., as the value of one such parameter changes relative to that of the others on the real axis.

A preliminary methodology is initially presented to ascertain and validate the inconsistency in solution profiles. The analysis is carried out by matching the coefficients of input and output terms in the models; the basic approach is to combine physical principles with mathematical analysis and expose the inconsistencies. In some cases, an initial discontinuity exposed through physical principles can't be accounted for through mathematical analysis. The value of that discontinuity is, thus, required for correct solutions of such cases for an impulse input. This effect is investigated for different systems and validated by the comparison of experimental and simulated solution profiles of nonlinear models of flow-level tanks. The same is also established by the calculations of time required for emptying the flow-level tanks using impulse responses and verifying them with physical principles. Right through all of these, the significance of putting the theoretical analysis consistent with the physical principles is indicated. This preliminary methodology brings out the qualitative effects of initial discontinuities.

Following the above analysis and building upon its results, a general framework of methodology to quantitatively describe the transient response of nonlinear first-order ODE systems, is, then, proposed. It works on the basis of using original non-transformed models, and initializing them through the following alternative methods: Direct inclusion of singularities in the *cause* through initial integration of the models (Initialization A), whose accuracy in making a reliable estimation is quantified by comparison with the method of application of physical balances to the initial *effects* of singularity (Initialization B); the latter is, thus, closer to the real as ascertained in the last paragraph. For many cases, the initial conditions calculated from initialization A are inconsistent with that calculated from initialization B. The solution profiles thus obtained are also compared with that obtained by using an increasingly sharpened Gauss pulse function for impulse (Initialization C).

It is found that whereas the Gaussian pulse approximation can't reliably model the singularity of the $\delta$-Dirac function, it can be done fairly accurately through the procedure of initialization A. The ready-to-use initialization A can be adequately used for a system operated not significantly far off from its normal operating conditions. The validity of

initialization A is substantiated by its conformity to the definitely known cases, and to the well established Laplace transform approach for the linear time-invariant systems.

On application of the proposed framework to the linear systems, it is elicited that the $\mathcal{L}_+$ Laplace transform approach doesn't involve inconsistency and doesn't require physical balances on the effects for the simple cases; whereas, the $\mathcal{L}_-$ approach is inconsistent/inexact, especially, for many nontrivial chemical engineering cases indicated at the outset, as their models can't account for the initialization inconsistency under an impulse.

Various transformed and approximated models, viz., Laplace transformed models, linearized models; smoothened impulse models, symbolically manipulated models, etc. can't predict the native consistencies/inconsistencies of the physical systems, and lead to wrong solution profiles and convergence. The numerical solutions of the proposed framework that uses un-manipulated models are found to converge to the right values, predict accurate behaviors, and work over a wider range of inconsistent initial values, in contrast to the solutions of the implicit and symbolically modified indirect models. Thus, the proposed framework is direct and avoids the complicated machinery of generalized functions.

## Basic Definitions

*Lumped-parameter* systems are modeled by lumping all the resistance into one location and all the capacitance into another, the state of the system is independent of the spatial coordinates, and the system's dynamics can be represented by an ordinary differential equation. If the resistance and the capacitance are uniformly distributed throughout the medium, the state of the system varies with the spatial coordinates and this *distributed-parameter* modeling would lead to a partial differential equation. A singularity is in general a point at which a given function is not defined, or a point of an exceptional set where it fails to be well-defined or is non-differentiable. For example, the functions $\delta(t)$ and $1/t$ on the real axis have a singularity at $t = 0$, where they "explode" to $\pm\infty$ and are not defined. The function $|x|$ (absolute value) also has a singularity at $x = 0$, since it is non- differentiable there. So, singularities are either discontinuities or discontinuities of the derivative. A *singular solution* of an ordinary differential equation is a solution for which the initial value problem fails to have a unique solution at some point on the solution. The set on which a solution is singular may be as small as a single point or as large as the full real axis. Such solutions may or may not be singular functions. In mathematical analysis, a function that has derivatives of all orders is called a *smooth* function. A function $f$ is called a *monotonic* (or *monotonically increasing*), if for all $x$ and $y$, such that, $x \le y$ one has $f(x) \le f(y)$. If for $x \le y$ one has $f(x) \ge f(y)$, the function is called monotonically decreasing. A *non-monotonic* function, however, rises and falls and shows maximum/minimum. *Explicit* differential equations (or a set of them) are those in which the differential terms are expressed explicitly in terms of state variables $\mathbf{z}(t)$ and forcing functions $\mathbf{u}(t)$, i.e., $\dot{\mathbf{z}}(t) = f(t, \mathbf{z}(t), \mathbf{u}(t))$; $\dot{\mathbf{z}}(t), \mathbf{u}(t), \mathbf{z}(t) \in \Re^n$, is an explicit ordinary differential equation. *Implicit* differential equations or *differential-algebraic* equations, however, consist of a set of coupled differential equations of the form $F(t, \dot{\mathbf{z}}(t), \mathbf{z}(t), \mathbf{u}(t)) = 0$; $\dot{\mathbf{z}}(t), \mathbf{u}(t), \mathbf{z}(t) \in \Re^n$. Alternatively, these consist of *differential* equations of the form $\dot{\mathbf{y}}(t) = f(t, \mathbf{y}(t), \mathbf{z}(t), \mathbf{u}(t))$ coupled along with the *algebraic* equations $g(t, \mathbf{y}(t), \mathbf{z}(t), \mathbf{u}(t)) = 0$; $\mathbf{y}(t), \mathbf{u}(t), \mathbf{z}(t) \in \Re^n$. A singular matrix is one which has the determinant zero, and its inverse doesn't exist. An *ill-conditioned* matrix is an "almost-singular" matrix. These systems lead to convergence problems in Newton iteration. *Input multiplicity* means for different magnitudes of the step inputs to a system, a state variable exhibits the same value of output at the steady-state.

# 1 Introduction

## 1.1 Background

Many systems in chemical engineering are modeled as lumped-parameter systems that are represented by ordinary differential equations (ODE). These dynamic systems include continuous flow stirred tank reactors (CSTR), jacketed stirred tank heaters, condensers, distillation columns, etc. Singular inputs (impulse and derivative of step) create initial jump discontinuities in the physical systems. These initial discontinuities lead to inconsistency in the initial conditions of the state variables and their derivatives. Incorrect initial conditions lead to incorrect solution profiles. These initial errors, also, tend to blow up in a control system by the feedback action of a controller in the presence of dynamic lags in the loop and eventually influence the controller design. Presence of singularity and a short duration input cause difficulty in solutions. Singular inputs are not well defined mathematical functions, thereby making their mathematical treatment difficult. Owing to the discontinuity and inconsistency in initialization, the choice of the correct initial conditions becomes difficult as otherwise a different problem completely unrelated to the original one is solved. Thus, anticipation of the accurate magnitude of the initial discontinuities, before carrying out the solution, is essential. Also, the discontinuous inputs cause steep gradients and non-smoothness in output state variables thus making the numerical solution inefficient and inaccurate. Solutions of diverse initially discontinuous problems have been of much research interest (Ahuja, 2010; 2011; Casasús and Al-Hayani, 2002; Evangelista, F., 2009; Jena and Sharma, 2008, Karelsky *et al.*, 2006; Kelevedjiev *et al.*, 2004; Liu and Ballinger, 2004).

Inputs with jump discontinuities such as impulse, pulse, step, etc. are widely used for studying system behavior because of the ease of interpretation of their responses (Alopaeus, 2008; Chauhan and Srivastava, 2008; 2009; Chauhan *et al.*, 2009; Chaves *et al.*, 2004; Pour *et al.*, 2010; Zheng *et al.*, 2004). Besides, these stimuli are principally used for studying the residence-time distribution of fluids in non-ideal flow stirred-tanks, vessels and tubular reactors (Bansal *et al.*, 2007(a) & (b); Brouckaert, 1995; Cermakova *et al.*, 2003; Nauman, 2008; Wanchoo *et al.*, 2007). Changes in any of the operating

variables for a very short duration of time can be modeled as impulse function, e.g., a momentary activation of a safety valve when pressure exceeds a given value. Impulse has also been used in breakthrough curves (Srivastava *et al.*, 2008) and adsorption equilibrium studies (Tondeur *et al.*, 1996), leak locations in pipelines (Lee *et al.*, 2007), and in tuning of proportional-integral-derivative (PID) and other controllers (Ramasamy and Sundaramoorthy, 2008; Silva *et al.*, 2006; Zhang, 2006). Impulse stimulus-response finds extensive applications in allied disciplines too, such as, stress relaxation of materials, shock waves on liquids and solar wind, flow over surfaces in hydrodynamics and digital signal processing. Impulse, its derivatives, and the derivatives of step are difficult to treat mathematically as these are not well defined mathematical functions (singularities). The unit impulse or Dirac delta function, $\delta(t)$, is a function of time such that it is zero for all values of time except at zero time, where it is infinite, and its integral over the time interval $(-\infty, \infty)$ is equal to one.

Methods for the treatment of singularity include: (a) generalized functions that require theory of distributions; (Brigola & Singer, 2009) (b) method of moments; (Ramasamy and Sundaramoorthy, 2008) (c) smoothing of step and impulse by approximating them with continuous functions; (Zhang *et al*., 2010) (d) analytical transformations of equations to eliminate/separate the singular terms (Makila, 2006; Pilipchuk, 1999); (e) numerical approaches that use approximations of discontinuities with algebraic or differential functions (Al-Hayani and Casasús, 2006); (f) impulse matching (Lundberg *et al.*, 2007). Studies on singularity involve complicated and transformed mathematical equations. However, there are several advantages of working with the original models directly, rather than with the models transformed after mathematical manipulations and differentiations. These are: (a) the physical significance of various terms in the models is easily interpreted; (b) time consuming manipulations are avoided and fundamental information, that could have been lost through differentiation, is preserved; and (c) constitutive relations (state equations, phase equilibrium, kinetic equations, etc.) are easily included and/or changed whenever necessary (Brenan *et al.*, 1989; Murata and Bascaia Jr., 1997; Vieira and Bascaia Jr., 2000).

The Laplace transforms and the transfer function approach comes in as a handy tool to treat singularity in linear systems. However, the treatment involves inconsistencies

in initialization, and recent studies reported in the literature have generated interest in these inconsistencies (Brigola and Singer, 2009; Grizzle, 2004; Lundberg *et al.*, 2007; Makila, 2006). Inconsistencies arise as the initial values of the derived responses (post-initial state $0^+$) are inconsistent with the original initial conditions chosen (pre-initial state $0^-$) for deriving the responses to the singular inputs. The Laplace transform (based on the $0^+$ state) of the input $\delta$ Dirac function becomes zero.

There has been inconsistency in the treatment of singularity in the literature and the studies use approximate, convoluted, and transformed methods. The framework of the generalized functions has also been recommended for a consistent treatment of singularity (Brigola and Singer, 2009; Lundberg *et al.*, 2007). However, many authors have advocated against the use of the framework of generalized functions as being very demanding and involving many associated complications, especially for the case of the nonlinear systems that constitute most of the chemical engineering systems (Grizzle, 2004; Makila, 2006; Pilipchuk, 1999).

Various aforesaid approaches for the treatment of discontinuities and singularities involve mathematical technicalities such as symbolically manipulated models, smoothed impulse models, Laplace transformed models, models transformed to get the moments of response (method of moments), generalized functions, etc. Besides being approximate, complicated and indirect, the literature studies on the singular inputs deal mainly with electrical and mechanical engineering systems, and pure mathematical equations. These systems have been linear time-invariant, linear time varying, and systems with only a nonlinear term of a single variable. The chemical engineering systems are further complicated by flows along with mixing and chemical reactions, phase changes, and the interaction of material, thermal and mechanical energy (inertia) capacities, e.g., CSTRs, gravity-flow tanks, condensers, vaporizers, etc. Hence, these also contain nonlinear terms of products of output with other output/input variables. Direct methods for these nontrivial systems need to be thoroughly investigated for the singular inputs, as for them, the above approaches would become further complex.

## 1.2 Inconsistencies in Initialization

There are essentially two kinds of inconsistencies arising out of the initial jump discontinuities of the input functions. The first relates only to the discontinuities associated with a mathematical model that are exhibited in its numerical solution, and the second relates to the initial discontinuities exhibited in the actual physical system that are primarily due to the singular inputs.

The first kind of inconsistency arises out of symbolic manipulations and differentiations of the coupled differential and algebraic equation, i.e., DAE systems. Depending upon the solution approaches, these are done either for the transformation of the implicit DAEs into explicit ODEs or for the reduction in their index so as to use automatic DAE solvers. Index is defined as the number of differentiations required to convert a DAE system into an ODE system. In the extended set of equations, some of the state variables have inconsistent initial values. This leads to initial jump discontinuities and singular initial conditions of the state variables for a discontinuous (step) or non-smooth perturbation. In addition, the inconsistent initial values always lead to discontinuities in the solution during initial numerical integration step and result in errors and inefficient computation (Kroner *et al.*, 1997; Sincovec *et al*., 1981). Many rigorous and approximate approaches have been suggested based on algorithmic and direct methods for consistent initialization of such chemical engineering systems under the step input (Methekar *et al.*, 2011; Souza *et al*., 2005; Vieira and Biscaia Jr., 2001; Wu and White, 2001). However, the estimation of a consistent set of these initial conditions is a task even more challenging than the numerical integration itself, whereas, the available initialization approaches are complex and require index analysis of the model system, numerical differentiation, finite difference methods, and the solution of nonlinear algebraic equations; these steps lead to various inadequacies and inconsistencies. To overcome the above inconsistent initialization problems, some studies propose an approach of smoothing the step function by approximating it with a continuous function; the approach is direct as the convergence of an initialization algorithm is not required prior to the numerical integration (Kroner et al., 1997; Souza at al., 2005; Vieira and Biscaia Jr., 2000; 2001). However, this approach is also found to be inadequate even for a non-singular (step) input since some of the results don't converge to the right values.

With recent advancements in solvers and initialization routines, several successful strategies of solutions have emerged for the systems perturbed by nonsingular inputs. But these have not been useful with inconsistent initial conditions that are far off from the consistent initial conditions, as these lead to convergence problems of Newton iteration and the singular/ill-conditioned Jacobian matrix, and are not suitable for most practical applications (Methekar *et al.*, 2011).

Further, and more relevantly, the symbolic differentiations and manipulations involved with the above kind discussed are inadequate for the systems perturbed by the singular inputs. This inadequacy is due to the fact that the singular inputs cause significant initial discontinuities and inconsistencies in the state variables decently far from the consistent initial conditions. Also, the symbolic differentiation of the discontinuous state variables is bound to lead to further singularity, inconsistency, and serious errors. The present study is not directed towards this, first kind of inconsistency that is exhibited in numerical solutions in a mathematical sense and is associated only with a mathematical model. Rather, the prime focus of the present work is on the second kind of inconsistency, which is associated with the initial discontinuities in the actual *physical* system perturbed by the singular inputs. These initial discontinuities in the values and/or slopes of the state variables cause inherent inconsistency in the original symbolically non-transformed model and its solution profiles, and have a corresponding effect on the actual physical system.

Based upon the literature review and the gaps identified in Chapter 2, objectives of the present work have been set. Next section describes the aims and scope of the work.

## 1.3 Aims and Scope

Estimating reliably accurate initial conditions to quantitatively describe the dynamic response of the nonlinear lumped-parameter chemical engineering systems to the singular inputs and to increase the understanding of the effects of the initial discontinuities on these systems through a simple and direct approach are the main objectives of the present study. The specific sub-objectives of each chapter are listed below:

- Chapter 1: To provide necessary background information for understanding the problem. To briefly introduce the concepts required for the development of the research work. To outline the objectives, motivation, scope, and structure of the thesis along with the basic approach adopted and main results.
- Chapter 2: To review the existing literature related to the problem and identify the knowledge gaps.
- Chapter 3: To present lumped-parameter models representing mixing with chemical reaction, phase change, interaction of different capacities, closed-loop system with dead time, etc. that have been used in the discontinuity, singularity, nonlinearity, and initialization studies in the literature. Furthermore, to explore the general range of the behavior of these models by identifying their characteristic parameters.
- Chapter 4: To study the qualitative effects of initial discontinuities on linear and nonlinear systems. To develop strategies for discontinuity analysis and their qualitative comparison to reveal the initialization inconsistency, and to ascertain the consistent strategy. To validate these effects through experimental procedure and draining time calculations of flow-level tanks.
- Chapter 5: To propose a simple, direct, and comprehensive methodological framework for the quantitative description of the response of the nonlinear chemical engineering systems to the singular inputs. To estimate reliably accurate initial conditions and quantification of the errors/deviations involved in the initialization methods. To reveal the limitations of the smoothed impulse models, linearized models, and symbolically transformed models.
- Chapter 6: To apply the above methodological framework in order to reveal and resolve the inconsistencies in the Laplace transform treatment of the linear systems.
- Chapter 7: Conclusions and recommendations.

The focus is on the effects of the inconsistency associated with the actual physical systems and original non-transformed models that are caused by the singular inputs, i.e., of the second kind stated above (Section 1.2). Symbolically transformed models under singular perturbation are also considered occasionally. This is done to explore the possible errors of incorrect initialization and computation that can creep into the

framework proposed due to the use of these models. These transformed models can cause errors under the singular inputs as the state variables undergo initial jump discontinuities decently far from their pre-initial steady state—the pre-initial steady state happened to be consistent by default.

In the proposed methods, initial discontinuities are analyzed for the systems essentially by checking whether or not the inclusion of singularity in the input variables (cause) takes into account the inclusion of singularity in the output variables (effect). The basic approach is to combine physical principles with mathematical analysis and reveal the consistency/inconsistency; then use computer simulation to investigate and quantify the resultant effects.

The present study reveals exceptional behaviors in chemical engineering systems containing singular terms of derivatives of step and impulse inputs, which are: assorted profiles including input multiplicity, etc.; pole-zero cancellation, reduction to systems not containing differentials of the input terms, order reduction, and appearance/disappearance of the consistency/inconsistency upon linearization; paradoxical effect of the undetermined and/or the inconsistent initial conditions on the solution profiles; and, interesting cases of calculations of time required for emptying flow-level tanks, i.e., multiplicity, inconsistency with physical principles for different tanks, etc. Right through all of these, the significance of putting the theoretical analysis consistent with the physical principles is indicated (Ahuja, 2010; 2011). The discontinuity analysis, linearization, Laplace analysis and numerical solutions present very interesting results. The sequence of the treatment is described next.

Chapter 3 considers chemical engineering systems modeled through the lumped-parameter approach. Upon linearization, they exhibit numerator-dynamics behavior that is represented by ODEs with terms containing differentials of the input function, which exhibit initial discontinuities in their step and impulse responses. Initially, to explore the general range of their behavior, conditions are worked out for their assorted solution profiles to identify characteristic parameters. The solution profiles of these systems depend upon the value of one such parameter relative to that of the others on the real axis.

In Chapter 4, a preliminary analysis is carried out for the coupled, linear and nonlinear ODEs to ascertain and validate the effects of initial discontinuities. The initial

discontinuities are estimated by matching the coefficients of input and output terms in the models and making use of the physical balances. The results are substantiated by the comparison of the numerical and experimental data of the nonlinear flow-level tanks. This chapter brings out the qualitative effects of initial discontinuities that indicate the accuracy of the application of physical balances vis-à-vis the use of models. These results are used in the subsequent chapters. In Chapter 5, a general and comprehensive time-domain framework is proposed for a quantitative treatment of nonlinear chemical engineering systems while laying a special emphasis on the systems affected by the impulse inputs. The solutions obtained through three alternative ways (mentioned below) are compared and the error deviations are quantified. The framework is direct and should be useful for engineering practitioners as it doesn't assume a prior knowledge of mathematical techniques of methods of moments, Laplace transforms, advanced mathematical transformations, and generalized functions.

On application of the framework to the linear time-invariant systems in Chapter 6, unlike the studies in the literature, it is elicited that the $\mathcal{L}_+$ Laplace transform approach, that uses $0^+$ initial conditions for the solution, doesn't involve inconsistency and doesn't require physical balances for obtaining initial conditions for the simple cases; whereas, the $\mathcal{L}_-$ approach, that uses $0^-$ initial conditions for the solution, is inconsistent and inexact for many chemical engineering cases, as their models can't account for the initialization inconsistency under an impulse input.

So, in this thesis, a comprehensive framework is proposed for the treatment of linear and nonlinear systems for singular inputs. It is applicable to a set of first-order ODEs representing the lumped-parameter chemical engineering systems, and doesn't involve simplifying assumptions. The higher order chemical engineering systems are also composed of the first-order coupled ODEs. The framework first estimates the initial conditions using the model, and including singularity in the *cause* (Initialization A). Its accuracy in making a reliable estimation is quantified by comparison with the solution initialized through the application of physical balances to the *effects* of the singularity at the origin (Initialization B). The numerical solutions are also compared with that obtained by interpreting an impulse as the limit of an increasingly sharpened Gaussian pulse (Initialization C).

The proposed alternative methodologies, viz., initializations A and B are fundamental and first-principles, yet their potential for a direct treatment of singularity have not been explored so far. In this respect, only initialization B has been used, that too, only for the elementary linear cases of a *step* input to electric circuits that require entirely different physical principles than the aforesaid nontrivial chemical engineering systems that require complex concepts and the application of physical balances, especially, for an *impulse*. These also involve the nonlinear product of state variables in their models. The framework implements the above three methodologies in conjunction and their comparison reveals crucial information for the correct initialization of the nonlinear chemical engineering systems for the singular inputs. Its application, to the linear systems containing singular terms of derivatives of step and impulse, handles the inconsistency in the Laplace domain analysis, and reveals the results different from that for electrical/mechanical systems in the literature. The application of the framework also elicits the limitations of several transformed and approximated models in that they can't predict the native consistency/inconsistency of the physical systems, and lead to erroneous solution profiles and convergence.

Practical applications of the work such as the use of singular perturbations for the ease of interpretation of system behavior, residence-time distribution, leak location in pipe lines, stress relaxation of materials, influence of the inconsistency on the system's behavior and controller design, etc. have been listed in the beginning of this chapter. The mathematical treatment of dynamic lumped-parameter systems involves solving a set of differential equations for the singular perturbations under consideration. An accurate analytical or numerical solution of a set of linear and nonlinear ODEs would require a set of consistent initial conditions of the state. Their estimation to a reliable degree of accuracy without involving approximate methods and mathematical and numerical technicalities is of much practical significance in chemical engineering science. The benchmark models implemented in the present work are the ones that have been used consistently in the literature for the initialization and nonlinear dynamic studies. The treatments proposed are started with a general system, so that, these can be applied to any chemical process industry employing lumped-parameter chemical engineering systems such as distillation column, condenser, vaporizer, CSTR, etc. Further, distributed-

parameters systems can also be treated using the methods proposed as the partial differential equations can be decomposed into ordinary differential equations through separation of variables analytically. Initialization A procedure of the framework proposed in Chapter 5 is a simple and less time consuming procedure. It predicts reliably accurate initial conditions and solution profiles within an error of the order of 10% for operations not very far off from the normal operating conditions. Such operations are of significant practical importance in an actual plant. The general profiles described in Chapter 3 for the systems under consideration exhibiting maximum and minimum in step and impulse responses are also important from the perspective of design of the system. Any design must be based on maximum/minimum values rather than on the steady-state values; since during the dynamic changes, these values can be significantly beyond the steady state operating range of values.

# 2 Literature Review

## 2.1 Linear Systems

Studies on analysis of initial discontinuities and singularities should start with a background on the widely applied linear system dynamics thus describing the inconsistency in the treatment of initial conditions. The Laplace transform is widely used for the analysis of linear dynamic systems, and is a convenient tool for the treatment of singularity (Evangelista, 2009; Lundberg *et al.*, 2007; McCoy, 1987; Papadopoulos, 2001). Recent studies have generated an interest in the issue of $0^-$ and $0^+$ in the basic (unilateral) Laplace transform treatment (Brigola and Singer, 2009; Girard, 2005; Grizzle, 2004; Lundberg *et al.*, 2007; Makila, 2006).

In many texts on dynamics and control (e.g., Bequette, 2002; de Silva, 2009; Powers, 2010), the unilateral Laplace transform $f(s)$ of a function $f(t)$ and its derivative are defined as:

$$f(s) = \mathcal{L}\{f(t) = \int_0^\infty f(t)e^{-st}dt\,; \qquad \mathcal{L}\{f'(t) = sf(s) - f(0) \tag{2.1}$$

where $t$ is time, $\mathcal{L}$ is the Laplace operator and $s$ is the Laplace parameter. For systems perturbed by the singular inputs, there are initial jump discontinuities in the output functions and/or their derivatives. Hence, it becomes essential to specify the lower limit of the integral of Eq. (2.1). However, most texts don't specify this explicitly. Due to the discrepancy in the unilateral Laplace transform treatment, the initial values calculated from the derived responses (post-initial values $f(0^+)$) are inconsistent with the original initial conditions chosen for deriving these responses (pre-initial conditions $f(0^-)$) (Tanaka, 1989).

This inconsistency can be observed from the following elementary illustration. Consider the case of a lumped, linear second-order system having two poles and one zero (also called as second-order system with numerator dynamics) that is represented mathematically by a linear, ordinary differential equation having constant coefficients $A$ through $E$ as:

$$A\frac{d^2Y}{dt^2}+B\frac{dY}{dt}+CY=D\frac{dX}{dt}+EX \tag{2.2}$$

where $X$ is the input function, $Y$ is the output function and $t$ is the time. This type of model containing a derivative of the input term is considered in the literature frequently, because it contains a singular term even for a step input, and thus, exhibits discontinuities in the initial slope of the step response (Fig. 2.1) (unlike the standard second-order step response). So, this model contains mathematically unmanageable terms of the derivative of the step and the impulse inputs. Many chemical engineering models, upon linearization, yield such numerator-dynamics transfer functions (Chapter 3). See the next section for the physical systems corresponding to this model.

Assuming zero initial conditions:

$$Y(0)=0 \text{ and } Y'(0)=0 \tag{2.3}$$

For an under-damped case, Eq. (2.2) can be written as the following transfer function:

$$\frac{Y(s)}{X(s)}=P\frac{s+l}{s^2+2\zeta\tau s+1} \tag{2.4}$$

Taking constants $P$, $l$, $\zeta$ and $\tau \geq 0$

For a singular unit impulse input:

$$X(t)=\delta(t)$$

The output impulse response (and the slope of step response) signals can be obtained with the use of Eq. (2.4) and the inverse Laplace transform, this gives:

$$Y_{st}'(t)=Y_{imp}(t)=\frac{P}{\tau^2}e^{-\zeta t/\tau}\left[\cos\left(\frac{t}{\tau}\sqrt{1-\zeta^2}\right)+\frac{\tau l-\zeta}{\sqrt{1-\zeta^2}}\sin\left(\frac{t}{\tau}\sqrt{1-\zeta^2}\right)\right] \tag{2.5}$$

However, the initial values obtained from Eq. (2.5) are non-zeros:

$$Y(0^+)\neq 0 \text{ and } Y'(0^+)\neq 0 \tag{2.6}$$

Eq. (2.6) is inconsistent with the zero initial condition (2.3). See Fig. 2.1 representing the discontinuities in the initial values and/or initial slopes of the step and impulse response profiles of an under-damped numerator-dynamics second-order system.

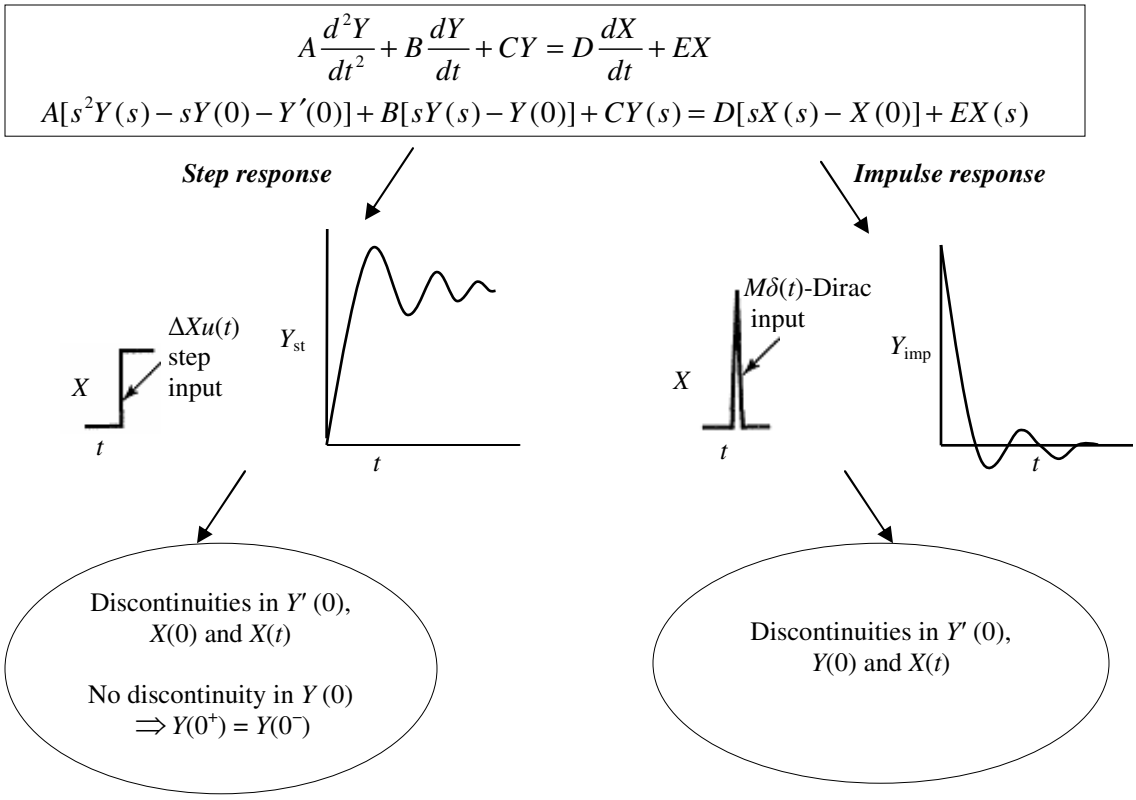


**Fig. 2.1** Schematic showing discontinuities in initial conditions for systems containing singular terms of differential of step and impulse inputs, where $X$, $Y$ are deviation variables for input and output; $\Delta X$, $M$ are magnitudes of step and impulse inputs, respectively

To overcome this inconsistency, $\mathcal{L}_-$ and $\mathcal{L}_+$ forms of Laplace transform have been suggested by taking $0^-$ and $0^+$ in the lower limit of the integral, and in $f(0)$ in Eq. (2.1) (Kailath, 1980).

$$\mathcal{L}_-\{f(t)=\int_{0^-}^{\infty} f(t)e^{-st}dt \tag{2.7}$$

$$\mathcal{L}_+\{f(t)=\int_{0^+}^{\infty} f(t)e^{-st}dt \tag{2.8}$$

And the corresponding Laplace transforms of the differentials as:

$$\mathcal{L}_{-}\{f'(t)\} = sf(s) - f(0^{-}) \tag{2.9}$$

$$\mathcal{L}_{+}\{f'(t)\} = sf(s) - f(0^{+}) \tag{2.10}$$

So, the $\mathcal{L}_{-}$ Laplace transform approach is the same as the one described above to get Eqs. (2.5) and (2.6), i.e., the use of the pre-initial conditions for the solution; the resultant post-initial values are inconsistent with the pre-initial ones. Recently, Grizzle (2004), Lundberg *et al.* (2007), etc. have advocated for the use of $\mathcal{L}_{-}$ Laplace transform along with its derivative rule, since the use of the $\mathcal{L}_{+}$ approach (described next) requires additional effort to calculate the post-initial values that are obtained on applying physical principles. Lundberg *et al.* (2007) asserts that the inconsistency in initial values can be treated by the uniform use of generalized functions. The framework of generalized functions is described in brief in Section 2.4 below. Brigola and Singer (2009) too have solved the initial value problems of linear systems under singular step inputs within the framework of generalized functions, however, along with the $\mathcal{L}_{+}$ approach.

Taking the $\mathcal{L}_{+}$ transform of Eq. (2.2) with $0^{+}$ initial conditions obtained, *a priori*:

$$Y(0^{-}) = 0, Y'(0^{-}) = 0 \text{ and } Y(0^{+}) \neq 0, Y'(0^{+}) \neq 0 \tag{2.11}$$

This gives:

$$A[s^2Y(s) - sY(0^{+}) - Y'(0^{+})] + B[sY(s) - Y(0^{+})] + CY(s) = D[sX(s) - X(0^{+})] + EX(s) \tag{2.12}$$

Solving this for $Y(s)$ and applying the inverse Laplace transform, it can be seen that this conforms to the solution for the step response and the impulse response given by Eq. (2.5) and satisfies the non-zero initial condition given by Eq. (2.11). The $\mathcal{L}_{+}$ approach (advocated by Brigola and Singer, 2009; Phillips *et al.*, 2003, etc.) resolves the inconsistency in the initial conditions. Brigola and Singer (2009) state that logically $\mathcal{L}_{+}$ approach can have the support on non-negative half line whereas $\mathcal{L}_{-}$ approach can only have a support on negative half line. Many authors (e.g., Lundberg *et al.*, 2007; Makila,

2006) assert that $\mathcal{L}_-$ and $\mathcal{L}_+$ approaches yield the same results invariably. However, the Laplace transform of the input Dirac function becomes zero as shown below. Since,

$$\delta(t) = \frac{d}{dt}u(t) \tag{2.13}$$

where, $u(t)$ is the unit step function. Taking the Laplace transform of this equation yields:

$$\mathcal{L}_+\{\delta(t)\} = su(s) - u(0^+) = s\frac{1}{s} - 1 \tag{2.14}$$

$$\mathcal{L}_+\{\delta(t)\} = 0 \tag{2.15}$$

which seems meaningless (Lundberg *et al.*, 2007). Many authors (Coughanowr and LeBlanc, 2009, etc.) implement the $\mathcal{L}_+$ transform approach tacitly, while retaining the Laplace transform of the Dirac function $\mathcal{L}_+\{\delta(t)\} = 1$. Some contributions have reported that this conflict can be resolved by taking the Dirac function completely to the right of $t = 0$ (Bernstein, 2005).

To overcome the aforesaid conflicts, some studies suggest the use of double-sided $\mathcal{L}_u$ and bilateral Laplace transform $\mathcal{L}_b$ (Schetzen, 2003, Tanaka, 1989, etc.). The double-sided Laplace transform $\mathcal{L}_u$ is defined in the domain $(-\infty, \infty)$:

$$\mathcal{L}_u F(t) = \int_0^\infty F(t)e^{-st}dt \tag{2.16}$$

And, the zero initial state function $F(t)$, which is zero for $t < 0$ is defined by:

$$F(t) = f(t)u(t) \tag{2.17}$$

where $u(t)$ is the unit step function.

Thus, $F(t) = 0$ for $t < 0$ and, $F(t) = f(t)$ for $t > 0$.

The following property was proved by induction:

$$\mathcal{L}_u\{F^n(t)\} = s^n f(s) \tag{2.18}$$

where $n$ stands for the $n^{\text{th}}$ derivative of a function. Thus, the initial conditions on the functions are not required. This approach avoids the inconsistency in the initial

conditions; Taking the double-sided transform of Eq. (2.2) according to Eq. (2.3) yields the same solution as given by (2.5) and with no inconsistency in the initial condition. However, it doesn't work in the face of non-zero and non steady state pre-initial conditions. For such situations, the output functions (or their deviations from the pre-initial state) don't fit into the frame of $F(t)$, since $F(t) = 0$ for $t < 0$. In the bilateral $\mathcal{L}_b$ transform, $f$ is retained as it is, and is not replaced by the function $F$ in Eq. 2.16. Graf (2004) and Schetzen (2003) have proposed to use Eqs. (2.8) and (2.10) instead (even for the bilateral Laplace transform). Graf (2004) has also provided a proof by starting with a function $f(t)$ that has a discontinuity at $t$ = a, and taking the limit of the resultant expression at $a = 0$. So, effectively, it reduces to the same $\mathcal{L}_+$ approach (Grizzle, 2004).

In his contribution, Makila (2006) has provided a mathematical treatment for solving step responses of the linear, constant coefficient differential equations with singular terms of derivative of the input (as in Eq. (2.2)). He has applied the first approach given by Eq. (2.1) to solve the system equation, and has stated that there is no need to use the $\mathcal{L}_-$, $\mathcal{L}_+$ and $\mathcal{L}_b$ approaches for these solutions. The basic Laplace transform can be stated as given in Eq. (2.1) without any need to indicate how the lower limit of the integration should be interpreted. The integral there is to be represented as the basic integral only. Further, the derivative rule:

$$\mathcal{L}\{f'(t) = sf(s) - f(0) \tag{2.19}$$

is sufficient and there is no need to specify the use of $0^-$ or $0^+$ (Eqs. (2.9) and (2.10)).

However, he has used a somewhat convoluted approach by rewriting the original ODE into a form consisting of differentials of the integrals. He, then, defined two new functions: one each for the integral of the input and the output. These two new functions are continuous functions and, thus, don't suffer from the singularity and the inconsistency caused by the term $f(0)$ on the right hand side of the derivative rule (2.1). Thus, the solution is derived from the new set of Laplace transformed equations by circumventing the inconsistency in the initial conditions. However, this strategy has been formulated for the step inputs, and should be laid out clearly before its possible extension to the impulse inputs (this is examined in Appendix I).

This study has also pointed out the limitations of the $\mathcal{L}_u$ and $\mathcal{L}_b$ transforms. Furthermore, it affirms that the framework of the generalized Laplace transform and the generalized functions is not required even to solve initial value problems involving singularity due to the differentials of inputs containing jump discontinuities. Many authors have advocated against the use of the framework of distributions (generalized functions) as being very demanding and involving many associated complications (Grizzle, 2004; Makila, 2006; Pilipchuk, 1999).

## 2.2 Physical Systems for the Singularity Studies

The studies on singularity mentioned above mainly involved pure mathematical equations containing differentials of the input function. Following physical systems have been employed in the literature, which also are the systems represented by differential equations with terms containing differentials of the input function. These studies comprise of electrical and mechanical engineering systems, and stand good potential for comparison with the corresponding physical cases in chemical engineering science.

### 2.2.1 Circuit example

Consider a high pass filter consisting of a resistance-capacitance (RC) circuit that is described by the following ODE with a term containing derivative of the input, $v_o$ and $v_I$ are output and input voltage, respectively (Lundberg *et al.*, 2007):

$$\frac{dv_o}{dt} + \frac{v_o}{RC} = \frac{dv_I}{dt} \tag{2.20}$$

The system is driven by the step change in input voltage:

$$v_I(t) = \begin{cases} 1 \text{ V}, & t < 0 \\ 0 \text{ V}, & t > 0 \end{cases} \tag{2.21}$$

A schematic of this system is shown in the following Fig. 2.2:

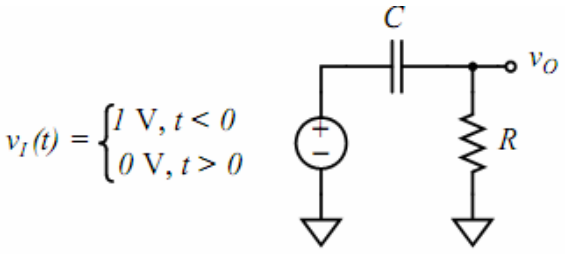


**Fig. 2.2** Schematic of a high pass electrical filter driven by a step from 1 to 0 at $t$ = 0. The initial state of this system is the capacitor voltage $v_C(0^-)$ = 1 V, and thus the initial output voltage is $v_o(0^-)$ = 0 V; Although the unilateral Laplace transform of the input $v_I$ ($t$) is $V_i(s)$ = 0, the presence of the non-zero pre-initial capacitor voltage produces a dynamic response

The pre-initial conditions are, $v_o(0^-) = 0$ V and $v_I(0^-) = 1$ V. Although the Laplace transform of the input voltage, $v_I(t)$ is $v_I(s) = 0$, the presence of the non-zero pre-initial capacitor voltage produces a dynamic response. The solution using the $\mathcal{L}_-$ approach is (Lundberg *et al.*, 2007):

$$v_o(t) = -e^{-t/\tau}, \quad t < 0 \tag{2.22}$$

Post-initial value of the response from this equation is:

$$v_o(0^+) = -1 \text{ V} \tag{2.23}$$

Another technique for solution is described in the above study that is based on impulse matching (Siebert, 1986). Since the input voltage is a step of −1 V at $t$ = 0, the input term in Eq. (2.20) becomes $dv_I/dt = -\delta(t)$. To match this term, the output term $dv_o/dt$ must have a $-\delta(t)$ term, so, $v_o$ is a step of −1 V at $t$ = 0. Using this as the initial condition and solving Eq. (2.20) through the $\mathcal{L}_+$ approach leads to the same Eq. (2.23). However, the required matching becomes increasingly complex as the system order increases; so this is not a practicable technique (Lundberg *et al.*, 2007).

### 2.2.2 Car wheel suspension example

This system (Fig. 2.3) consists of a spring and damper in parallel and is described by the following second-order ODE containing a derivative of the input term. Similar models

have been employed by other singularity studies (e.g., Pilipchuk, 1999). The momentum balance gives (Lundberg *et al.*, 2007):

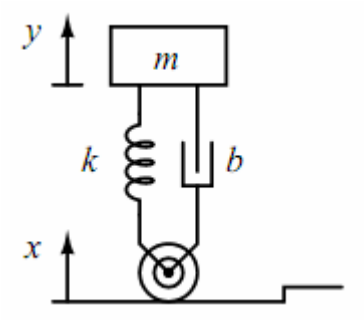


**Fig. 2.3** An idealized automobile-suspension system approaching a rectangular speed bump; in the analysis, the center of the wheel is assumed to follow the bump exactly

$$\ddot{y} = \frac{b}{m}(\dot{x} - \dot{y}) + \frac{k_s}{m}(x - y) \tag{2.24}$$

where $x$ is the input motion (displacement of the wheel in the vertical direction), $y$ is the output motion (displacement of the car-body in the vertical direction), $m$ is the mass of the car-body, $b$ is the damping coefficient of the suspension, and $k$ is the spring constant of the suspension. The system is under one-meter unit step input and $x(0^-) = 0$ m .

Three sets of initial conditions, viz. (a), (b), and (c) have been considered in the referred study. The mutual inconsistency in the corresponding post and the pre-initial value can be observed in the three cases. These very cases shall be used to apply the proposed framework to the linear systems for comparison purposes (Chapter 6).

(a) Initial rest conditions for the output and its derivative, i.e., $y(0^-) = 0$ m and $\dot{y}(0^-) = 0$ m/s . From the $\mathcal{L}_-$ approach the solution is:

$$Y(s) = \frac{bs + k}{s(ms^2 + bs + k)} \tag{2.25}$$

The post initial values calculated from this equation are, $y(0^+) = 0$ m and $\dot{y}(0^+) = b/m$ m/s . Note the discontinuity and inconsistency in the pre and post initial values of initial velocity, which is due to the singularity contained in the derivative of the input.

(b) Initial position $y(0^-) = 1$ m with initial velocity $\dot{y}(0^-) = 0$ m/s . From the $\mathcal{L}_-$ approach the solution is:

$$Y(s) = \frac{1}{s} + \frac{b}{ms^2 + bs + k} \tag{2.26}$$

The post initial values calculated from this equation are, $y(0^+) = 1$ m and $\dot{y}(0^+) = b/m$ m/s .

(c) The third set is selected to yield immediate convergence to the final value of the response, i.e., $y(0^-) = 1$ m and $\dot{y}(0^+) = -b/m$ m/s , such that the initial velocity is exactly cancelled by the force impulse from the damper (the non-steady state pre-initial condition). From the $\mathcal{L}_-$ approach the solution is:

$$Y(s) = \frac{ms^2 + bs + k}{s(ms^2 + bs + k)} = \frac{1}{s} \tag{2.27}$$

The post initial values calculated from this equation are, $y(0^+) = 1$ m and $\dot{y}(0^+) = 0$ m/s .

The mutual inconsistency in the corresponding post and the pre-initial values can be observed in the cases discussed in the above two examples. However, from the above two examples, it is seen that the $\mathcal{L}_-$ approach yields correct results in the presence of non-zero and non-steady state pre-initial values and input functions containing singularity, and calculates the right post-initial conditions from the initial value theorem. Lundberg *et al.* (2007) have reported that this approach is better than the $\mathcal{L}_+$ approach that requires physical considerations or techniques of impulse matching (Section 2.2.1) to calculate the post-initial conditions, although both approaches give the same solution. However, these

remarks need further critical examination for the nontrivial chemical engineering systems.

### 2.2.3 Model for car-body subjected to applied force

The same physical system of Section 2.2.2 represents this equation but, now, $y$ becomes the car-body upward velocity and $x$ the force applied.

$$\ddot{y} = 1(\dot{x} - \dot{y}) + 1(0 - y) \tag{2.28}$$

Grizzle (2004) has used this model containing differential of input. Advocating in favor of the $\mathcal{L}_-$ approach in his article, Grizzle (2004) has reported that since for a step input in $x$, the $\mathcal{L}_+$ Laplace transformed of $\dot{x}$ through Eqs. (2.13)–(2.15) is zero; the solution of the system Eq. (2.28) from the $\mathcal{L}_+$ approach is identically zero as long as the initial values of the output and its derivative are zero. And, on this very basis, he has commented that the use of $\mathcal{L}_+$ form of the Laplace transform with the corresponding derivative rule, from a systems engineer's perspective, is unfortunate. However, this argument seems to suffer from fallacies and needs further inspection (Chapter 6).

In chemical engineering science, the velocity of a manometer column under applied pressure difference also follows the same dynamics. The same model also applies to an analogous RLC series circuit, with current $I$ analogous to the velocity $y$ and applied voltage $E$ to the force $x$.

## 2.3 Nonlinear Chemical Engineering Studies for Nonsingular Inputs

### 2.3.1 Lumped-parameter modeling

Lumping of parameters has been an effective approach in modeling chemical engineering systems (Bhargava *et al.*, 2008; Botchwey *et al.*, 2006; Dasila *et al.*, 2012; Dua, 2011; Gupta *et al.*, 2010; Pareek *et al.*, 2003; Patel *et al.*, 2007; Sangal *et al.*, 2012; Wu *et al.*, 2007). A lumped-parameter system is one whose parameters such as temperature,

concentration, density, velocity, etc. are uniform throughout the space and change with only one independent variable (usually time for dynamic systems). These systems are modeled by lumping all the resistance into one location and all the capacitance into another and the state of the system is independent of the spatial coordinates. This facilitates writing unsteady state physical balances of mass, energy, and momentum on the system as a whole as the system can be considered a lumped-free body, and, so, its dynamics can be represented by an ordinary differential equation. In contrast to this a distributed-parameter model involves spreading out of the capacitance and resistance over the entire space and the state of the system is dependent on the independent spatial coordinates in addition to time. So, the unsteady state physical balance cannot be written on the system as a whole. Rather, the physical balances are written over a representative infinitesimally small control volume element that has uniform characteristics of temperature, composition, density, velocity, etc.

Lumped-parameter systems are quite common in process industries, a stirred-tank heater being a classic example. A tank heater is rigorously modeled as a distributed-parameter system. Alternatively, it can be modeled as a series of lumped tanks-in-series, or as a lumped-parameter model with dead time, e.g., a first-order model with dead time model (FOPDT) (Coughnamowr and LeBlanc, 2009; Goswami *et al.*, 1997; Harriott, 1972; Jotshi *et al.*, 2001). Even for the cases where complex representation is necessary as in heat exchangers, distillation columns, packed-bed reactors, etc., equivalent lumped-parameter models are considered for convenience and computational efficiency, without compromising much with the accuracy (Harriott, 1972; Patranbis, 1996). The partial differential equations of distributed-parameter systems can be equivalently represented by ordinary differential equations through model reduction, through separation of variables, or through descretization; the proofs of their equivalency are available in Patranbis (1996). Non-ideal flow packed-bed reactors are also modeled as a series of lumped tanks-in-series, which has been found to be as accurate as a distributed axial dispersion model in predicting the RTD and conversion. Furthermore, the lumped tanks-in-series model is simple to solve than the dispersion model, the latter also involves complications of open and closed vessel boundary conditions (Fogler, 2005, Levenspiel, 2004).

There is limited availability of chemical engineering studies on singular inputs (singular inputs are discussed in Section 2.4). However, discontinuity/inconsistency for the non-singular inputs caused by symbolic manipulations and differentiations has been studied extensively (i.e., of the first kind mentioned in Section 1.2). These are discussed below. The direct methods for handling these are discussed in the next Subsection 2.3.2.

***Single-component condenser model***

The following lumped-parameter index-2 DAE vapor-phase dynamics model of a single component condenser presented by Pantelides *et al.* (1988) has been considered frequently in the literature. A schematic of the condenser is shown in Fig. 2.4 below.

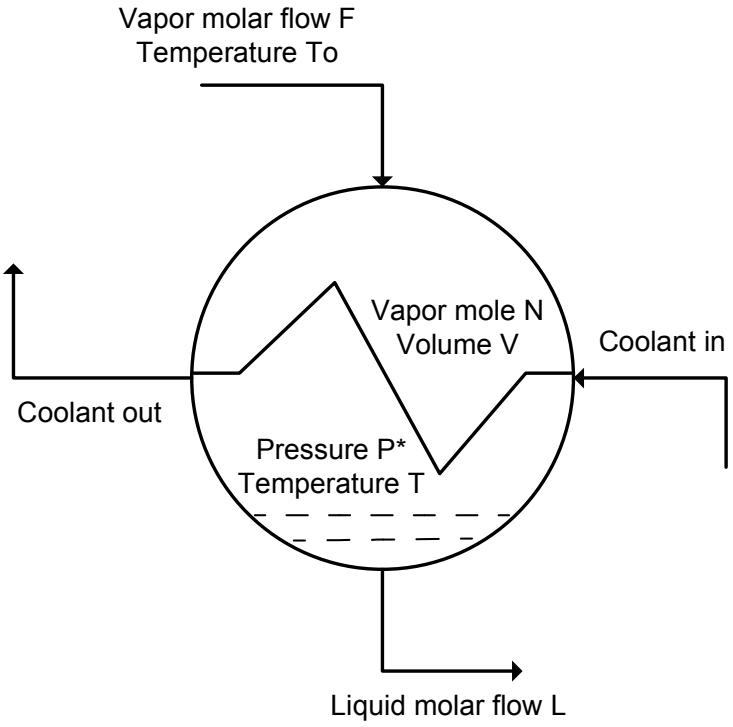


**Fig. 2.4** Schematic of a single component condenser

$$\frac{dN}{dt} = F - L \tag{2.29}$$

$$NC_p \frac{dT}{dt} = FC_p(T_o - T) + L\Delta H + UA_h(T_j - T) \tag{2.30}$$

$$P^* = A\exp\left(-\frac{B}{T+C}\right) \tag{2.31}$$

$$V = \frac{NRT}{P^*} \tag{2.32}$$

where $A$, $B$, $C$ are Antoine's constants; $R$, $U$, $A_h$, $C_p$ and $\Delta H$ are universal gas constant, heat transfer coefficient, heat transfer area, heat capacity of vapor and heat of condensation, respectively; $F$, $T_o$, $N$, $P^*$, $V$, $T$ are inlet vapor molar flow, inlet temperature, moles of the vapor in the condenser, vapor pressure, volume of vapor (assumed constant), and temperature of vapor and liquid in tank, respectively; $L$ and $T_j$ are outlet molar flow rate of liquid and jacket temperature (assumed constant), respectively.

Although being non-rigorous and contrived, this model for phase change has been used quite consistently in initialization studies. Several studies have employed this model (Chowdhary *et al.*, 2004; Kröner *et al.*, 1997; Majer *et al.*, 1995; Pantelides *et al.*, 1988; Unger *et al.*, 1995; Vieira and Biscaia Jr., 2001). It consists of differential and algebraic equations. This model is employed to illustrate the inconsistency of the symbolically transformed models; inconsistent initialization and limitations of these models are outlined next.

### 2.3.2 Inconsistency due to symbolic manipulations

Depending upon the solution approaches, the coupled differential and algebraic equations have to be transformed for conversion to the explicit ODEs or for the reduction in their index, to use the automatic DAE solvers. This involves the differentiation of the algebraic equations, and substitution of known expressions of time derivatives to get new algebraic and differential equations (extended system). No general method is available for the

solution of DAE systems of index ≥ 2; however, index-1 DAE systems have been solved in a number of studies.

Index is defined as the number of differentiations required to convert a DAE system into an ODE system. In extended system, some of the output variables have inconsistent initial values (they don't satisfy the extended system) for discontinuous inputs. This leads to initial jump discontinuities and singular initial conditions of the output variables for systems with terms containing differential of the output. In addition, the inconsistent initial values always lead to discontinuities in the solution during initial numerical integration step and result in errors and inefficient computation (Kroner *et al.*, 1997; Sincovec *et al.*, 1981). Many rigorous and approximate approaches have been suggested and extensive literature is available on algorithmic and direct methods of consistent initialization of such chemical engineering systems under the step input. However, the DAE approach is unsatisfactory for impulse inputs, and the symbolic differentiations of discontinuous outputs cause singularity.

As remarked, the extended system of equations doesn't satisfy the initial conditions for all the output variables for discontinuous forcing functions, which leads to inconsistent initialization. Several algorithms and numerical methods have been developed to solve the system starting with inconsistent initial conditions (Gopal and Biegler, 1988; Kröner *et al.* 1997; Leimkuhler *et al.*, 1992; Rabier and Rheinboldt. 1996; Ressig *et al.*, 2002; Unger *et al.*, 1995). However, it has been affirmed that these rigorous methods of initialization rely on numerical differentiation of the system, finite difference methods, and on the solution of a set of nonlinear algebraic equations. Hence, they are inexact and give rise to convergence problems and may not be suitable for most practical applications (Vieira and Biscaia Jr., 2001). Some algorithms, e.g., implicit Euler step methods, cause their own initial jump discontinuities in the output variables, and a solution altogether different from the actual physical system is obtained (Kröner, 1992). Moreover, significant errors are introduced in the solution due to inconsistent initial conditions (Kröner *et al.*, 1997). Besides, the solution through reduced index equivalent system starts degrading after some time (Soares and Secchi, 2005). These methods are, also, computationally less efficient and slow. Also, due to the presence of points of discontinuities, and due to the non-monotonic and non-smooth functions arising out of

the discontinuous inputs, numerical differentiation is likely to fail, leading to convergence problems.

In the solvers based on the above approaches, the estimation of a consistent set of initial conditions is essential and is the most challenging step of the numerical solution (more challenging than the numerical integration itself), whereas, the available initialization approaches are complex (requiring a structural analysis to find the index) and inadequate. In spite of the recent advancements, many of the available DAE solvers and initialization algorithms mentioned above fail due to convergence problems. When convergence criteria of Newton iteration are not satisfied, these solvers reduce the integration step size. This approach works well only for nearly consistent initial conditions. Due to a very small step size, Jacobian matrix becomes singular/ill-conditioned, resulting in failure of these solvers for the systems far off from the consistent initial conditions (Methekar *et al.*, 2011; Wu and White, 2001).

To overcome the inconsistent initialization problems, some studies propose a direct approach of smoothening of the step function by approximating it with a continuous function (Kröner *et al.*, 1997; Souza *et al.*, 2005; Vieira and Biscaia Jr., 2000; Vieira and Biscaia Jr., 2001). These studies use initial steady state values for initialization as it has been proved that a steady state is always a consistent initial set regardless of the type of the DAE system (Bachmann et al., 1990). Although being less rigorous and seemingly direct, this approach is inadequate as significant errors are introduced even if consistent initialization is achieved (Kröner *et al.*, 1997).

As remarked in the Introduction (Section 1.2), the above kind of inconsistency for the non-singular inputs is due to the discontinuities occurring only in a mathematical sense and not in the actual physical systems. The prime concern of the present study, however, is the singular inputs and the initial discontinuities affecting the physical systems.

### 2.3.3 Direct methods for initialization

Due to the several reasons stated above, many researchers rely on the simple and computationally more efficient direct methods. There are several other advantages of working with the original models directly rather than with symbolically transformed

models above (Brenan *et al.*, 1989; Murata and Bascaia Jr., 1997; Vieira and Bascaia Jr., 2000). They are efficiently solved, physical significance of various terms is retained, time consuming manipulations are avoided and fundamental information, that could have been lost through differentiation, is preserved. Quite contrary to the indirect approaches discussed above, some very recent contributions have proposed modeling and initialization approaches of either directly converting the DAE systems to explicit ODE systems, or solving them without symbolic manipulations and differentiations.

In their contribution, applicable to index-1 DAE systems, Methekar *et al.* (2011) have used a very small, constant perturbation parameter $\varepsilon$ in the algebraic equation, and expanded it by Taylor's series to get an explicit ODE form. The explicit ODEs have, then, been solved using easily available ODE solvers to obtain a consistent set of initial conditions corresponding to the steady state. This approach is computationally efficient, works well with inconsistent initial conditions, and doesn't require a nonlinear solver for initialization. However, in some studies, consistent initialization is achieved, *a priori*, e.g., by directly substituting the derivative of the differential variables with their initial values, so as to convert the ODEs into algebraic equations, and solving them to obtain a consistent set of initial conditions. These initial conditions have, then, been used for the integration of the ODE or the DAE system (Dones *et al.*, 2010; Lima *et al.*, 2009; Manenti *et al.*, 2009; Manenti and Rovaglio, 2008). Manenti *et al.* (2011) have presented a *radically* simplified and computationally efficient model of an original heterogeneous DAE model of methanol synthesis by converting it to an explicit ODE model and removing the algebraic equations through the simplifying pseudo-homogeneous assumption of no concentration and temperature gradients between gas and solid phase, and, so, merging the equations of the two phases. Their numerical results have clearly shown that the pseudo-homogeneous ODE model represents a good compromise between model accuracy and reduced computational effort, and a clear and reliable alternative for the original heterogeneous DAE model.

The above direct methods have been successful in achieving consistent initialization for the nonsingular inputs. These again handle the kind of inconsistency caused due to the discontinuities occurring only in a mathematical sense and not in the actual physical systems. No study is, however, available on the direct methods for the

singular inputs and the initial discontinuities in the physical systems emerging from them for the nonlinear ODE systems that constitute lumped-parameter chemical engineering systems.

## 2.4 Treatment for Singularities and Initial Discontinuities

The framework of generalized functions that have developed over a long period of time, have been the most rigorous technique for the treatment of singularities. However, as stated above, it involves mathematical technicalities and complications. A glance at this framework for the linear systems is made here (see Lundberg *et al.*, 2007 for more details).

A sparse set $S$ of numbers is first selected, which contains only finite number of elements. A piecewise continuous and smooth function $f(t)$ on $[0, \infty)$ is assumed, i.e., for every $a \in [0,\infty)$, left and right limit, and all the derivatives exist on the complement of the sparse set. Singularity functions are defined by the following sum of the impulse and its $l^{\text{th}}$ derivatives:

$$f_s(t) = \sum_{k,l} c_{k,l} \delta^{(l)}(t - a_k) \tag{2.33}$$

where $a_k$ is a non-decreasing sequence in $[0,\infty)$ and $\delta^{(l)}(t)$ is the $l^{\text{th}}$ derivative of the Dirac function. The constants $a_k$ for which some $c_{k,l}$ are nonzero are the singular points of $f_s(t)$. The singularity at $t = a$ of $f_s(t)$ is the part of the sum corresponding to $a_k = a$. Generalized functions consist of regular part $f_r(t)$ and singular part $f_s(t)$ as follows:

$$f(t) = f_r(t) + f_s(t) \tag{2.34}$$

whose regular part $f_r(t)$ is determined by a piecewise-smooth function and whose singular part $f_s(t)$ is a singularity function. The regular part contributes the pre-initial conditions:

$f^{(n)}(0^-) = f_r^{(n)}(0^-)$.

Two piecewise-smooth functions define the same generalized functions, if and only if, they differ from each other on a sparse set. For generalized functions, the specific

values $f(a)$ are irrelevant, rather, the one-sided limits $f(a^+)$ and $f(a^-)$ are referred to, which are always defined (even for $a \in S$ ) even if a finite number of values of $f(t)$ are changed.

The generalized derivative of a piecewise-smooth function $f(t)$ is a generalized function. The regular part of $f'(t)$ is smooth on the complement of $S$, and is given by the ordinary derivative of $f_r(t)$ on the complement of $S$. The singular part of $f'(t)$ is given by summing Dirac functions that arise from the jumps in the graph of $f(t)$, i.e.,

$$f_s'(t) = \sum_{a \in S} (f(a^+) - f(a^-))\delta(t-a) \tag{2.35}$$

Multiplication of smooth function $g(t)$ with a generalized function is worked out by defining the product of $g(t)$ with $f_s(t)$ as:

$$g(t)\delta^{(n)}(t-a) = \sum_{k=0}^{n} (-1)^k \binom{n}{k} g^{(k)}(a)\delta^{(n-k)}(t-a) \tag{2.36}$$

The usual product rule for differentiation and the integration-by-parts rule is valid for any smooth function $g(t)$ and generalized function $f(t)$.

The machinery of generalized functions involves an intuitive treatment of the Dirac function, and has many associated complications and ad hoc interpretations when the Dirac function is multiplied with a discontinuous function, and, hence, some studies prefer to use the basic integral notion rather than the generalized integral notion (Grizzle, 2004; Makila, 2006). These remarks are more apt for the nonlinear systems for which the machinery involves further mathematical technicalities (Pilipchuk, 1999).

Various other methods that are described in the literature for the treatment of singularity and initial discontinuity are briefed below.

Method of moments, and regression analysis have been used in many of the contributions (Brouckaert *et al.*, 1995; McCoy, 1987; Ramasamy and Sundaramoorthy, 2008; Tondeur *et al.*, 1996). These approximations rely on the comparison of the mean (first moment), the variance (second moment), third moment, etc., of the impulse response predicted from some theoretical correlations (or through Maclaurin's series of the transfer function truncated up to first three terms), with the moments that are obtained from the desired or the experimental response profiles. However, these methods involve

inaccuracy as the equality of the moments doesn't guarantee the closeness to the actual response. Alternatively, the physical system is imagined as a combination of units of known models and the predicted response is compared with the experimental response by least square regression analysis. However, it requires a rigorous trial and error procedure.

Smoothening of step and impulse functions by approximating them with continuous functions have been in use for quite a long time (e.g., Gauss, rectangular, pulse, and regularization series functions of exponential, polynomial, ramp or sine forms) (Gezici *et al*., 2005; Souza *et al.*, 2005; Zhang, *et al.*, 2010). However, fundamental limitations of smoothing of step inputs have been discussed in detail (Kroner *et al.*, 1997). The type of smooth approximation has a significant impact on the accuracy of the transient solution, and there have been problems as these errors can't be made arbitrarily small by choosing the smoothing time interval arbitrarily small.

Several studies adopt analytical transformations of equations to eliminate/separate the singular terms, e.g., as discussed above in Section 2.1 (see also Appendix I) (Makila, 2006; Yan, 2008). Some studies considered linear and nonlinear mechanical systems under discontinuous and impulsive excitation and presented solutions through the application of special non-smooth saw-tooth temporal transformations to these systems (Pilipchuk *et al*., 1997; 1998; Pilipchuk, 1999; Vakakis *et al.*, 1996). These transformations lead to elimination of singularities. Solutions of the ODEs of motion were represented in a special form which contained a standard pair of non-smooth periodic functions and possessed a convenient structure and explicit forms of analytical solutions. The systems considered were linear first-order viscous damper, second-order harmonic oscillator, Duffing oscillator, etc. These were linear time-invariant, linear time varying, and systems with an only nonlinear term of single variable.

Several numerical approaches approximated the discontinuous behavior with auxiliary algebraic or differential functions (Al-Hayani and Casasús, 2006; Casasús and Al-Hayani, 2002; Hogarth, *et al.*, 1990; Mao and Petzold, 2002). In some of these methods, the solution of the linear and nonlinear ODE was approximated by an infinite series. The nonlinear term of the ODE was decomposed into Adomian polynomials consisting of differential functions of the components of the solution series. An iterative algorithm was then determined in a recursive way by substituting these functions into the

ODE. The systems considered were linear time-invariant and systems with nonlinear term of single variable (Al-Hayani and Casasús, 2006). There were significant errors involved for singular inputs, and there were problems of convergence for nonlinear cases. In some studies, spline collocation was used (Khuri and Sayfy, 2009; Pederson and Tanoff, 1982; Saranen and Wendland, 1987). In this method, different polynomials as solution functions were assumed for different parts of the domain. For each polynomial of certain degree, certain collocation points were selected. The polynomial function must satisfy the differential equation at all these points, which gives a number of equations. These equations were solved to give the constant coefficients of the solution polynomial. However, the discontinuous and singular inputs create steep gradients in solutions, and in these regions, a high density of collocation points are needed for accuracy, which also requires the behavior of the solution to be known in advance. Also, high degree polynomials are required for high accuracy.

The generalized functions that require theory of distributions is described above (Brigola and Singer, 2009; Corinthios, 2005; 2007; Lundberg *et al.*, 2007; Rabier and Rheinboldt, 1996). The technique of impulse matching, also, is illustrated in Section 2.2.1 above (Lundberg *et al.*, 2007).

Limitations of approximate and technically complicated methods are laid out in this chapter. Many of these methods require series expansion of the model system, approximate regression analysis, smoothing of discontinuous functions, finite difference methods, cumbersome methodologies of generalized functions, mathematical transformations of equations, and symbolic manipulations, etc.; these steps lead to various approximations and complications. The symbolic differentiations and manipulations are seriously inadequate for systems perturbed by the singular inputs due to the fact that these inputs cause significant initial discontinuities in the state variables, which make them non-differentiable. So, as clarified in Section 1.2 of the Introduction, the present study is not directed towards this kind of inconsistency that occurs only in a mathematical sense and only with a mathematical model. Rather, the prime focus of the present work is on the inconsistency associated with the initial discontinuities in the actual physical systems caused by the *singular* inputs. These jump discontinuities in the initial values and/or slopes of the state variables present inherent initialization

inconsistency in the solution profiles of the original non-transformed model, and directly affect the actual physical system. In this context, the following gaps are identified.

- Several approaches have been suggested in the literature for the treatment of the lumped-parameter dynamic systems perturbed by the discontinuous inputs. However, especially for the initial discontinuities pertaining to the singular inputs to the physical systems, the approximation with smooth inputs, complicated techniques, and the demanding framework of generalized functions have been suggested.
- Besides being complicated and indirect, the literature studies on the singular inputs deal mainly with electrical and mechanical engineering systems, and pure mathematical equations. These systems have been linear time-invariant, linear time varying, and systems with an only nonlinear term of single variable. The chemical engineering systems involve additional complexities associated with flows along with mixing and chemical reactions, phase changes, and the interaction of material, thermal and mechanical energy (inertia) capacities, e.g., CSTRs, gravity-flow tanks, condensers, vaporizers, etc. Hence, these also contain nonlinear terms of products of discontinuous outputs with other output/input variables. Direct methods for these systems remain to be thoroughly investigated for the singular inputs, as for them, the above approaches would become further complex.
- Laplace transform has been an effective technique in handling singularity. However, as seen above in Section 2.1, a significant confusion and inconsistency also prevails on the issue of singular inputs, especially, the impulse input (and its derivative) to the widely used linear time-invariant systems in the Laplace domain.

A direct treatment for the inconsistency due to the singular inputs outlined in the Introduction has not been investigated so far. The studies on singularity deal mainly with electrical and mechanical engineering systems and pure mathematical equations, and advocate either the use of the approximate methods, or the convoluted, complicated methods, and the framework of generalized functions. These approaches reported in the literature are demanding, mathematically complicated, indirect (use transformed models), and, are not easily applicable on a routine basis in practical situations.

# 3 Mathematical Modeling

In this chapter, representative lumped-parameter nonlinear ODE models, involving mixing with chemical reaction, phase change, interaction of different capacities, closed loop system with dead time, and interacting and coupled systems are considered. Two examples of inherent linear second-order systems with derivative of the input are included in Section 3.8. For convenience in comparison of alternative initializations in subsequent chapters, the native models rather than the dimensionless forms are used. These models are different in their physical structure, analysis for the effect of initial discontinuities and the effect of linearization.

The models considered contain coupled ODEs, which on simultaneous solution for one of the output variables yields ODEs with terms containing differentials of the input function. Upon linearization, such models yield second-order numerator-dynamics transfer functions, which exhibit initial discontinuities in their profiles. To explore the general range of their behavior, conditions are worked out for their assorted solution profiles to identify characteristic parameters, which unfold interesting cases of maximum, minimum, inflection, input multiplicity, pole-zero cancellation, reduction to standard systems, etc., as the value of one such parameter changes relative to that of the others on the real axis. These profiles would be discussed later in this chapter. The profiles exhibiting maximum and minimum in step and impulse responses respectively are not observed in the standard over-damped systems, and become important even from the point of view of design of the system. During the dynamic changes, the operating variables can attain maximum/minimum values that are significantly beyond the steady state range of values. The design is certainly influenced due to these dynamic changes and must be based on the maximum/minimum values as the design based on steady state values would be unsatisfactory.

## 3.1 Non-isothermal CSTR

A benchmark model that has been used to study nonlinear dynamics in the literature, i.e., a non-isothermal CSTR, is considered first (Inamdar *et al.*, 2011; Lemoine-Nava *et al.*, 2006; Moudgalya and Jaguste, 2001; Prasad and Bequette, 2003; Prasad *et al.*, 2002; Ray, 1995; Salehi and Shahrokhi, 2008). With changes in the inlet flow rate, material and thermal capacities are interacting. This model is considered in Sections 5.3 and 5.4 to study inconsistencies from singularities and illustrate the framework of methodology for the analysis of discontinuities and initialization for the numerical solution for the impulse inputs.

The constant density, jacketed, non-isothermal CSTR is carrying out a liquid-phase, first-order reaction $A \rightarrow R$ with rate constant $k$ and enthalpy $(-\Delta H_R)$. The feed contains only $A$. Assuming that the jacket fluid is at saturated condition, thus, its temperature $T_j$ is constant and uniform throughout. Heat capacity of the reaction mass $C_p$ also stays constant throughout. $C_A$ and $C_R$ are concentrations of $A$ and $R$. $v_o$, $v$, $T_o$ and $T$ are respectively flow rates and temperatures of feed and exit. $k_o$ and $E$ are Arrhenius parameters, $R$ is the universal gas constant. Writing material and energy balances give (Coughanowr and LeBlanc, 2009):

$$\frac{dV}{dt} = v_o - v \tag{3.1}$$

$$\frac{d(VC_A)}{dt} = v_o C_{Ao} - vC_A - kC_A V \tag{3.2}$$

$$\rho C_P \frac{d(VT)}{dt} = \rho C_P (v_o T_o - vT) + (-\Delta H_R) kC_A V + U_h A_h (T_j - T) \tag{3.3}$$

$$k = k_o exp\left(-E / RT\right) \tag{3.4}$$

### 3.1.1 Linearized model

The tank is now assumed closed and always fully filled, so that, its hold-up volume $V$ can be taken constant. Linearizing the above model (using Taylor's series expansion of the nonlinear terms in the neighborhood of initial steady state and ignoring the terms of order

greater than or equal to two), taking the Laplace transforms of the linearized equations, and solving these simultaneously, the following transfer functions are obtained (valid for step perturbations in jacket temperature):

$$\frac{\bar{T}}{\bar{T}_j} = K\frac{s+l}{s^2+(l+d)s+ld-e} \qquad \frac{\overline{C_A}}{\bar{T}_j} = K''\frac{1}{s^2+(l+d)s+ld-e} \tag{3.5}$$

where $K = \frac{U_h A_h}{\rho V C_P}$, $l = \frac{v}{V} + k_s$, $d = \frac{v}{V} + K + \frac{\Delta H_R}{\rho C_P} C_{As} k_s \frac{E}{RT_s^2}$, $e = \frac{\Delta H_R}{\rho C_P} C_{As} k_s^2 \frac{E}{RT_s^2}$ (3.6)

Subscript *s* and over bar represent initial steady state and the deviations of variables from their initial steady states, respectively.

## 3.2 Isothermal CSTR

It is a constant hold-up volume tank carrying out a liquid-phase constant-density reaction $A \rightarrow R$ having first-order rate constant *k*. Assume that the system is closed and is always fully filled, so that, the hold-up volume of the tank remains unchanged. Only reactant *A* is in the feed and is dissolved in an inert solvent *I*. The component material balance for *R* and *A* respectively are:

$$\frac{dC_R}{dt} = -\frac{v_o}{V}C_R + kC_A \tag{3.7}$$

$$\frac{dC_A}{dt} = \frac{v_o}{V}C_{A_O} - \left(\frac{v_o}{V} + k\right)C_A \tag{3.8}$$

If the volumetric flow rate of feed $v_o$ is perturbed at zero time. The differential equation for $C_R$ is derived from Eqs. (3.7) and (3.8), and is given below.

$$\frac{d^2C_R}{dt^2} + \left(2v_o/V + k\right)\frac{dC_R}{dt} + \left(v_o^2/V^2 + kv_o/V\right)C_R = (kC_{A_O}/V)v_o - (C_R/V)\frac{dv_o}{dt} \tag{3.9}$$

This is a nonlinear ODE with a term containing differential of the input function $v_o$.

Eqs. (3.7) and (3.8) are derived as follows. The first term in the transient material balance (3.7) is the rate accumulation of *R* in tank; the inflow rate of *R* is *zero*; the second

term is the rate of out-flow of $R$ and the third term is the rate of formation of $R$. In Eq. (3.8), the first term is the rate accumulation of $A$; the second term is the inflow rate of $A$; the third term is the rate of out-flow of $A$ plus the rate of disappearance of $A$. All these terms are in moles per unit time and volume. Where, $C_A$, $C_R$ and $C_I$ are concentrations of $A$, $R$ and $I$ respectively in the tank and in the exit stream; $C_{Ao}$ is the feed stream concentration; $v$ is the volumetric feed rate and $V$ is holdup volume.

### 3.2.1 Linearized model

The system is assumed to be at steady state at time $t \rightarrow 0^-$. For a perturbation in volumetric flow rate of feed $v_o$, linearizing Eqs. (3.7) and (3.8) and converting to deviation variables, gives:

$$\frac{d\overline{C_R}}{dt} = -\frac{C_{R_s}}{V}\overline{v_o} - \frac{v_s}{V}\overline{C_R} + k\overline{C_A} \tag{3.10}$$

$$\frac{d\overline{C_A}}{dt} = \left(\frac{C_{A_o} - C_{A_s}}{V}\right)\overline{v_o} - \left(\frac{v_s}{V} + k\right)\overline{C_A} \tag{3.11}$$

For impulse perturbation in $C_{Ao}$, the system of Eqs. (3.8) and (3.7) behaves as standard first and second order respectively for $A$ and $R$. However, considering the effect of initial discontinuity (discussed in Section 4.2.4 for the linear systems) would yield a second-order numerator-dynamics form for $R$ as it would lead to an un-accounted discontinuity in $C_R(0)$. This gives the following Eq. (3.12), where ($s$) denotes Laplace parameter, over-bar denotes deviation of a variable from its initial steady state value and subscript $s$ denotes the initial steady state value:

$$\frac{\overline{C_R}}{\overline{C_{A_O}}} = \frac{\overline{C_R}(0^+)\left((s + (v_o/V + k)\right)/M + kv_o/V}{\left(s + (v_o/V + k)\right)\left(s + v_o/V\right)} \tag{3.12}$$

Thus, this transfer function would have reduced to the standard second-order transfer function, if $\overline{C_R}(0^+)$ was zero, i.e., the discontinuity was ignored.

## 3.3 Semi-batch Reactor

Consider a variable holdup semi-batch reactor, in which, *A* was already in the reactor and *B* was being fed continuously at constant rate $v_o$ for time $t \leq 0^-$. No outlet stream is there. *M* ($m^3$) of reactant *B* is fed suddenly at $t \rightarrow 0^+$. This is equivalent to an impulse perturbation (in *B*) volumetric flow rate of feed $v_o$ at $t \rightarrow 0^+$. For the elementary reaction $A + B \rightarrow R$, the component molar balance for *B* and *A* respectively are (Fogler, 2005):

$$\frac{d(VC_B)}{dt} = v_o C_{Bo} - kC_A C_B V \tag{3.13}$$

$$\frac{d(VC_A)}{dt} = -kC_A C_B V \tag{3.14}$$

## 3.4 Single-component Condenser

This model is also used in literature (Chowdhary *et al.*, 2004; Kröner *et al.*, 1997; Majer *et al.*, 1995; Pantelides *et al.*, 1988; Unger *et al.*, 1995; Vieira and Biscaia Jr., 2001). The symbols were defined in the last chapter.

$$\frac{dN}{dt} = F - L \tag{3.15}$$

$$NC_p \frac{dT}{dt} = FC_p(T_o - T) + L\Delta H + U_h A_h(T_j - T) \tag{3.16}$$

$$P^* = A \exp\left(-\frac{B}{T + C}\right) \tag{3.17}$$

$$V = \frac{NRT}{P^*} \tag{3.18}$$

### 3.4.1 Revised model

In the above literature model of Section 3.4, Eq. (3.16) is obtained by applying differentiation rule of the product of variables *N* and *T* in the accumulation term of the original energy balance equation, and substituting material balance Eq. (3.15) for the

differential of *N*. This model might work for the step input. However, the *impulse* input causes initial discontinuities in *N* and *T* that make these variables non-differentiable, and, so, the symbolic manipulations and differentiations are bound to lead to errors. Hence, for the impulse input, the first principles energy balance must replace Eq. (3.16).

The original energy balance equation for the vapor phase is re-formulated as:

$$C_p \frac{d(NT)}{dt} = FC_pT_o + U_hA_h(T_j - T) - L(C_pT - \Delta H) \tag{3.19}$$

The first term is the accumulation of energy, the second term is enthalpy of inlet vapors, the third term is heat transfer to the cooling jacket, and the fourth term is the enthalpy of outlet condensed liquid.

The comparisons of this model with others are made in Sections 5.13 and 5.14.

### 3.4.2 Model obtained through symbolic manipulations

If *V* is a variable, the above model has one degree of freedom for perturbation in *F*, and, so, *V* has been assumed constant in the above literature model. Assuming constant volume, the model has zero degree of freedom. For solution, the model can be converted to a different form after symbolic differentiations and manipulations. Limitations of the symbolic manipulations were outlined in Section 2.3.1 of the last chapter. The model formulated here will be used to illustrate the inconsistencies arising out of symbolic manipulations and differentiations in Section 5.13. Consider a step disturbance in the molar feed rate *F* introduced into the single component condenser model with volume *V* held constant at $V_o$. The above model is converted to explicit ODE system in order to use the standard explicit ODE solvers. To obtain *L* explicitly from the above equations, the model is converted to the following form after symbolic differentiations and manipulations. Eq. (3.18) is first written as:

$$N = \frac{P^*V_o}{RT} \tag{3.20}$$

Then, an explicit equation for *L* is obtained by cumbersome manipulations: differentiating Eqs. (3.17) and (3.20), and combining them together to give Eq. (3.21).

Substituting Eq. (3.21) and the value of $\frac{dT}{dt}$ obtained from Eq. (3.16) into Eq. (3.15), finally gives the following Eq. (3.23) for *L*.

$$\frac{dN}{dt} = Z\frac{dT}{dt} \tag{3.21}$$

where $$Z = \frac{BV_oP^*}{RT(T+C)^2} - \frac{V_oP^*}{RT^2} \tag{3.22}$$

$$L = \frac{FNC_p - Z\{FC_p(T_o - T) + U_hA_h(T_j - T)\}}{NCp + Z\Delta H} \tag{3.23}$$

Hence, an alternative system consisting of Eqs. (3.15), (3.16), (3.17), (3.22), and (3.23) is obtained.

However, for *N*, there is a choice of including either the differential Eq. (3.15) or the algebraic Eq. (3.20). These alternative systems are solved using explicit ODE solvers for a step and impulse perturbation in *F*, and many unsatisfactory results are exhibited. The analysis of discontinuities and the numerical results of these alternative systems, exposing their inconsistencies are presented in Section 5.13.

### 3.4.3 Linearized model

The system is assumed to be at steady state at time $t \rightarrow 0^-$. Linearizing Eq. (3.19) and using Eq. (3.15), for no change in the jacket temperature, the following equation is obtained:

$$C_pN_s\frac{d(\overline{T})}{dt} = C_p(T_o - T_s)\overline{F} - (U_hA_h + L_sC_p)\overline{T} + (\Delta H)\overline{L} \tag{3.24}$$

Subscript *s* and over bar represent initial steady state and the deviations of variables from their initial steady states, respectively.

Various tank models are considered next. The flow-level tanks and their draining times are used in the next chapter to validate the initialization effects as these are clearly

observed in the level responses. Coupled and interacting flow-level tanks, stirred-tank heaters, reactors, etc. have been reported quite often in the literature studies (Engin *et al.*, 2004; Gatzke *et al.*, 2000; Oh and Yeo, 1996; Roy, 2003; Sundaram and Radhakrishnan, 2003; Thakkar and Gaikwad, 2005; Watt *et al.*, 2010).

## 3.5 Gravity-flow Tank

A gravity-flow tank consists of a tank with an inflow stream and a straight, horizontal outflow pipe at the bottom exit (Fig. 3.1). It is unique in the respect that it has interacting material (tank) and mechanical energy (pipe) capacities. This results in coupled differential equations. Plug flow is assumed in the pipe and, hence, the velocity profile is flat. This facilitates the application of momentum balance on the pipe fluid as it can be considered as a lumped free body. Writing transient material and momentum balances (Luyben, 1990) gives the following two Eqs. (3.25) and (3.26). These equations may be solved for $h$ to yield a cumbersome nonlinear ordinary differential equation that contains a term with a differential of the input function $q$ (see Eq. (3.27)). $A_T$ is x-sectional area of the tank, $h$ is level, $q$ is volumetric feed rate, $u_p$ is efflux velocity in the pipe, $f$ is friction factor $A_p$, $L$, $D_p$ are respectively x-sectional area, length and diameter of the pipe.

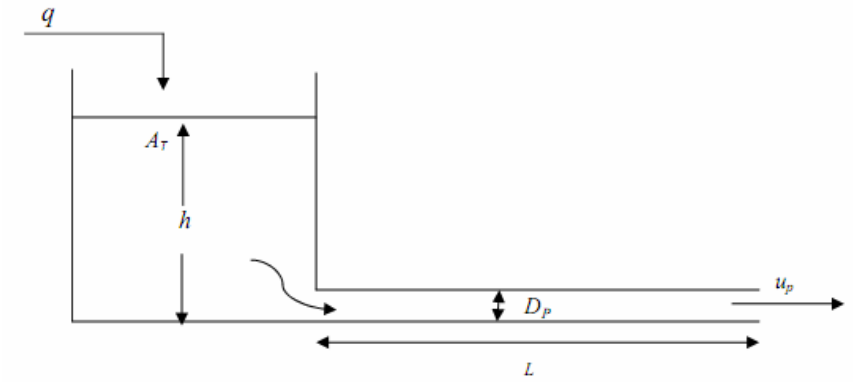


**Fig. 3.1** Schematic of a gravity-flow tank

$$\frac{dh}{dt} = -\frac{A_p}{A_T}u_p + \frac{q}{A_T} \tag{3.25}$$

$$\frac{du_p}{dt} = \frac{g}{L}h - \frac{2f}{D_p}u_p^{\,2} \tag{3.26}$$

### 3.5.1 Linearized model

The system is assumed to be at steady state at time $t \rightarrow 0^{-}$. Linearizing, combining and taking Laplace transforms of these equations, give:

$$s^2H(s) - sH(0) - H'(0) + \frac{B}{A}\left[sH(s) - H(0)\right] + \frac{C}{A}H(s) = K\left[sQ(s) - Q(0)\right] + K\frac{B}{A}Q(s) \tag{3.27}$$

where $K = 1/A_T$, $A = A_P L$, $B = \left(4fLQ_S\right)/\left(D_P\right)$, $C = gA_P^{\,2}/A_T$

Capitals *H, U* and *Q* are deviation variables corresponding to variables of lower case. These deviations are from their initial steady states. Subscript *s* represents initial steady state and superscript (′) represents derivative. The corresponding transfer function form (valid for step inputs, see next chapter, Section 4.2.2) becomes:

$$\frac{H(s)}{Q(s)} = \frac{1}{A_T}\frac{(\rho A_P L)s + \left(4fL\rho Q_S\right)/D_P}{(\rho A_P L)s^2 + \left[\left(4fL\rho Q_S\right)/D_P\right]s + \left(\rho g A_P^2\right)/A_T} \tag{3.28}$$

It is rewritten in a different version as:

$$\frac{Y(s)}{X(s)} = K'\frac{s + l}{As^2 + Bs + C} \tag{3.29}$$

where $K' = \rho A_P L / A_T$, $l = (4fQ_S)/(A_P D_P)$, $A = A_P L$, $B = (4fLQ_S)/(D_P)$, $C = gA_P^{\,2}/A_T$

## 3.6 Interacting Tanks System

The first tank of the two interacting liquid-level tanks-in-series is considered (Fig. 3.2). Writing transient material balances gives the following two Eqs. (3.30) and (3.31). These equations may be solved for the level of the first tank $h_1$ to yield a cumbersome ordinary differential equation that contains a term with differential of input function *q*. Here, *q* stands for volumetric inflow rate to the first tank; $A_1$ and $h_1$ are cross-sectional area and level rate of the first tank, respectively; $q_{21}$, $h_2$ and $q_2$ are the input flow, level and output flow of the second tank.

$$\frac{dh_1}{dt} = -\frac{q_{21}}{A_1} + \frac{1}{A_1}q \qquad (3.30(a)); \qquad \frac{dh_2}{dt} = -\frac{q_2}{A_2} + \frac{1}{A_2}q_{21} \qquad (3.30(b))$$

For non-linear resistances the flow-head relationships with constants $k_1$ and $k_2$ are:

$$q_{21} = k_1\sqrt{h_1 - h_2}\ ; \qquad q_2 = k_2\sqrt{h_2} \qquad (3.31)$$

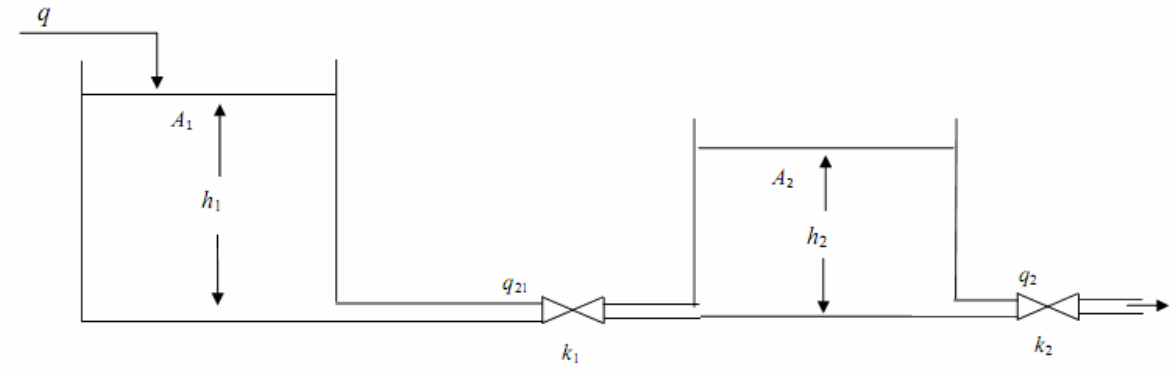


**Fig. 3.2** Schematic of the two interacting tanks system

### 3.6.1 Linearized model

The system is assumed to be at steady state at time $t \rightarrow 0^-$. Assuming the outflows from tanks 1 and 2 are related to the liquid levels with constant linear resistances $R_1$ and $R_2$:

$$Q_{21} = \frac{H_1 - H_2}{R_1} \qquad (3.32(a)); \qquad Q_2 = \frac{H_2}{R_2} \qquad (3.32(b))$$

Combining Eqs. (3.30) and (3.32), and solving for $H_1$ gives:

$$\tau_1\tau_2\frac{d^2H_1}{dt^2} + (\tau_1 + \tau_2 + A_1R_2)\frac{dH_1}{dt} + H_1 = (R_1 + R_2)Q + \tau_2R_1\frac{dQ}{dt} \qquad (3.33)$$

Capitals $Q_{21}$, $H_1$, $Q_2$, $H_2$ are deviation variables corresponding to variables of lower case.

$\tau_1 = A_1R_1$ and $\tau_2 = A_2R_2$.

The above system Eq. (3.33) is written in the following useful Laplace transform version:

$$\tau_1\tau_2[s^2H_1(s) - sH_1(0) - H_1'(0)] + [(\tau_1 + \tau_2 + A_1R_2)]\times[sH_1(s) - H_1(0)] + H_1(s) = (R_1+R_2)Q(s) + \tau_2R_1[sQ(s) - Q(0)] \qquad (3.34)$$

The transfer function form for the first tank is (see next chapter, Section 4.2.2):

$$\frac{H_1}{Q} = \frac{(\tau_2 R_1)s + (R_1 + R_2)}{(\tau_1 \tau_2)s^2 + (\tau_1 + \tau_2 + A_1 R_2)s + 1} \tag{3.35}$$

It is rewritten in a different version as:

$$\frac{Y(s)}{X(s)} = K' \frac{s + l}{As^2 + Bs + C} \tag{3.36}$$

where $K' = \tau_2 R_1$, $l = (R_1 + R_2) / (\tau_2 R_1)$, $A = \tau_1 \tau_2$, $B = \tau_1 + \tau_2 + A_1 R_2$, $C = 1$

## 3.7 Closed-loop Stirred Tank Heater with Dead Time

This model is selected to illustrate the effect of initial conditions on the closed-loop systems in the presence of dynamic lags in Chapter 5. Consider a stirred tank heater system that consists of a constant holdup tank of volume $V$ and a horizontal pipe at the bottom exit. Liquid of density $\rho$ and specific heat $C_p$ enters at a flow rate $v_o$ and temperature $T_o$, and it is heated in the tank to a temperature $T$ with a thyristor controlled electric heater. Temperature transmitter senses the temperature $T_m$ at the pipe exit, and transmits the signals to the control module. The process temperature is controlled through a proportional controller of gain $K_c$ by manipulating heat input to the process $Q$. A tank heater is rigorously modeled as a distributed-parameter system, or a lumped-parameter system with dead time (Goswami *et al.*, 1997; Jotshi *et al.*, 2001). Here, it is modeled as a first-order system with dead time $\tau_d$ (FOPDT). There is no lag in any other component of the control loop. Writing energy balance and using the controller equation, the following delay differential equation (DDE) of the regulator system perturbed by inflow rate $v_o$ is obtained (Coughanowr and LeBlanc, 2009):

$$\frac{dT_m}{dt} = K_1 Q(0^-) - K_1 K_c T_m(t - \tau_d) + K_1 K_c T_m(0^-) + K_3 v_o(t - \tau_d) - K_2 v_o(t - \tau_d) T_m$$
$$\text{where } K_1 = 1/(\rho C_p v_o),\ K_2 = 1/V,\ \text{and } K_3 = T_o / V \tag{3.37}$$

An FOPDT model has been a prevalent model of process plant dynamics, and has been of considerable research interest (Arbogast *et al.*, 2007, Banu and Uma, 2008;

Juneja *et al.*, 2009; Kanagaraj *et al.*, 2009; Kaya, 2004; Skogestad 2004; Toscano, 2005; Vilanova and Pedret, 2010), as the presence of a significant dead time makes the closed system oscillatory, unstable and difficult to design and control. This DDE can't be solved through ordinary means; hence, a numerical algorithm based on fourth order Runge-Kutta method is developed for the solution (refer to Appendix II).

### 3.7.1 A degenerate system – linearized jacketed stirred tank heater

In a stirred-tank heater, material and thermal energy capacities are interacting. It consists of a perfectly stirred tank of variable hold up $V$, which heats the incoming liquid stream of flow rate $v_o$, using a jacket fluid of temperature $T_j$. The leaving stream is thus at a higher temperature $T$. Let the incoming temperature $T_o$ be a constant. The jacket fluid is saturated. The input variable considered here is the inflow rate $v_o$. The material and energy balance equations respectively are (Coughanowr and LeBlanc, 2009):

$$\frac{dV}{dt} = v_o - v \tag{3.38}$$

$$\rho C_P \frac{d(VT)}{dt} = v_o \rho C_P T_o + U_h A_h (T_j - T) - v \rho C_P T \tag{3.39}$$

Assume constant linear resistance $R$, i.e., $v = V / R$. The system is assumed to be at steady state at time $t \rightarrow 0^-$. Introducing deviation variables, linearizing the non-linear terms and solving simultaneously, gives:

$$\frac{\bar{T}}{\bar{v}_o} = -\frac{(T_s - T_o)(Rs+1)}{V_s(Rs+1)(s + v_s / V_s + U_h A_h / \rho C_P)} = -\frac{(T_s - T_o)}{V_s(s + v_s / V_s + U_h A_h / \rho C_P)} \tag{3.40}$$

Hence, this linear system behaves as a first-order negative gain system due to pole-zero cancellation.

## 3.8 Inherent Second-order Systems with Derivative of the Input

### 3.8.1 U-tube manometer

Such systems are the linear systems with terms containing derivative of the input function, i.e., inherent numerator-dynamics. Consider a simple U-tube manometer that measures a pressure difference $\Delta P$ imposed on its two legs. It contains a liquid of density $\rho$ and viscosity $\mu$. The mass of the liquid column is $m$, total length of the column is $L$, and its cross sectional area is $A$, $g$ is acceleration due to gravity, $u$ is the velocity of the liquid column, and $y$ is the deviation of liquid level from the initial rest position if the levels in the two legs were equal. $U$, $Y$, & $\Delta\overline{P}$ are the corresponding deviations from the pre-initial state. Assuming laminar flow in the tube but ignoring radial variations in velocity so that the system can be modeled through the lumped-parameter approach. This facilitates application of momentum balance on the column as a whole as it can be considered a free body; this gives the following equations for $Y$ and $U$ (Coughanowr & LeBlanc, 2009):

$$m\ddot{y} = -a\dot{y} - by + A(\Delta P) \qquad \text{or} \qquad m\ddot{Y} = -a\dot{Y} - bY + A(\Delta\overline{P}) \tag{3.41}$$

$$m\ddot{u} = -a\dot{u} - bu + A(\Delta P)$$
$$\text{where} \quad a = 8\pi\mu LA, \quad b = 2\rho gA \qquad \text{or} \qquad m\ddot{U} = -a\dot{U} - bU + A(\Delta\dot{\overline{P}}) \tag{3.42}$$

The last equation is derived by noting that $u = \dot{y}$

### 3.8.2 Car wheel suspension example

This system described in the last chapter (Fig. 2.3) consists of a spring and damper in parallel and is described by Eq. (2.24) of the last chapter, i.e., a second-order ODE containing a derivative of the input term (Lundberg *et al.*, 2007).

### 3.8.3 Model for car-body subjected to applied force

This system described in the last chapter (Fig. 2.3) again consists of a spring and damper in parallel and is described by Eq. (2.28) of the last chapter, i.e., a second-order ODE containing a derivative of the input term. The above three systems shall be used in the treatment of inconsistencies in the Laplace transforms in Chapter 6.

As can be seen in the above models, the governing equations, in general, yield second-order ODEs with terms containing differentials of the input function. In particular, Eqs. (3.5), (3.9), (3.12), (3.28), (3.33), (3.36), (3.40), and (3.42) exhibit this fact. These systems are called second-order numerator-dynamics systems in their linearized, transfer function adaptations, because their transfer functions contain a variable term in the numerator. These systems contain singular terms of differentials of the input function even for the step perturbation, and, thus, exhibit initial discontinuities in initial values and/or slopes of the step and impulse responses. To explore the range of behavior of these systems in general, their comprehensive treatment is provided in the next section (Ahuja, 2010). Their general profiles are derived and their characteristic parameters are identified. The solution profiles of these systems depend upon the value of one such parameter relative to that of the others on the real axis. These conditions unfold different types of profiles exhibiting initial discontinuity, maximum, minimum, inflection, input multiplicity, etc., when applied to the models presented above. Negative real part poles are considered, deviation variable are used and the magnitudes of the inputs are taken as positive throughout.

## 3.9 Second-order Numerator-dynamics Transfer Functions

The second-order numerator-dynamics systems represented by Eq. (2.2) exhibit an assortment of behavior. For such systems, the same three types of step and impulse responses viz. over-damped, under-damped and critically-damped as encountered in the standard second order systems are exhibited. However, there are some differences, which can be observed from response profiles shown in the figures in the following sections. There are discontinuities in initial values and/or initial slopes, and the over-damped case exhibits maximum and minimum in step and impulse responses respectively, which are not there in the standard second-order systems, i.e., not containing the derivative of the input terms. In general, the responses are faster than that of standard counterparts because the relative order is one. Relative order: (order of denominator – order of numerator) of the transfer function. The speed of the response is not given only by the parameters $\tau$ (time constant) and $\zeta$ (damping coefficient), but also by the relative magnitudes of the constants in the numerator of their transfer functions. Eq. (2.2) is repeated below:

$$A\frac{d^2Y}{dt^2} + B\frac{dY}{dt} + CY = D\frac{dX}{dt} + EX \qquad (2.2)$$

### 3.9.1 Over-damped response

The over-damped step response of these systems, unlike the standard second-order systems, is found to exhibit a range of behavior: (a) a response similar to first-order systems, (b) a curve containing a maximum with a point of inflection, and (c) a curve containing a point of inflection at origin as a limiting case (this limiting case will be shown to be valid for the gravity-flow tank system). They are shown in Figs. 3.3(a) through 3.3(d) below.

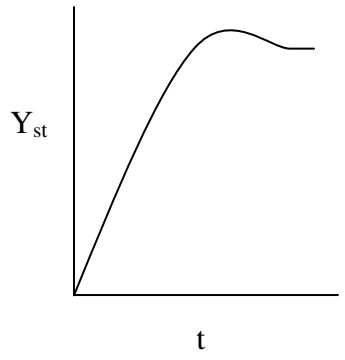


**Fig. 3.3(a)**

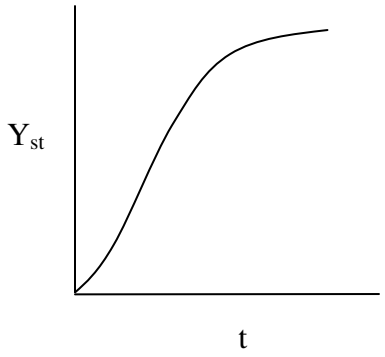


**Fig. 3.3(b)**

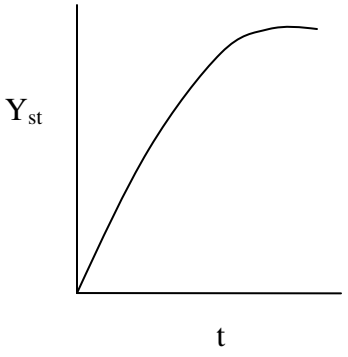


**Fig. 3.3(c)**

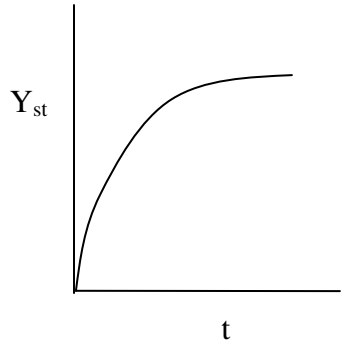


**Fig. 3.3(d)**

**Fig. 3.3** Step responses of non-oscillatory numerator-dynamics systems, (a) for Cases (A) and (D); (b) for Cases (B.1) and (E); (c) for Case (B.2); (d) for Cases (B.3) and (F) discussed later in this section and represented on the real axis

Note that the initial slope is not zero for any of these cases, unlike the standard second-order systems. The impulse response is found to exhibit even more number of cases, viz. (a) one like a first-order system, (b) a curve containing a point of inflection at zero time, (c) a curve containing a maximum near zero time with a point of inflection, and finally (d) one like a standard second-order impulse as a limiting case. These curves are shown in the Figs. 3.4(a) through 3.4(e). The conditions of the respective profiles can be found. Since the roots of the characteristic equation for the over-damped case are real and unequal, Eq. (2.2) can be written in a different form:

$$\frac{Y(s)}{X(s)} = K\frac{s+l}{(s+m)(s+n)} \tag{3.43}$$

where constants $K$, $l$, $m$, $n \geq 0$ and $l \neq m, n$

The solution for unit step input, obtained through inverse Laplace transforms, is:

$$Y_{st}(t) = K\left(\frac{l}{mn}\right)\left[1+\frac{n}{l}\left(\frac{m-l}{n-m}\right)e^{-mt} - \frac{m}{l}\left(\frac{n-l}{n-m}\right)e^{-nt}\right] \quad \text{For } m \neq n \tag{3.44}$$

One of the two roots of the quadratic characteristic equation is smaller (say $m$) than the other (say $n$) for the over-damped case. The derivative of Eq. (3.44) is the following equation, which also represents the unit impulse response:

$$Y_{st}'(t) = Y_{imp}(t) = K\left[\left(\frac{l-m}{n-m}\right)e^{-mt} + \left(\frac{n-l}{n-m}\right)e^{-nt}\right] \quad \text{For } m \neq n \tag{3.45}$$

***Maximum for the step response and zero for the impulse response*** Differentiating the step response and equating it to zero finds the condition for the step response curve containing a maximum. Equating Eq. (3.45) to zero gives:

$$t_{\max} = \frac{1}{n-m}\ln\frac{n-l}{m-l} \quad \text{For } m \neq n \tag{3.46}$$

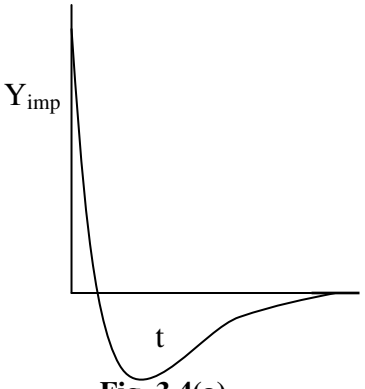


**Fig. 3.4(a)**

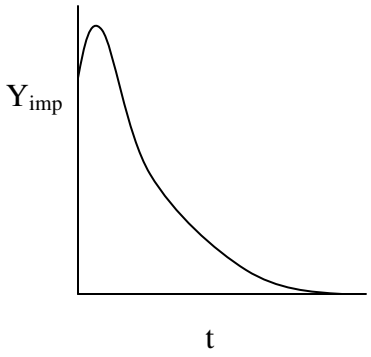


**Fig. 3.4(b)**

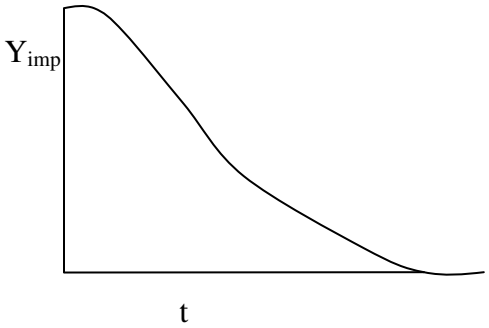


**Fig. 3.4(c)**

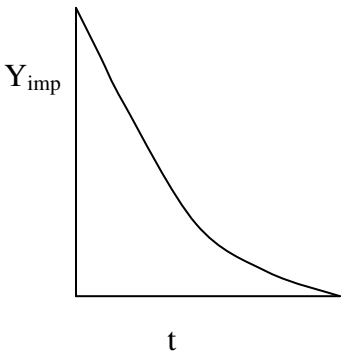


**Fig. 3.4(d)**

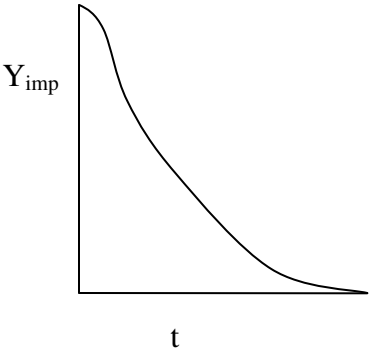


**Fig. 3.4(e)**

**Fig. 3.4** Impulse responses of non-oscillatory numerator-dynamics systems, (a) for Cases (A) and (D); (b) for Cases (B.1) and (E); (c) for Case (B.2); (d) for Cases (B.3.a) and (F); (e) for Case (B.3.b) discussed later in this section and represented on the real axis

For a feasible value of $t_{max}$, the quantity within the logarithm term should be positive. This is possible under two conditions {namely Case (A) and Case (B)}: Case (A) $l$ should be less than both $m$ and $n$; Case (B) $l$ should be more than both $m$ and $n$. The condition (B) gives a negative value of time, whereas (A) gives a positive value of time, which corresponds to Fig. 3.3 (a), note that this curve depicts a point of infection. This time also corresponds to the zero value of the impulse response in Fig. 3.4 (a). The feasibility condition for Eq. (3.46) corresponding to the Case (A) is reiterated mathematically as:

**Case (A):** $l < min\ (m, n)$ (3.47)

***Minimum/maximum for the impulse response and inflection for the step response*** The impulse response corresponding to Case (A) depicts a minimum in Fig. 3.4 (a) at the time when the step response depicts a point of inflection in Fig. 3.3 (a). Differentiating Eq. (3.45) and equating it to zero gives this time. The derivative of Eq. (3.45) is as follows:

$$Y_{st}''(t) = Y_{imp}'(t) = -K\left[\left(\frac{l-m}{n-m}\right)me^{-mt} + \left(\frac{n-l}{n-m}\right)ne^{-nt}\right] \quad \text{For } m \neq n \tag{3.48}$$

Equating it to zero gives:

$$t_m = \frac{1}{n-m}\ln\left[\left(\frac{n-l}{m-l}\right)\frac{n}{m}\right] \quad \text{For } m \neq n \tag{3.49}$$

From this Eq. (3.49), the condition for a positive value of this time for the Case (A) is:

$$l < m + n \tag{3.50}$$

It may be noted that Eq. (3.50) is always true for Case (A) and, hence, gives a minimum for impulse because the further derivative of Eq. (3.48) results in a negative value at $t_m$.

And from Eq. (3.49) again, the following condition for a positive value of this time under **Case (B)** is obtained:

$$l \geq m + n \tag{3.51}$$

***Subdivisions of Case (B)*** The feasibility condition for Case (B) is reiterated as:

**Case (B):** $l > max\,(m, n)$ (3.52)

Combining Eqs. (3.51) and (3.52), lead to three subdivisions of Case (B). These are discussed below as (B.1), (B.2) and (B.3):

**Sub-case (B.1):** $l > m+ n$. This corresponds to Figs. 3.3 (b) for the step response and 3.4 (b) for the impulse response. They show an inflection for the step response and a maximum for the impulse response, respectively. Note that for the impulse input, the same Eq. (3.49) corresponds to the time of minimum for Case (A) but to the time of maximum for Case (B).

**Sub-case (B.2):** $l = m+ n$. This corresponds to Figs. 3.3 (c) for the step response and 3.4 (c) for the impulse response. Note that in this case the point of inflection in the step response and the maximum in the impulse response are occurring at the zero value of time.

**Sub-case (B.3):** $l < m+ n$. This corresponds to Figs. 3.3 (d) and 3.3 (c) for the step response, and 3.4 (d) and 3.4 (e) for the impulse response. There is no maximum/minimum for step or impulse responses.

***Inflection for the impulse response*** The above Sub-case (B.3) is further bifurcated into following two cases on the basis of inflection for impulse:

**Case (B.3.a):** $l < (n^2 + m^2 + nm) / (n + m)$ (3.53)

**Case (B.3.b):** $l > (n^2 + m^2 + nm) / (n + m)$ (3.54)

The former of the two correspond to no point of inflection for the impulse response as shown in Fig. 3.4 (d) but the latter yields to a point of inflection for the impulse response as shown in Fig. 3.4 (e). Other cases and sub-cases do not yield this bifurcation because of the following reasons (inflection is either present or absent throughout their domain).

For Case (A), the condition for impulse showing an inflection is reversed, i.e., Eq. (3.53) is valid for inflection and not Eq. (3.54). But Eq. (3.53) always holds for Case (A). This is shown below.

Since $n > m$, the condition given by Eq. (3.47) reduces to $l < m$. Combining it with Eq. (3.53) gives the following condition:

$$m < (n^2 + m^2 + nm) / (n + m) \tag{3.55}$$

This yields $n^2 > 0$, which is always true. Thus, Case (A) always depicts an inflection in the impulse response as depicted in Fig. 3.4 (d). The time of inflection is given by:

$$t_i = \frac{1}{n-m} \ln \left[ \left( \frac{n-l}{m-l} \right) \frac{n^2}{m^2} \right] \text{ For } m \neq n \tag{3.56}$$

Likewise, for Case (B) the governing equation becomes $l > n$. For Case (B.1), combining this with Eqs. (3.51) and (3.54) gives:

$$m + n > (n^2 + m^2 + nm) / (n + m) \tag{3.57}$$

This yields $2 > 1$, that again is always true and, thus, Case (B.1) always shows inflection throughout its domain, the time of inflection is given by the same Eq. (3.56). Whereas, for the Case (B.2), the time for inflection in the impulse response is given by placing:

$$l = n + m$$

in Eq. (3.56), one gets:

$$t_i = \frac{1}{n-m} \ln \frac{n}{m} \quad \text{For } m \neq n \tag{3.58}$$

Eq. (3.58) is always feasible because $n > m$. Thus, the Case (B.2) also, always shows inflection for the impulse response, throughout its domain.

The only condition that still remains uncovered is the Case (C), it is given below:

**Case (C):** $m < l < n$, for which there is neither a maximum/minimum, nor any inflections. Its response curves are shown in Figs. 3.3 (d) and 3.4 (d).

The above inequalities are comprehensively represented on the real axis:

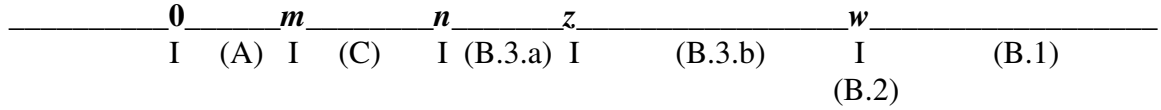


where $w = m + n$ $z = (n^2 + m^2 + nm) / (n + m)$

To summarize, $l$ can lie in any of the regions shown: Region (A) corresponds to maximum and inflection for the step response and minimum for the impulse response, (B.1) to inflection for the step response and maximum for the impulse response. (B.2) is the limiting Case of (B.1) in which the inflection and the maximum are at zero time, (B.3) and (C) depict no extremes. The response curves corresponding to all these regions are shown in this order in Figs. 3.3 (a), 3.3 (b), 3.3 (c) and 3.3 (d) respectively for the step response, and 3.4 (a), 3.4 (b), 3.4 (c), and 3.4 (d) respectively for the impulse response.

Finally, initial slopes for the impulse response curves of all the cases are given by:

$$Y_{imp}'(0) = K (l - n - m) \tag{3.59}$$

**3.9.2 Critically damped response** This case can be worked out similarly. Let $m = n$ in Eq. (3.43) for this case yields the following Regions D, E, and F on the real axis.

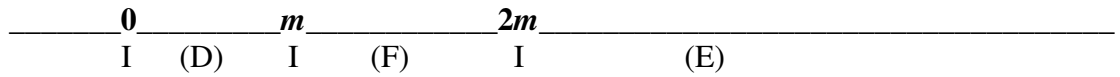


**Case (D):** This depicts maximum for the step response and minimum for the impulse response in Figs. 3.3 (a) and 3.4 (a), respectively.

**Case (E):** This gives a maximum for the impulse response similar to Fig. 3.4 (b).

**Case (F):** This case can again be bifurcated at the mid-point on the basis of inflection for impulse: The left half shows no maximum/ minimum or inflection but the right half depicts inflection for impulse at the time given by:

$$t_i = (3m - 2l) / (m - l) \tag{3.60}$$

**3.9.3 Under-damped response** For oscillatory response, better use $\zeta$ and $\tau$ of second-order systems and the transfer function becomes:

$$\frac{Y(s)}{X(s)} = P\frac{s+l}{\tau^2 s^2 + 2\zeta\tau s + 1} \tag{3.61}$$

Unit impulse response for this case is:

$$Y_{st}'(t) = Y_{imp}(t) = \frac{P}{\tau^2} e^{-\zeta t/\tau}\left[\cos\left(\frac{t}{\tau}\sqrt{1-\zeta^2}\right) + \frac{\tau l - \zeta}{\sqrt{1-\zeta^2}}\sin\left(\frac{t}{\tau}\sqrt{1-\zeta^2}\right)\right] \tag{3.62}$$

The initial slope of the impulse response is given by:

$$Y_{imp}'(0) = Y_{st}''(0) = P(\tau l - \zeta)/\tau^3 - P/\zeta\tau \tag{3.63}$$

The impulse response curves are similar to those for the standard second-order systems, except that they are faster and with initial value non-zero. Depending upon whether the initial slope is positive, negative or zero, they are of different shapes. These are shown in Figs. 3.5 (a), 3.5 (b) and 3.5 (c), respectively. Step response is also similar to its standard counterpart, except that its initial slope is a non-zero positive, is faster, has more overshoot and higher final value.

### 3.9.4 Applications of the results

It is further illustrated how the conditions of Sections 3.9 unfold for different numerator-dynamics cases.

***Input multiplicity*** If $l = 0$ and gain is positive, the step response undergoes a maximum and eventually returns to the same initial value irrespective of the magnitude of the input as shown in Fig. 3.6. The impulse response undergoes a minimum and goes below zero as shown in Fig. 3.4 (a) irrespective of the magnitude of the input. Velocity transfer function of a damped vibrator under perturbation in applied force (Fig. 2.3 and Section 2.2.3.), velocity of the liquid manometer column under applied pressure or current in the RLC circuit under applied electro motive force (voltage) exhibit such a behavior.

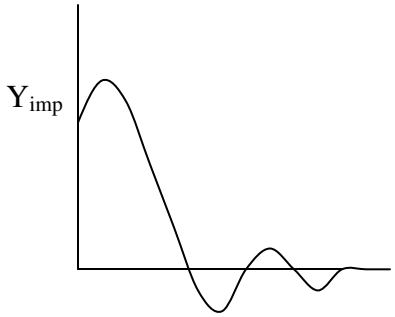


**Fig. 3.5(a)**

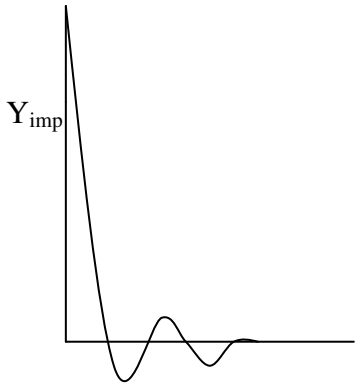


**Fig. 3.5(b)**

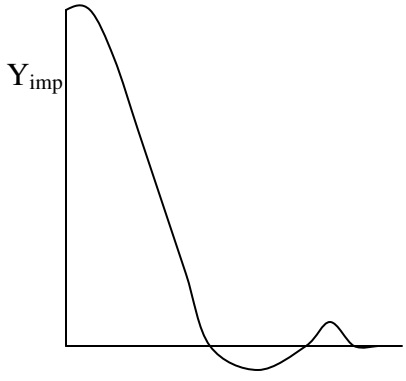


**Fig. 3.5(c)**

**Fig. 3.5** Impulse responses for oscillatory numerator-dynamics systems with (a) positive, (b) negative, and (c) zero initial slopes discussed in Section 3.9.3

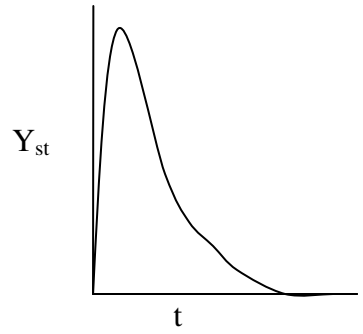


**Fig. 3.6** Step response of non-oscillatory numerator-dynamics system exhibiting input multiplicity discussed in Section 3.9.4

***Pole-zero cancellation*** In case, $l$ = ($m$ or $n$) in the system transfer function Eq. 3.43, the system reduces to first order as shown in the stirred tank heater example in Sections 3.7.1 and non-isothermal CSTR example in Eq. (3.77) below. These systems, thus, do not show numerator-dynamics form.

***Two interacting-tanks system*** For Region (A) on the real axis for this system, i.e., the condition given by Eq. (3.36) requires the following two conditions to be met simultaneously:

$$Al < B/2 \text{ and } Al > B - C/l \tag{3.64}$$

And for Region (B) on the real axis (condition given by Eq. (3.51)):

$$Al > B/2 \text{ and } Al > B - C/l \tag{3.65}$$

$$Al > B - C/l, \text{ gives } \tau_2 R_2 < 0 \tag{3.66}$$

which is not possible. Hence, Regions (A) and (B) are non-feasible regions. The only feasible Region is (C), the curves for which neither show any maximum/minimum nor any point of inflection.

***Coupled CSTRs*** Consider coupled constant flow isothermal CSTRs having a recirculation loop given in Figs. 3.7 (a) and 3.7 (b). They are carrying out an incompressible liquid phase, first-order reaction $A \rightarrow R$.

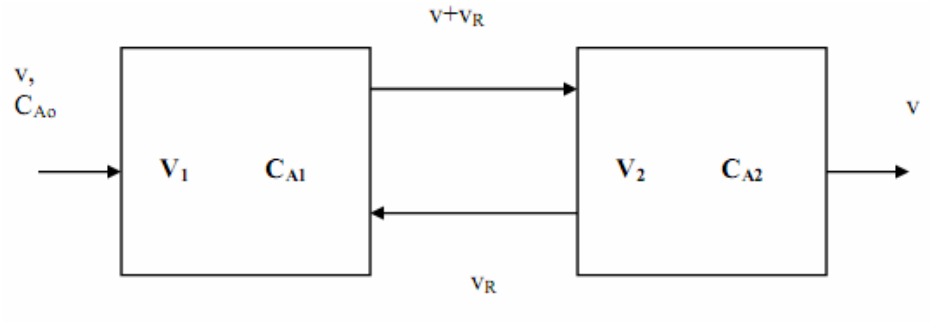


**Fig. 3.7(a)**

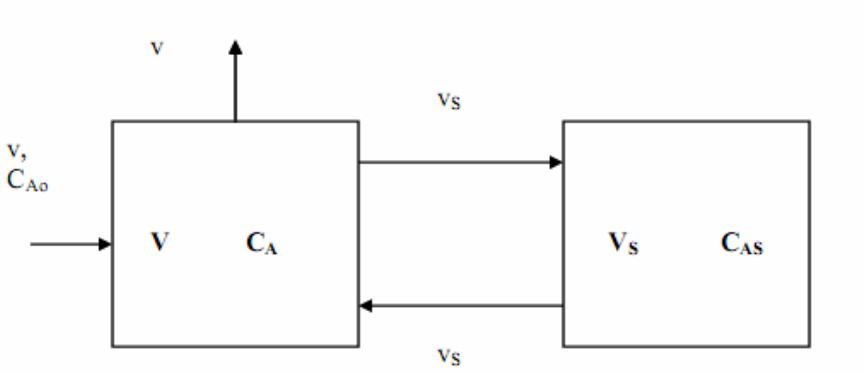


**Fig. 3.7(b)**

**Fig. 3.7** Schematic of coupled CSTRs containing recirculation loops

For the first of the two coupled tanks, the numerator-dynamics transfer functions $C_A/ C_{Ao}$, are found out corresponding to Figs. 3.7 (a) and 3.7 (b). The transfer functions are found by applying unsteady material balance of $A$. On comparison of the transfer function of Fig. 3.7 (a) with the equation of type (3.36), one gets:

$$l = (kV_s + v_s) / V_s,\ A = VV_s,\ B = k\,V_sV + v_sV + vV_s + kVV_s + v_sV_s,$$
$$C = kvV_s + k^2VV_s + kv_sV_s + vv_s + kVv_s, \tag{3.67}$$

Cases (A) and (B) on the real axis are not feasible because for $Al > B - C/l$:

$$v^2{}_sV_s < 0 \tag{3.68}$$

For the second Fig. 3.7 (b); finding $l$, $A$, $B$, and $C$ and applying, $Al > B - C/l$:

$$v_R / v + v_R kV_2 / v\left(v + v_R\right) < 0 \tag{3.69}$$

which is again not possible. So, such systems fall only in Region (C) on the real axis. Thus, they are never under-damped. Also, note that the value of the damping factor $\zeta \geq 0$. It can also be checked that $l < (m + n)$ (the equality never holds), and the initial slope of their impulse response obtained from Eq. (3.59) is non-zero and negative due to this. These findings apply across all the interacting systems discussed above.

All interacting and coupled systems composed of first-order systems, in general, come under Case (C) on the real axis.

***Gravity-flow tank*** From Eq. (3.28) for this system, the sum $(m + n)$ is equal to $B/A$, and this gives:

$$l = m + n \tag{3.70}$$

Eq. (3.70) implies that the system coincides with point *w* or (B.2) on the real axis, and Eq. (3.51) and (3.57) are valid. The response thus shows a point of inflection at the origin for the step input and corresponds to that shown in Fig. 3.3 (c). For the impulse input it shows a maximum at zero time and an inflection near zero time and shown in Fig. 3.4 (c).

***Jacketed non-isothermal CSTR***

From Eqs. (3.5) and (3.6) for this system, $K$ and $l$ are always positive. But $d$ and $e$ can be negative or positive. To detect that, following two cases are taken: (1) If the reaction is exothermic, $\Delta H_R$ is negative and, (2) if the reaction is endothermic, $\Delta H_R$ is positive. Note that the first case can give unstable poles. Also, recall that only stable cases are being dealt with for which $(l + d)$ and $(ld - e)$ are positive. The exothermic case is treated first.

***Exothermic reaction*** This system can exhibit maximum for impulse too. For this case, $e$ is negative but $d$ can either be positive, negative or zero. The over-damped domain is first considered.

For Case (A) to be valid $l < m$. Applying this condition and using the roots of the quadratic gives, $e < 0$ and $l < d$. (3.71)

For Case (B) to be valid $l > n$. Applying this condition and using the roots of the quadratic gives, $l > d$ and e $< 0$. (3.72)

For Sub-case (B.1) to be valid, $l > (m + n)$, that gives, $d < 0$. (3.73)

For Sub-case (B.3) to be valid, $l < (m + n)$, that gives, $d > 0$. (3.74)

For Sub-case (B.2), $d = 0$. (3.75)

So, it is found that all the above cases are feasible and even the conditions of stability do not make them non-feasible.

The Case (C) is, however, not feasible.

The results are analogous for critically-damped case too. This system is over-, critical- and under-damped depending on the following conditions, respectively.

$$(l-d)^2 + 4e > 0, \qquad (l-d)^2 + 4e = 0, \qquad (l-d)^2 + 4e < 0 \tag{3.76}$$

Thus, if $l = d$ this system is oscillatory.

***Endothermic reaction*** For this case *K, l, d, e* are all positive and non-zero. Only feasible region in this Case is (C). Also, this case can *only* be over-damped. This is, therefore, one of the kinds of the first-order interacting and coupled systems in series.

***Reaction enthalpy zero*** **($\Delta H_R = 0$)**

For this case of no heat effect, the system Eqs. (3.5) and (3.6) reduce to first-order as shown:

since, $e = 0$

$$\frac{\bar{T}}{\bar{T}_j} = K\frac{s+l}{s^2+(l+d)s+ld-0} = K\frac{s+l}{(s+l)(s+d)} = \frac{K}{s+d} \tag{3.77}$$

Another numerator-dynamics case, i.e., a stirred tank heater too, invariably turned out to be standard first-order in Section 3.7.1.

### 3.9.5 Discussion

Figs. 3.3 through 3.5 reveal the variation in the nature and speed of the response profiles as $l$ changes on the real axis. The *impulse* response of the over-damped case of second-order numerator-dynamics system derived in Section 3.9 is given by Eq. (3.45) with parameters $K$, $l$, $m$, $n \geq 0$. Observe the effect of parameter $l$ on the response from Eq. (3.45). Initial discontinuity, initial value and final value of the response don't depend on $l$. Eq. (3.45) contains two terms involving $l$, namely, $le^{-mt}/(n-m)$, and $-le^{-nt}/(n-m)$. If $l$ is decreased (keeping all other parameters constant), the first term increases but the second one decreases, however, since $m < n$ the first term dominates and there is a net decrease in the magnitude of impulse response. Thus, the response for a lower value of $l$ always lies below the one with a higher value of $l$. Hence, the decrease of the response is faster on decreasing $l$. Looking at the curves of Figs. 3.3(b), 3.3(c), 3.3(e), 3.3(d) and finally 3.3(a) serially in this order, it is seen that as $l$ decreases, the response decreases faster. In Fig. (2.a), it even goes below the initial value and exhibits minimum.

However, as $l \to \infty$, the impulse response of the numerator-dynamics system approaches the impulse response of a standard second-order system. Thus, the impulse response increases initially, rather than decreasing, and has positive initial slope and has no initial discontinuity, i.e., the one corresponding to a standard second-order system. On comparing the transfer function of the second-order numerator-dynamics with the standard second-order transfer function, the limiting case is obtained:

$$Standard\ \ second-order\ \ response = \lim_{l \to \infty} \left\{ \begin{matrix} Second-order \\ numerator-dynamics\ \ response\ /\ l \end{matrix} \right\}$$

The above facts are equally true of critically-damped and oscillatory responses. For the *step* response of Eq. 3.44, the same pattern is observed, the speed of the *rise* in the response increases with decrease in $l$, and is maximum at $l = 0$ that exhibits input multiplicity (Fig. 3.6). However, as $l \to \infty$, the system approaches a standard second-order one exhibiting no initial discontinuity.

So, it is seen that the lumped-parameter models presented in this chapter can be represented by second-order ODE with terms containing differential of the input function. These systems are called second-order systems with numerator-dynamics in their linear, transfer form adaptation. These systems present themselves with an initial discontinuous behavior for initially discontinuous inputs like step and impulse, unlike the standard second-order system. Numerator-dynamic behavior is different and has more classified branches than its standard counterpart. Different behaviors and their characteristic conditions are obtained in various Sub-sections of Section 3.9, for negative real part poles, and represented concisely on the real axis in the same section.

Second-order numerator-dynamics systems of relative order one, such as, gravity-flow tank, isothermal/non-isothermal CSTR, interacting tanks system, RLC circuit, single-component condenser, damped vibrator, etc. show an assortment of behaviors viz. maximum, minimum, inflection, input multiplicity and oscillations depending upon the characteristic system parameters and the conditions identified, these behaviors shall also be encountered in the corresponding nonlinear cases in next chapters, particularly in Chapter 5, where their numerical solutions will be carried out. It can also be observed that the magnitude, speed and nature of these response profiles changes as a result of the effect of initial discontinuities. This happens because the parameter $l$ undergoes changes with initial discontinuities and the systems change their positions on the real axis and switch over the regions on the real axis, or could result in the appearance of numerator-dynamics behavior for standard systems (see Eq. (3.22), Section 3.3.1 above).

ODE models representing lumped-parameter systems were considered in this chapter and the treatment in the following chapters applies to them. Distributed-parameter systems in two dimensions, however, lead to partial differential equations. Nevertheless, ODEs are also generally obtained by the reduction of partial differential equations through separation of variables to give an accurate analytical treatment (e.g., Kumar *et al.*, 2000; 2008).

# 4 Effects of Initial Discontinuities

Initial conditions of the response to the inputs with jump discontinuities are, generally, not obvious. Because of the discontinuity, the initial conditions of the response have to be selected circumspectly. An incorrect choice of the initialization route leads to a solution inconsistent with the physical realities of the system. To address and reveal these inconsistencies, a methodology based on two alternative routes of initialization is presented in this chapter. This methodology is implemented in the Laplace domain for the linear systems in Section 4.2 (Ahuja, 2010). Following this, the methodology is extended in the time domain, and is implemented to the nonlinear systems in Section 4.3 to study the qualitative effects of discontinuities on the solution profiles. These effects are validated in Sections 4.4 through 4.8 (Ahuja, 2011). However, a comprehensive, methodological framework for the analysis and direct initialization to quantitatively describe the response for the nonlinear systems to the singular inputs shall be worked out in the next chapter.

## 4.1 Systems with Differentials of the Input Function

Models considered in the last two chapters were the systems represented by nonlinear second-order ordinary differential equations with terms containing differentials of the input function (see, e.g., Eqs. 3.9, 3.33, 3.42, etc.). Solution profiles of these systems exhibited initial jump discontinuities under the aforesaid inputs, which are not exhibited by the systems not containing the differentials of the input term (standard second-order systems). Besides, as mentioned at the outset of Chapter 2, these models include singularities contained in the differentials of the input terms of the equation even for the step perturbation and, thus, exhibit discontinuities in the initial slopes of the response profiles. Their solution profiles were discussed at length in Section 3.9 of the last chapter and can be observed in Fig. 4.1 below. However, the methodology presented here is general and is applicable to other lumped-parameter models including the standard systems.

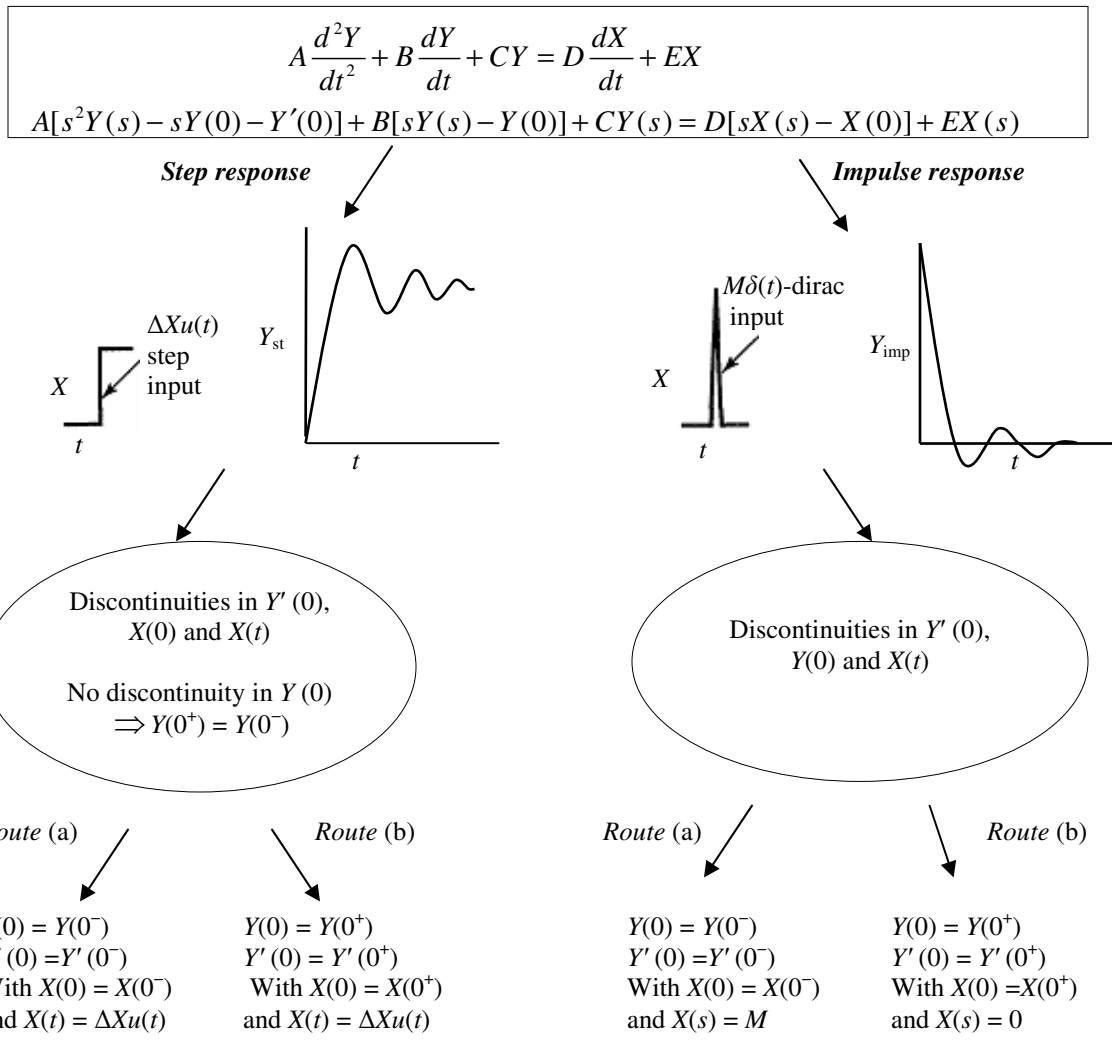


**Fig. 4.1** Schematic showing methodology for analysis and initialization of systems containing differential terms of step and impulse inputs, where $X$, $Y$ are deviation variables for input and output; $\Delta X$, $M$ are magnitudes of step and impulse inputs, respectively; $A$ through $E$ are constants

### 4.1.1 Methodology of the discontinuity analysis

A schematic diagram of the methodology for the analysis of initial discontinuities for the linear systems is outlined in Fig. 4.1 for the step and impulse inputs. Discontinuities are analyzed for the linear and the nonlinear systems by checking whether or not the input discontinuity takes into account the initial discontinuities in the output variables. As seen from Fig. 4.1, there are essentially two alternative initialization routes for addressing the

impulse function. The first is to include impulse in the cause (i.e., the input function), i.e., Route (a) with the all the initial conditions of the input and output evaluated at $t \rightarrow 0^-$; and the second, to include impulse in the effect (The effect of the impulse is included in the output functions, and the Laplace transform of the input impulse function is zero according to Eq. (2.15)), i.e., Route (b) with the input and all the initial conditions evaluated at $t \rightarrow 0^+$. For the step response also, the initialization Route (a) implies taking all the initial conditions of the inputs, outputs, and their derivatives at $t \rightarrow 0^-$, and the initialization Route (b) implies taking all the initial conditions of the inputs, outputs, and their derivatives at $t \rightarrow 0^+$ (Note that by doing so for the step input for $X$, the $(dX/dt)$ term becomes zero and, thus, all the singularities are included in the effect). Initial conditions at $t \rightarrow 0^+$ corresponding to Route (b) are based on the application of physical balances to the system conditions at the time of singularity. For the linear systems, Route (a) corresponds to the $\mathcal{L}_-$ approach, whereas Route (b) corresponds to the $\mathcal{L}_+$ approach. The Laplace domain dynamics will be treated in detail separately in Chapter 6 by the application of the framework of Chapter 5.

CSTR and gravity-flow tank under feed rate perturbation, non-isothermal CSTR under jacket temperature perturbation, etc., are some nonlinear systems with derivatives of the input function, the response profiles for which would be affected by the discontinuities. For such systems, an initial discontinuity in the response identified on applying physical balances (mass/momentum etc.) through Route (b) won't get accounted for in the initial discontinuity of the stimulus through Route (a). Hence, Route (b) won't reduce to Route (a), and the value of this discontinuity in the response would be required for the correct solution. Simply knowing the magnitude of the input would not be sufficient to obtain the correct solution to these systems. So, these systems are said to be affected by discontinuities throughout the text as they yield inconsistent initial conditions.

However, some other systems such as the U-tube manometer, first unit of the two interacting units-in-series, jacketed stirred tank heater under feed rate perturbation, etc. also give rise to ODE with the derivative of the input. But discontinuities of such systems get accounted for as Route (b) would reduce to Route (a). A few nonlinear systems may undergo order reduction to standard linear systems (i.e., containing no derivative term of the input) upon linearization due to pole zero cancellation, and may turn into being

unaffected by discontinuities (e.g., Eqs. 3.40 and 3.77). However, some standard systems exhibit numerator-dynamics form due to the effect of initial discontinuities (Eq. 3.12). These kinds of special cases shall be treated in Section 5.12.1 of Chapter 5. The present methodology investigates the existence and validation of the qualitative effects of initial discontinuities. Validation will be done by the comparison of experimental and simulated data of non-linear models of flow-level tanks (Ahuja, 2011).

## 4.2 Application to the Linear Time-invariant Systems

The methodology introduced above is aimed at a simple and effective treatment of linear systems containing derivatives of the input terms, especially, the ones that are inherently of this kind (i.e., of Sections 2.1, 2.2, and 3.8). Now, the linear U-tube manometer, isothermal CSTR, and the linearized flow-level tank models will be used to illustrate the procedure. It is intended to extend the procedure later to the maiden nonlinear systems and validate it by the corresponding nonlinear flow-level tank models.

### 4.2.1 Example 1

***Impulse input***

Consider the U-tube manometer presented in Section 3.8.1 of the last chapter. The system is at a state at time $t \rightarrow 0^-$. An impulse perturbation of magnitude $M$ (Pa-s) in the applied pressure difference $\Delta P$ is imposed on its two legs. Input function $\Delta P(t)$ and the initial conditions need to be specified in order to solve this equation, viz., the values of $Y$, $U$, and $dU/dt$ at $t \rightarrow 0$. Discontinuities are analyzed using the following Laplace transformed form of the system Eq. (3.42) and by referring to Fig. 4.1.

$$m[s^2U(s) - sU(0) - \dot{U}(0)] + a[sU(s) - U(0)] + bU(s) = sA\Delta\overline{P}(s) - A\Delta\overline{P}(0) \qquad (4.1)$$

Applying physical balance, i.e., momentum balance in this case for Route (b); as an impulse is applied, the effect of the impulse is to give initial velocity to the liquid column. Consequently, there is discontinuity in $U(0)$. But no such discontinuity exists in $Y(0)$ due to inertia of the column and the resistance offered, so $Y(0^+) = 0$ . The value of

$U(0^+)$ is obtained by noting that the magnitude of the applied impulse force $AM$ equals the change in the initial momentum, thus the initial discontinuity in $U(0)$ is given by:

$$mU(0^+) = AM \tag{4.2}$$

As the velocity increases suddenly, its derivative at the origin would contain a singularity. To relate $U(0^+)$ and $\dot{U}(0^+)$, momentum balance Eq. (3.41) is used at $t \to 0^+$:

$$m\dot{U}(0^+) = -aU(0^+) - bY(0^+) + A\Delta\overline{P}(0^+) = -aU(0^+) - 0 + A\Delta\overline{P}(0^+) \tag{4.3}$$

Impulse input, thus, causes an initial discontinuity in $U(t)$ and, hence, $\dot{U}(t)$. The following analysis shows that these discontinuities are accounted for in the magnitude of the impulse input. The aforesaid two Routes (a) and (b) are applied to analyze Eq. (4.1):

- Route (a): take initial values $U(0) = U(0^-) = 0$ and $\dot{U}(0) = \dot{U}(0^-) = 0$, with $\Delta\overline{P}(0) = \Delta\overline{P}(0^-) = 0$, and $\Delta\overline{P}(s) = M$
- Route (b): take initial values as $U(0) = U(0^+)$ and $\dot{U}(0) = \dot{U}(0^+)$ (i.e., Eqs. (4.2) & (4.3)), with $\Delta\overline{P}(0) = \Delta\overline{P}(0^+)$ and $\Delta\overline{P}(t) = M\delta(t - t_o)$, $t_o = 0^+$, $\Delta\overline{P}(s) = 0$

Now, if the given impulse perturbation is to account for all the initial discontinuities, Route (b) should reduce to Route (a). For Route (b), the terms on the left of Eq. (4.1) are evaluated in the following two equations:

$-smU(0^+) = -sAM$ (From Eq. (4.2))

$-m\dot{U}(0^+) - aU(0^+) = +aU(0^+) - A\Delta\overline{P}(0^+) - aU(0^+) = -A\Delta\overline{P}(0^+)$ (Using Eq. (4.3))

Placing these values in Eq. (4.1) and following Route (b), it is seen that Eq. (4.1) simplifies to one corresponding to Route (a). Thus, the initial discontinuities in $U(t)$ and $\dot{U}(t)$ are accounted for in the magnitude of the impulse input.

***Step input***

Analyzing the initial discontinuities for a step input in the applied pressure, again by applying momentum balance (for Route (b)) reveals that $U(0^+) = 0$. There is no discontinuity in the initial velocity due to the inertia of the liquid column. Discontinuities are there in $\Delta P(0)$ and $\dot{U}(0)$, but the force applied is equal to mass times the acceleration:

$$m\dot{U}(0^+) = A\Delta\overline{P}(0^+)$$

So, employing Route (b) of Fig. 4.1 for the step response case implies that for Eq. (4.1), the initial discontinuities in $\Delta P$ and $U$ exactly cancel each other. The same happens for Route (a) by taking all the initial conditions at $t \rightarrow 0^-$, as all the initial conditions are zero. Hence, Route (b) reduces to Route (a), and both the routes are consistent and would yield correct solution profiles.

It is, thus, observed that the initial discontinuities of the output functions are accounted for in the discontinuous input functions. Thus, the transfer function approach is valid, and the transfer function form can be written for the U-tube manometer system for the step as well as impulse inputs. The transfer function approach assumes that the initial conditions of all the input and the output functions are zero.

### 4.2.2 Example 2

Consider the linearized model of gravity-flow tank presented in Section 3.5.1 of the last chapter. Input function $Q(t)$ and two initial conditions need to be specified in order to solve this equation, viz. $H$ and $dH/dt$ at $t \rightarrow 0$. Discontinuities are analyzed using the Laplace transformed system Eq. (3.27) and Fig. 4.1.

The system is at a state at time $t \rightarrow 0^-$. Volumetric feed flow rate $q$ is perturbed impulsively at $t \rightarrow 0^+$. The ideal *impulse* input can be realized by plunging a measured amount of liquid into the tank, all in one go (with no change in the inflow rate $q$), with the magnitude of disturbance $M$ ($m^3$) equal to the volume of liquid added.

Material balance applied at this instant of perturbation for Route (b) reveals that the impulse in the volumetric feed rate equivalently results in the initial increase in the liquid holdup in tank. Hence, there are two values of level at *zero* time $t$, at $t \rightarrow 0^-$ and at

$t \rightarrow 0^+$. This leads to initial discontinuity in level $h(0)$ and, hence, in the efflux velocity $u(0)$ for discontinuous impulse disturbance $q(t)$. The initial change in level $h(0)$ equals magnitude of the impulse (i.e., volume of liquid added), divided by the area of tank:

$$H(0^+) = M \,/\, A_T \tag{4.4}$$

Moving further with the physical principles, direct dependence of the outflow rate on the head is utilized. With the sudden change in level, simultaneously there is a resultant sudden increase in the efflux velocity in the pipe. Also, since there is an initial discontinuity in the level as the level increased suddenly, its derivative at the origin, $H'(0^+)$, would contain a singularity, i.e., an impulse. The increase in the efflux velocity is related to $H'(0^+)$ using Eq. (3.25) at $t \rightarrow 0^+$:

$$H'(0^+) = \frac{Q(0^+)}{A_T} - \frac{A_p}{A_T} U(0^+) \tag{4.5}$$

Impulse input, thus, causes an initial discontinuity in $H(t)$ and, hence, $U(t)$ (and $H'(t)$). The following analysis shows that the discontinuity in $H(0)$ is accounted for in the magnitude of the impulse input, but the same is not true for $H'(0)$. In this system, the aforesaid two routes are applied to analyze the Laplace transformed Eq. (3.27):

- Route (a): take initial values $H(0) = H(0^-) = 0$ and $H'(0) = H'(0^-) = 0$, with $Q(0) = Q(0^-) = 0$ and $Q = M\delta(t)$ or $Q(s) = M$
- Route (b): take initial values as $H(0) = H(0^+) = M/A_T$ and $H'(0) = H'(0^+)$ (i.e., Eqs. (4.4) & (4.5)), with $Q(0) = Q(0^+)$ and $Q(s) = 0$

Now, if the introduced impulse perturbation was to account for all the initial discontinuities, Route (b) would reduce to Route (a) for Eq. (3.27). This is checked by the comparison of the two routes in the following equations, where the left of the equations/in-equations corresponds to Route (b), and their right corresponds to Route (a):

$sH(0^+) = KsQ(s)$ (Because $A_T H(0^+) = M$ and $K = 1/A_T$)

$\frac{B}{A} H(0^+) = K \frac{B}{A} Q(s)$ (Same reason)

Hence, the discontinuity in $H(0)$ is accounted for in the magnitude of the impulse input. Whereas,

$$H'(0^+) - \frac{Q(0^+)}{A_T} \neq 0 \text{ (From Eq. (4.5))}$$

Hence, the discontinuity in $H'(0)$ could not be accounted for in the magnitude of the impulse input. Route (a), which corresponds to the transfer function approach, assumes: $H'(0^+) = \frac{Q(0^+)}{A_T}$, or $U(0^+) = U(0^-) = 0$, which are not true because of simultaneous increase in the initial level and velocity in the pipe.

Route (b), which is a valid one, yields the following equation for Eq. (3.27):

$$s^2 H(s) + \frac{B}{A} sH(s) + \frac{C}{A} H(s) = K\left[ sM + \frac{B}{A} M - A_P U(0^+) \right] \tag{4.6}$$

It cannot be reduced to Route (a) and the transfer function form since $U(0^+) \neq 0$. Route (a) would yield inaccurate solution profiles. The transfer function approach, thus, does not work for this system under impulse perturbation. Also, the value $H'(0^+)$ or $U(0^+)$ is required for the correct solution of the system Eq. (4.6) for obtaining the impulse response, and paradoxically, it shall not be known unless the profile is obtained.

Now analyzed are the initial discontinuities for the *step* response of gravity-flow tank. Physical principles reveal that the discontinuities are absent in $H(0)$ and $U(0)$ because of inertia the pipe liquid. Hence, $H(0^+) = H(0^-) = 0$ and $U(0^+) = U(0^-) = 0$. Thus, discontinuity $H'(0^+)$ can be calculated from Eq. (3.25) by placing $Q = Q(0^+)$ at $t \rightarrow 0^+$.

$$H'(0^+) = (1/A_T)Q(0^+) = KQ(0^+) \tag{4.7}$$

Now, Eq. (3.27) is considered and is analyzed using Fig. 1. Following Route (b), all the initial values of all the input and output functions are taken at $t \rightarrow 0^+$, these values have been worked out above. Doing this, it is seen that the $H'(0)$ term cancels with the $KQ(0)$ term using Eq. (4.7). So, only the transfer function Eq. (3.28) is left. The same happens for Route (a) by taking all the initial conditions at $t \rightarrow 0^-$, as all the initial conditions are

zero. Hence, the Route (b) reduces to the Route (a), and both the routes are consistent and would yield correct solution profiles.

It is, thus, observed that the initial discontinuities of the output functions are accounted for in the discontinuous input functions. Thus, the transfer function approach is valid, and the transfer function Eq. (3.28) can be written for the gravity-flow tank system for step inputs.

### 4.2.3 Example 3

The first of the two interacting liquid-level tanks in series of Section 3.6 is, now, analyzed. The linearized model of Section 3.6.1 is used for the analysis.

The system is at a state at time $t \rightarrow 0^-$. Volumetric flow rate is perturbed impulsively at $t \rightarrow 0^+$. It can be introduced as in the last section, which leads to discontinuity in $H_1(0)$. The initial value of $H_1$ at $t \rightarrow 0^+$ is, in effect, the same as the magnitude of the impulse, i.e., the volume of liquid added divided by the area:

$$H_1(0^+) = M / A_1 \tag{4.8}$$

Physical principles reveal that discontinuities are there for both $H_1(0)$ and $H_1'(0)$ but are absent in $H_2(0)$, hence, $H_2(0^+) = 0$. The dynamic lag of the first tank prevents a discontinuity in the second tank level. Impulse, however, causes a discontinuity in out-flow rate from the first tank $Q_{21}$. Following analysis shows that the discontinuity of $H_1(0)$ and $H_1'(0)$ are accounted for in the magnitude of the impulse input. In this case, the two alternative routes to solve Eq. (3.34) become:

- Route (a): take initial values as $H_1(0) = H_1(0^-) = 0$, $H_1'(0) = H_1'(0^-) = 0$, with $Q(0) = Q(0^-) = 0$ and $Q = M\delta(t)$ or $Q(s) = M$
- Route (b): take initial values as $H_1(0) = H_1(0^+) = M/A_1$ from Eq. (4.8) and $H_1'(0) = H_1'(0^+) = Q(0^+)/A_1 - H_1(0^+)/A_1 R_1$ (obtained using Eqs. (3.30(a)) and (3.32(a))), with $Q(0) = Q(0^+)$ and $Q(s) = 0$

Route (b) reduces to Route (a) as seen by substituting the following two equations in Eq. (3.34), where the extreme L.H.S. of the two equations correspond to Route (b), and their extreme R.H.S. correspond to Route (a).

$$s\tau_1\tau_2 H_1(0^+) = s\tau_1\tau_2 M \,/\, A_1 = s\tau_2 R_1 Q(s)$$

$$-\tau_1\tau_2 H_1'(0^+) + (\tau_1 + \tau_2 + A_1 R_2) H_1(0^+) + \tau_2 R_1 Q(0^+) = (R_1 + R_2) Q(s)$$

From the above analysis, it is seen that the two routes are the same.

When the *step* response is considered, there is a discontinuity in $Q(0)$ and $H_1'(0)$. No discontinuity exists for $H_1(0)$ and $H_2(0)$. Consequently, $H_1(0)$ and $H_2(0)$ both are zero. To solve Eq. (3.34) through Route (b), take initial value, $H_1'(0) = H_1'(0^+)$. Initial value of $Q$ is $Q(0) = Q(0^+) = A_1 H_1'(0^+)$ from Eq. (3.30(a)). This implies that the initial discontinuities in $Q$ and $H_1$ exactly cancel each other in Eq. (3.34). Thus, Route (b) reduces to Route (a). The system model (3.34) therefore remains unaffected by initial discontinuities both for the step and the impulse perturbations.

### 4.2.4 Example 4

Consider an *impulse* input to the feed stream concentration $C_{Ao}$ to the constant density constant holdup CSTR of Section 3.2. Let $M$ (mol)(s)/(m$^3$) be the magnitude of the impulse perturbation. This perturbation is equivalent to plunging $Mv_o$ (mol) of pure liquid $A$ into the tank suddenly. The analysis could have been carried out in the above manner. However, the analysis of Eqs. (3.7) and (3.8) are, now, done directly without combining the two equations, *a priori*. This procedure would prove to be more convenient for the nonlinear systems that are to be described in the next section.

Application of material balance at the perturbation instant (for Route (b)) for component $A$ reveals that the sudden insertion of $Mv_o$ (mol) of pure liquid $A$ into the tank causes the same initial increase in the number of moles of $A$ in the tank, this increase divided by the holdup volume (constant), gives the value of initial discontinuity in the concentration of $A$ in the tank, $C_A$. This leads to (in terms of deviation variables):

$$\overline{C_A}(0^+) = Mv_o \,/\, V \tag{4.9}$$

The Laplace transformed Eqs. (3.7) and (3.8) respectively are:

$$s\overline{C_R}(s) - \overline{C_R}(0) = -(v_o / V)\overline{C_R}(s) + k\overline{C_A}(s) \tag{4.10}$$

$$s\overline{C_A}(s) - \overline{C_A}(0) = (v_o / V)\overline{C_{Ao}}(s) - (v_o / V + k)\overline{C_A}(s) \tag{4.11}$$

Eq. (4.11) is first analyzed for $C_A$ as it doesn't have $C_R$. It can be seen that the discontinuity in its second term $\overline{C_A}(0)$ through Route (b) (given by Eq. (4.9)), is accounted for in the magnitude of the impulse input in the third term of Eq. (4.11) through Route (a). All other terms are same in the two routes. Thus, Eq. (4.11) is not affected by the discontinuity in $C_A$.

Eq. (4.10) is now analyzed. Moving further with physical principles (Route (b)), as the holdup is constant, concentrations of $R$ and $I$ fall suddenly with the sudden initial rise in the concentration of $A$ in the tank. The following constant density condition can be applied in the deviation form at $t \rightarrow 0^+$ for the impulse input, considering that pure $A$ is put directly into the tank with no change in $C_{Ao}$ and volume $V$, this gives:

$$[\overline{C_R}(0^+)]M_R + [\overline{C_A}(0^+)]M_A + [\overline{C_I}(0^+)]M_I = 0 \tag{4.12}$$

$$\text{or, } \overline{C_R}(0^+) = -[MC_{Ao} / V]M_A / M_R - [\overline{C_I}(0^+)]M_I / M_R \neq 0 \tag{4.13}$$

which yields a non-zero value of the initial discontinuity in the concentration of $R$ in the tank, $C_R$. $M_A$, $M_R$, and $M_I$ are the molecular weights of $A$, $R$, and $I$, respectively. This discontinuity in $\overline{C_R}(0)$, i.e., ($C_R$ ($0^+$) – $C_R$ ($0^-$)), in the second term of Eq. (4.10) through Route (b) is not accounted for in the initial discontinuity of impulse input through Route (a), as there is no impulse input term in Eq. (4.10). If Routes (a) and (b) were to give the same results, $\overline{C_R}(0^+)$ would have been zero, and Route (a) would have reduced to Route (b), but this is clearly not so as seen from Eq. (4.13). The fourth term of Eq. (4.10) containing $C_A$ doesn't influence the analysis because $C_A$ was not affected by the discontinuity and had the same value through Routes (a) and (b) as shown above. The solution of Eq. (4.10) would, thus, be affected by the discontinuity. This discontinuity in $C_R(0)$ results in the modified form of transfer function Eq. (3.12) for $C_R$, which was marked by the appearance of the numerator-dynamics form.

Also, one needs to know the value of $C_R(0^+)$ to solve the system, and paradoxically, it shall not be known unless the profile is obtained. This leads to the undetermined value of initial discontinuity in $C_R$. Thus, the impulse response of this system, too, is affected by initial discontinuities. Following the treatment of this section, it can be shown that the step response of this system, however, remains unaffected of initial discontinuities.

## 4.3 Application to the Nonlinear Systems

Extending the methodology of Section 4.2.4 for the nonlinear systems, initial discontinuities will be analyzed again by checking whether the discontinuity in the stimulus takes into account the initial discontinuities in the response. Recall that Route (b) registered all the initial discontinuities in the output variables, whereas, Route (a) was valid only in case the discontinuous input takes all the initial discontinuities of the outputs into account. However, the Laplace transform approach is not applicable now; hence a time domain strategy is to be developed. Revision in the methodology is, hence, essential. Also, deviation variables cannot be used for the analysis in the nonlinear equations. Considering the aforesaid facts, a revised strategy is followed and is illustrated in the following cases (Ahuja, 2011).

### 4.3.1 Example 1

First consider *impulse* input in volumetric feed rate $q$, as in the Section 4.2.2, to the gravity flow tank system represented by the non-linear Eqs. (3.25) and (3.26). Corresponding to Eq. (4.4), mass balance reveals that initial change in level $h(0)$ equals magnitude of the impulse (i.e., volume of liquid added), divided by the area of tank, thus:

$$h(0^+) = h(0^-) + M \,/\, A_T \tag{4.14}$$

For the analysis of initial discontinuities, the methodology described in Fig. 1 for the case of impulse response is again followed, where the first Route (a) implies to include impulse in the cause (i.e., the input time varying forcing function), and the second Route (b) implies to include impulse in the effect (i.e., in the initial values of the output

functions). Mathematically, Route (b) implies to take initial conditions of all the output variables and their derivatives at $t \rightarrow 0^+$, with input $q(t) = q(0^-)$; Route (a) implies to take the initial values of the output variables at $t \rightarrow 0^-$, with the input at $t \rightarrow 0^+$ given by:

$$q(t) = q(0^-) + M\,\delta(t) \tag{4.15}$$

- Following Route (a), the disturbance variable is given by Eq. (4.15). The extent of initial discontinuity in the third term ($q/A_T$) of Eq. (3.25) is calculated using the integral form of Eq. (4.15) at $t \rightarrow 0^+$,

$$\int_{0-}^{0+} \frac{q(t) - q(0^-)}{A_T} dt = \int_{0-}^{0+} \frac{M\,\delta(t)}{A_T} dt = \frac{M}{A_T}$$

  The integral of the impulse input is $\int M\delta(t).dt = M\int\delta(t).dt = M$.

- Following Route (b), the perturbation variable volumetric feed rate $q$ becomes: $q(t) = q(0^-)$. In the integral form of Eq. (3.25), the integral of the first term at the time of introduction of input, i.e., at $t \rightarrow 0^+$ gives:

$$\int_{0-}^{t} \frac{dh}{dt} dt = h(t) - h(0^-) = h(0^+) - h(0^-)$$

  Thus, the extent of initial discontinuity of the level of the liquid in the tank, as given by Eq. (4.14), is:

$$h(0^+) - h(0^-) = (M/A_T)$$

This implies that into the integral form of Eq. (3.25), the introduction of the impulse disturbance, through Route (a), causes the third term, i.e., the feed rate term ($q/A_T$), to change by an amount ($M/A_T$). This happens to be the same as the initial discontinuity in the first term (i.e., the tank level from Eq. (4.14)) of Eq. (3.25) from Route (b). In other words, the initial discontinuity in the input function $q(t)$ in the third term through Route (a), is equal to, the initial discontinuity in the output variable $h$ of the first term through Route (b). All other terms have no discontinuity as their integrands are limited, which don't contribute anything to the integral form of Eq. (3.25). Thus, Eq. (3.25) is unaffected by initial discontinuities and can be solved through either of the two

routes. However, since Eqs. (3.25) and (3.26) are coupled through the parameter $u_p$; analysis of Eq. (3.26) is also required. That is done as follows.

The discontinuity in $u_p$ (0), i.e., ($u_p(0^+)$ – $u_p(0^-)$), in the first term of Eq. (3.26) through Route (b) is not accounted in the initial discontinuity of impulse input through Route (a) as there is no impulse input term in Eq. (3.26). Note that there is a change in the initial velocity in pipe as seen in Section 4.2.2, thus:

$$u_p(0^+) - u_p(0^-) \neq 0 \tag{4.16}$$

Route (b), therefore, doesn't reduce to Route (a). Hence, the impulse response of the level and velocity of this system gets affected by the initial discontinuities. Hence, Route (a) is inconsistent with the physical principles applied to the system as expressed in Eq. (4.16). Also, one needs to know the value of $u_p$ ($0^+$) to solve the system, and, paradoxically, it shall not be known unless the profile is obtained.

Now, for a *step* input, there is no discontinuity in $h(0)$ and $u_p$ (0) because of inertia of liquid and resistance to flow in the pipe, i.e., the initial rise in tank level is zero, and, hence, no initial change of velocity in the pipe. But there is a discontinuity in $h'$ (0); nevertheless, discontinuity in $h'$ (0) is not needed in Eqs. (3.25) and (3.26). Hence, the step response of the system is not affected by the initial discontinuities.

Thus, only the impulse response of this system is affected by initial discontinuities and exhibits a paradox. Numerical solution of this nonlinear system is discussed in Section 4.6.

### 4.3.2 Example 2

Consider an impulse perturbation in the volumetric feed rate $q$ to the first tank of the two interacting tanks-in-series. Application of physical principles gives the following two equations. The level in the second tank is not immediately affected by the change in the level of the first tank, because of the presence of the dynamic lag in the first tank.

$$h_1(0^+) - h_1(0^-) = M/A_1 \tag{4.17}$$

$$h_2(0^+) - h_2(0^-) = 0 \tag{4.18}$$

Following the same procedure as above, it can be shown that the initial discontinuities from the two routes balance each other, and Route (b) reduces to Route (a). Hence, the system is not affected by the initial discontinuities unlike in the last case. The same happens for the step response too. This system doesn't exhibit the paradox noted above.

### 4.3.3 Example 3

Consider an *impulse* input in the volumetric feed rate $v_o$ to the constant density constant holdup CSTR of Section 3.2. Impulse input can be brought about by plunging a measured volume $M$ ($m^3$) of pure liquid $A$ into the tank. The magnitude of impulse is equal to the magnitude of liquid added. *It is further assumed that this magnitude is small enough* (*or the holdup is large enough*) *not to cause any change in the exit volumetric flow rate*. Refer again to the impulse response case of Fig. 1 for initial conditions; there would be discontinuities in the output variables $C_A$ (0), $C_R$ (0) and in the input variable $v_o$. The system model described by Eqs. (3.7) and (3.8) is considered.

Application of material balance for component $A$ at the initial instant for its use in Route (b) leads to the following. Impulse disturbance of magnitude $M$ ($m^3$) in feed flow rate $v_o$, is equivalent to introducing ($MC_{Ao}$) (moles) of pure liquid $A$ directly into the tank, all in one go (with no change in feed stream flow or feed stream concentration). The sudden increase in the number of moles of $A$ in tank divided by the holdup volume gives the increase in $C_A(0^+)$, i.e., the initial concentration of $A$ in the tank.

$$C_A(0^+) = C_A(0^-) + MC_{Ao} / V \tag{4.19}$$

Concentrations of $R$ and $I$ fall suddenly with the sudden rise in the concentration of $A$. The constant density reaction condition can be applied in the deviation form at $t \longrightarrow 0^+$ for the impulse input considering that pure liquid $A$ is put directly into the tank with no change in $C_{Ao}$ and volume, this gives $C_R(0^+)$ as in Section 4.2.4:

$$\begin{aligned} C_R(0^+) &= C_R(0^-) - [C_A(0^+) - C_A(0^-)]M_A / M_R - [C_I(0^+) - C_I(0^-)]M_I / M_R \\ C_R(0^+) &= C_R(0^-) - \left(MC_{Ao} / V\right) - [C_I(0^+) - C_I(0^-)]M_I / M_R \end{aligned} \tag{4.20}$$

This equation is obtained by the combination of the constant density condition and Eq. (4.19). Discontinuities are now analyzed using Eqs. (3.7) and (3.8), by referring to Fig. 1.

- Following Route (a), the perturbation variable volumetric feed rate $v_o$ in Eq. (3.8) becomes:

$$v_o(t) = v_o(0^-) + M\,\delta(t) \tag{4.21}$$

Initial discontinuity in the second term ($v_oC_{Ao}/V$) of Eq. (3.8) comes from Eq. (4.21):

$$\int_{0-}^{0+} \left(v_o(t) - v_o(0^-)\right)\frac{C_{Ao}}{V}dt = \int_{0-}^{0+} M\,\delta(t)\frac{C_{Ao}}{V}dt = \frac{MC_{Ao}}{V} \tag{4.22}$$

- Following Route (b), the perturbation variable volumetric feed rate $v_o$ in Eq. (3.8) is: $v_o(t) = v_o(0^-)$. In the integral form of Eq. (3.8), the integral of the first term evaluated at time $t \rightarrow 0^+$ is equal to $\int_{0-}^{0+} \frac{dC_A}{dt}dt = C_A(0^+) - C_A(0^-)$. This extent of initial discontinuity in the tank concentration is: $(C_A(0^+) - C_A(0^-)) = (MC_{Ao}/V)$, as seen in Eq. (4.19).

This implies that in the integral form of Eq. (3.8), the introduction of the impulse disturbance causes the second term, i.e., feed rate term ($v_oC_{Ao}/V$) to change by an amount ($MC_{Ao}/V$). This happens to be the same as the initial discontinuity in the first term of the integral form of Eq. (3.8). Hence, the initial discontinuity in the feed rate in the second term through Route (a) is equal to the initial discontinuity in concentration of the first term through Route (b). Note that no initial discontinuity in the exit rate in the third term is considered by the virtue of the small magnitude (or large holdup) assumption. Thus, the initial discontinuities in the output function are accounted for in the magnitude of the impulse input function. Thus, Eq. (3.8) is not affected by the discontinuities. However, the initial discontinuity in $C_R$, i.e., $(C_R(0^+) - C_R(0^-))$ in the first term of Eq. (3.7) through Route (b) is not accounted for in the initial discontinuity of the impulse input through Route (a) as there is no impulse input term in Eq. (3.7). As seen from Eq. (4.20),

$$C_R(0^+) \neq C_R(0^-) \tag{4.23}$$

If it were not so, the solution would not have been affected by discontinuities. To summarize, Eq. (3.8) can be solved by either of the two routes, whereas, Eq. (3.7) only through Route (b). Hence, Route (b) does not reduce to Route (a), and Route (a) is inconsistent with the facts elicited on the application of physical balances to the system as expressed in Eq. (4.23). The value $C_R(0^+)$ is, thus, required to solve the system Eq. (3.7) as the impulse disturbance cannot take the discontinuity in $C_R(0)$ into account. Its value shall be estimated in the framework presented in the next chapter.

The impulse response is, thus, affected by the initial discontinuities. The step response of this system, however, remains unaffected of the initial discontinuities.

## 4.4 Validation of the Effects of Discontinuities on Nonlinear Models

The inconsistencies due to singular inputs as a result of the effect of the initial discontinuities discussed above were validated by the comparison of experimental and numerical data of non-linear models of flow-level tanks. Their level responses and draining time calculations clearly revealed these initialization effects. These are described in the following sections. For validation, two nonlinear flow-level tank systems, discussed in the last chapter, were considered, viz., gravity-flow tank and interacting level-tanks. Impulse response experiments were performed on these systems. The nonlinear differential equations describing these systems cannot be solved analytically. Hence, numerical solutions were obtained. Numerical experiments simulating the above systems were performed at different initial conditions. The initial condition was guessed initially and a tentative solution profile was obtained. Further guess trials were, then, made and the impulse solution profiles, thus obtained, were compared with the experimental data to substantiate the effect of initial discontinuities. Nonlinear models were considered to avoid the errors due to linearization, so that, the error deviations of the values of the simulated profiles ($y_i$) from that of the experimental ones ($b_i$) are reliable; root mean square deviations (RMSD) were calculated:

$$RMSD = \sqrt{\frac{\sum_{i=1}^{m} (b_i - y_i)^2}{m}} \tag{4.24}$$

As described in Section 4.8, the effects of initial discontinuities can also be validated by the calculations of the time required for emptying these flow-level tanks. It will be shown that the impulse solution profiles can be used to calculate the time required for emptying the flow-level tanks. Not accounting for the effect of initial discontinuities, however, will yield the same calculated value of the time required to empty a gravity-flow tank, irrespective of the initial level, which is obviously incorrect. Some other interesting features of calculations of time required to empty flow-level tanks shall be discussed. The prerequisites, i.e., the calculations of the over-damped and the under-damped profiles for the systems of interest have been discussed comprehensively in Section 3.9, Chapter 3 (Ahuja, 2010; 2011).

## 4.5 Experimental Section

Experiments on gravity flow tank were carried out in a set up made of steel consisting of a rectangular tank of dimensions 0.4 m $\times$ 0.4 m $\times$ 0.7 m with a horizontal pipe at the outlet of internal diameter 0.024 m and length 4.27 m (Fig. 3.1). To maintain constant inflow, inlet to the tank was obtained from the downstream of an overhead tank having a mechanism to maintain water at a constant level. The system was allowed to attain a steady state. Impulse disturbance was introduced by inserting a measured amount of water into the tank, all in one go. Level response was measured from the graduated transparent tube fitted to the tank. The steady inflow rate was $2.95\times10^{-4}$ $m^3/s$, initial level was 0.202 m and the magnitude of impulse disturbance was $1.5\times10^{-2}$ $m^3$. Reynolds number was calculated and turbulent flow in the pipe ensured.

Experiments on interacting tanks were performed in a set up consisting of two interacting transparent acrylic graduated cylindrical tanks each of internal diameter 0.101 m and height 0.3 m (Fig. 3.2). The inlet water to the first tank came from an overhead tank similar to the one mentioned above. To evaluate the constants in the flow-head relationships of Eqs. (3.31), $k_1$ and $k_2$, four steady state runs were performed and the constants were calculated from the slopes of the flow versus head plots. The transient experiments were carried out in similar manner as in gravity flow tank and the level response of the first tank was recorded. The initial steady state conditions were as

follows. Inflow rate was $8.33 \times 10^{-6}$ m$^3$/s, the first tank level was 0.11 m, second tank level was 0.091 m and the magnitude of the impulse input was $5.0 \times 10^{-4}$ m$^3$.

## 4.6 Validation by Numerical Solution

To validate the results of the inconsistencies due to singularities, the above two systems, namely, gravity-flow tank and interacting level-tanks, were numerically solved from their non-linear models. Comparing the fit of experimental data for these systems substantiates the effect of initial discontinuities in this section. Numerical solutions were carried out in the following manner.

Nonlinear Eqs. (3.25) and (3.26) were employed for the gravity-flow tank solution. The system is affected by initial discontinuities (refer to Section 4.3.1). There are initial discontinuities in level, efflux velocity and the impulse input. To simulate the above experimental procedure, $q(t)$ was taken as a constant equal to its initial steady-state value, i.e., $q(t) = q(0^-)$ as that mentioned in Route (b) in Section 4.3.1, while the experimental values of $h(0^+)$ and $u(0^+)$ were needed instead of $h(0^-)$ and $u(0^-)$ respectively. The value of $h(0^+)$ is given by Eq. (4.14). Differential equations were solved using Polymath which employs Runge-Kutta-Fehlberg algorithm (RKF45) of initial step size = $10^{-6}$ and truncation error tolerance = $10^{-6}$ (Gerald and Wheatley, 2004). As mentioned, a tentative solution was first obtained as the value of $u(0^+)$ was paradoxically unknown. For doing this, the initial discontinuity in the velocity of fluid in the pipe was ignored, so, the initial velocity was assumed as $u(0) = u(0^-)$, as a first estimate for the simulation. Initial discontinuity in $u(0)$ was then incorporated and successive higher values of $u(0)$ were assumed for further guess trials.

To simulate the experimental behavior of the impulse response of the first tank of interacting tanks system, Eqs. (3.30) were used. The methodology of numerical solution was the same as in the preceding paragraph. However, the values of $k_1$ and $k_2$ in the flow-head relationship Eqs. (3.31) for the first and the second tank were needed. These were obtained from the data analysis of the steady state experimental runs. The steady state data of the four runs were plotted as $q_s$ values versus $\sqrt{h_{1_s} - h_{2_s}}$ values; and $q_s$ values versus $\sqrt{h_{2_s}}$ values at steady state, and it was found that these give a straight line plot

passing through the origin, thus confirming the flow-head relationships. These values were found to be:

$$k_1 = 6.10 \times 10^{-5}\,\mathrm{m}^{2.5}/\mathrm{s} \text{ and } k_2 = 2.76 \times 10^{-5}\,\mathrm{m}^{2.5}/\mathrm{s} \tag{4.25}$$

For the non-linear model of interacting tanks system the initial discontinuities are accounted for in the magnitude of the impulse input (refer Section 4.3.2). Initial discontinuities are there in the impulse input and the level of the first tank, and in the input to the second tank, but are absent in the level and the outflow of the second tank. To solve this model numerically for impulse input in $q(t)$ the volumetric flow rate was taken to be $q(0^-)$ and initial values were taken as $h_1(0^+)$, $h_2(0^-)$, and $q_2(0^-)$. Eqs. (4.17) and (4.18) were used; the rest of the procedure was the same as that followed for the gravity-flow tank system.

## 4.7 Results and Discussion

Tables 4.1, 4.2, Figs. 4.2 and 4.3 present the results of the comparison of the numerical and experimental level response data for the gravity-flow tank and the first tank of the interacting tanks systems. The RMSD values of the comparison were calculated for different assumed values of the discontinuity of a particular variable mentioned above.

For the gravity-flow tank data in Table 4.1, the experimental response correspond to the initial steady state exit velocity of 0.65 m/s and the impulse of magnitude $1.5 \times 10^{-2}$ m$^3$. For the numerical solutions, the value of $q(t)$ was taken as $2.95 \times 10^{-4}$ m$^3$/s, and the discontinuous value of the level $h(0) = h(0^+)$ of $2.96 \times 10^{-1}$ m for all the five cases of Table 4.1. This Table shows a specific trend of RMSD values. On increasing the discontinuity in the exit velocity, the RMSD first decreased and then increased. For the case at S. No. 1, $u(0) = u(0^-)$, as obtained through Route (a) in Section 4.3.1 was taken for simulation as an initial estimate; the corresponding RMSD value exhibited was $5.00 \times 10^{-3}$ m. As further trials were made at successively higher values of $u(0)$ (as indicated through Route (b)), the RMSD value decreased considerably. For example, at S. No. 3 in Table 4.1, the RMSD value was $3.61 \times 10^{-3}$ m. However, when the value of $u(0)$ further

**Table 4.1** Comparison of the experimental and numerical results for the level response of gravity-flow tank for different assumed values of efflux velocity $u(0)$

| S. No. | Assumed values of $u(0)$ m/s | RMSD $\times 10^3$ m |
|---|---|---|
| 1. | 0.65[1] | 5.00 |
| 2. | 3 | 4.12 |
| 3. | 8 | 3.61 |
| 4. | 30 | 4.38 |
| 5. | 100 | 5.53 |

[1]Corresponding to steady flow rate of $2.95 \times 10^{-4}$ m$^3$/s

increased, the RMSD value started increasing. For example, at S. No. 5, the RMSD value was $5.53 \times 10^{-3}$ m, that is even more than that at S. No. 1 obtained by ignoring the initial discontinuity. These facts indicate that the actual value of $u(0^+)$ is higher than $u(0^-)$, and lies somewhere in between these assumed values. The aforesaid observations support the analysis carried out above that $u(0^-)$ can't be used in place of $u(0^+)$, and, hence, it is necessary to account for the initial discontinuities in the gravity-flow tank system. However, the value of $u(0^+)$ cannot be calculated from the initial slope of the experimental level response $h'(0^+)$. The level changes very fast initially for the impulse response, it is difficult to accurately measure its initial rate as it is not possible to accurately draw the tangent at zero time in the absence of the left hand branch of the curve (Mickley *et al.*, 1975).

Some corresponding numerical results are also plotted along with the experimental curve in Fig. 4.2. These are for $H$, i.e., the deviation of level from the initial steady state. The experimental curve was fitted by eye (bold curve); the actual data points are not shown here to avoid a clutter on the graph. The numerical solutions converge at the initial steady-state value at $t \to \infty$.

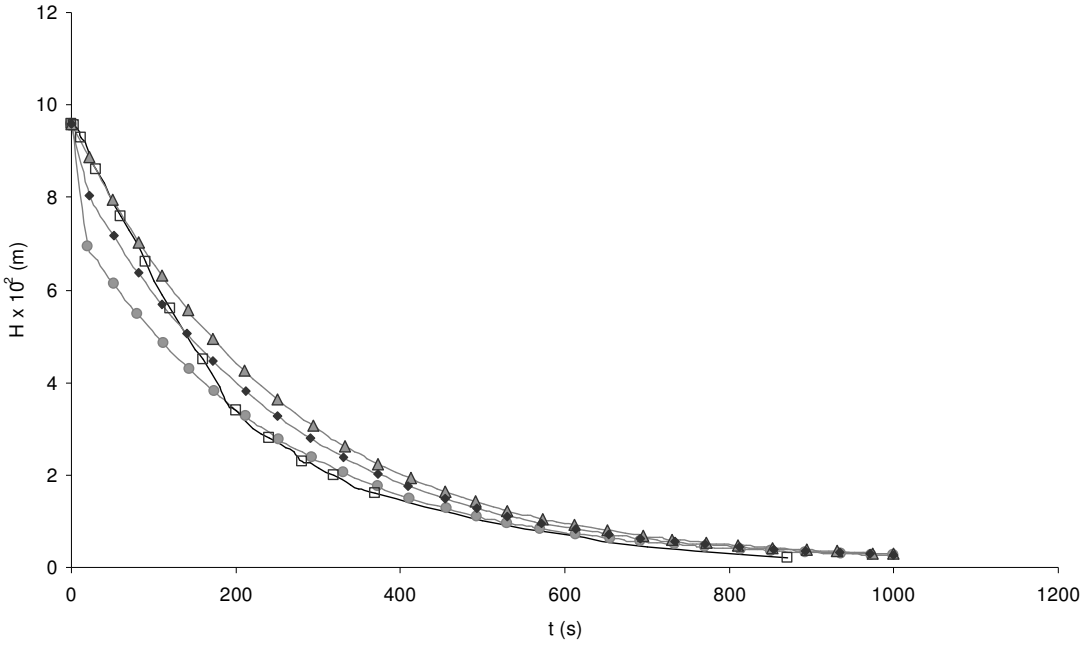


**Fig. 4.2** Response of gravity-flow tank for impulse input of magnitude $15\times\ 10^{-3}$ m$^3$ for different assumed values of $u(0)$

- Experimental (bold);
- $u(0) = u(0^-) = 0.65$ m/s, $q(0^-) = 2.95\times 10^{-4}$ m$^3$/s;
- $u(0) = 8$ m/s;
- $u(0) = 100$ m/s.

The numerical results for the first tank of the two interacting tanks-in-series are compared with the corresponding experimental results in Table 4.2. The experimental data corresponds to the initial steady state, i.e., inflow rate, $8.33\times 10^{-6}$ m$^3$/s, the first tank level, $1.1\ \times 10^{-1}$ m, the second tank level, $9.1\times 10^{-2}$ m, and the magnitude of the impulse input, $5.0\ \times\ 10^{-4}$ m$^3$. For the numerical solutions, the values of $q(t)$, $q_{21}(0^-)$, and $q_2(0^-)$ were taken as the corresponding initial steady state value above, while $h_1(0) = h_1(0^+)$ of $1.72\ \times\ 10^{-2}$ m was taken for all the five cases of Table 4.2. This Table clearly shows increase in RMSD of one order when the initial value of the efflux flow rate of the first tank was changed from that calculated through physical considerations, i.e., at S. No. 1; For which, value of $q_{21}(0) = q_{21}(0^-) = 1.74\times 10^{-5}$ m$^3$/s, obtained using Eq. (4.18) through either Routes (a) or (b) in Section 4.3.2 was used for solution. A very good agreement with an RMSD of only $4.35\times 10^{-4}$ m was obtained. If the initial value of $h_2(0)$ was changed (increased or decreased, to see the effect of $q_{21}(0)$) from $h_2(0^-)$, the RMSD value

**Table 4.2** Comparison of the experimental and numerical results for the level response of the first tank of the two interacting liquid-level tank system for different assumed values of exit flow rate $q_{21}(0)$

| S. No. | Assumed values of $q_{21}(0)$ $\times 10^5$ $m^3/s$ | RMSD $\times 10^3$ m |
|---|---|---|
| 1. | 1.74[1] | 0.435 |
| 2. | 1.52 | 3.56 |
| 3. | 1.69 | 1.75 |
| 4. | 1.79 | 1.12 |
| 5. | 1.85 | 1.81 |

[1]Corresponding to steady value of level of second tank of 0.091 m

increased by one order. For example, the case at S. No. 2 exhibited (at an increased value of $q_{21}(0)$) an RMSD of $3.56\times10^{-3}$ m, which is one order more than that at S. No. 1. Similarly, at S. No. 5 (at a decreased value of $q_{21}(0)$), the RMSD was $1.81\times10^{-3}$ m, which is again one order more than that at S. No. 1. Some corresponding numerical results of the impulse level response are plotted in Fig. 4.3 along with the experimental response profile (bold curve). It supports the observations made. The curve for the case at S. No. 1 practically overlaps with the experimental curve, while other cases deviate substantially from the experimental curve. Thus, the results are just the opposite of that seen in gravity-flow tank system, as the numerical solutions deviated from the experimental findings if the initial discontinuities were incorporated. These results support the preceding analysis that there is an undesirable consequence of deviating from the value of $h_2(0)$ determined from physical principles for the interacting tanks system. Hence, this system already accounts for the initial discontinuities in $h_1(0)$ and $q_{21}(0)$, and is, thus, not affected by the same.

To summarize, it is shown that the numerical solution of the gravity-flow tank moves closer to the experimental response as the initial discontinuity in the efflux velocity of the liquid, identified upon the application of momentum balance at the initial instant of the introduction of the perturbation, is taken into account. Conversely, the numerical solution of the first of the two interacting tanks system deviates away from the experimental response as the value of an initial discontinuity is deviated away from that evaluated upon the application of the physical principles. The distinct results of the two

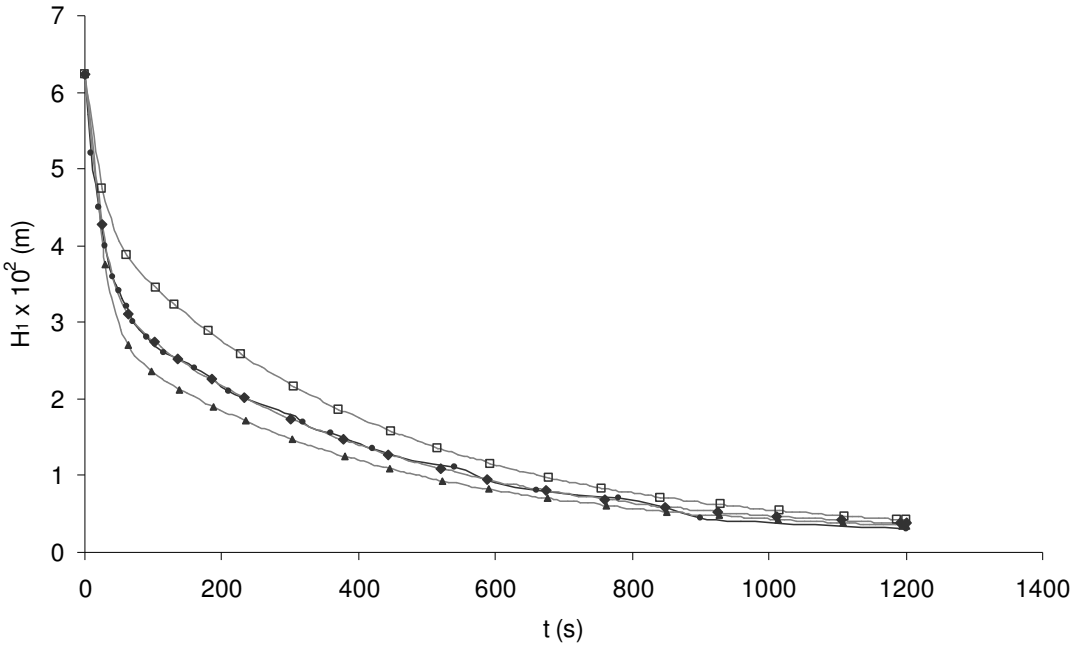


**Fig. 4.3** Response of the first tank of the two interacting liquid-level tanks for impulse input of magnitude $5 \times 10^{-4}$ m$^3$ for different assumed values of $q_{21}(0)$

● Experimental (bold);
◆ $q_{21}(0) = 1.74 \times 10^{-5}$ m$^3$/s, $h_2(0) = h_2(0^-) = 0.091$ m;
□ $q_{21}(0) = 1.52 \times 10^{-5}$ m$^3$/s;
▲ $q_{21}(0) = 1.85 \times 10^{-5}$ m$^3$/s.

systems studied substantiate the analysis carried out in Sections 4.1 through 4.3. Further evidence to this effect is provided in the next section.

## 4.8 Time Required for Emptying the Tanks

For further validation, calculations of the time required for emptying (time-to-empty) flow-level tanks are now described. These calculations under gravity-powered flows can be tricky because the head changes with time (Kossik, 2000; Loiacono, 1987; Shoaei and Sommerfeld, 1989; Sommerfeld and Stallybrass, 1992). However, in the present study, the impulse responses are used indirectly to describe these calculations here. The linearized models in terms of the deviation variables defined in Sections 3.5.1 and 3.6.1 are employed to see the effect. Recall the two routes for impulse response calculations. Route (a) includes the initial discontinuities in the stimulus, while Route (b) includes them in the response and was found to be the valid route as it took all the initial

discontinuities into account. Consider impulse input to an initially empty tank with inflow and outflow equal to zero at $t \rightarrow 0^-$, i.e., $Q(t) = Q(0^-) = 0$, $H(0^-) = 0$, $U(0^-) = 0$.

The impulse perturbation to the tank can be introduced by plunging a certain amount, i.e., $M$ ($m^3$) of liquid suddenly into the tank, all in one go. Corresponding to Route (a), i.e., $H(0) = H(0^-) = 0$, $U(0) = U(0^-) = 0$, and $Q(t) = M\delta(t)$. Alternatively, corresponding to Route (b), i.e., $H(0) = H(0^+) \neq 0$, $U(0) = U(0^+) \neq 0$. *Linearized* models are used for the calculations of time-to-empty gravity-flow tank and the first tank of the two interacting tanks system.

The effect on time-to-empty gravity-flow tank is discussed as follows. The deviation variables $H$, $U$ and $Q$ are the same as respective true values of level $h$, efflux velocity in pipe $u$ and inflow rate $q$, as the initial steady state values are all zero. Subscript $s$ represents initial steady state and superscript ($'$) represents derivative. The rest of the symbols were defined in Chapter 3. Linearized model Eq. 3.27 is repeated here for convenience:

$$s^2H(s) - sH(0) - H'(0) + \frac{B}{A}\left[sH(s) - H(0)\right] + \frac{C}{A}H(s) = K\left[sQ(s) - Q(0)\right] + K\frac{B}{A}Q(s) \tag{4.26}$$

where, $K = 1/A_T$, $A = A_P L$, $B = \left(4fLQ_S\right)/\left(D_P\right)$, $C = gA_P{}^2/A_T$

Giving an impulse input to initially empty tank as per Route (a), is first considered. In Eq. (4.26), $Q(s) = M$, and all the initial conditions become zero. The equation is solved for $H(s)$. Then, $H(s) = 0$ is substituted as the empty tank condition. As the left hand side of Eq. (4.26) becomes *zero*, time-to-empty the tank is invariably independent of the amount $M$ of liquid added (as $M$ gets cancelled out of the equation), which is erroneous and physically impossible. Thus, Route (a) yields incorrect solutions and the system is affected by initial discontinuities as also shown in the previous sections.

However, one can calculate the right value of the time-to-empty the tank by using Route (b). Route (b), which includes the initial discontinuities in the response $H(s)$, resulted in Eq. (4.6) above. It is repeated here for convenience:

$$s^2H(s) + \frac{B}{A}sH(s) + \frac{C}{A}H(s) = K\left[sM + \frac{B}{A}M - A_P U(0^+)\right] \tag{4.27}$$

Solving for $H(s)$, inverting it, and finding the value of the time when the level response $H(t)$ reaches the *zero* value gives the time for emptying. But the solution requires the value $U(0^+)$, which is unknown. However, the qualitative nature of the response can be looked at if the response is plotted against time. The time read from this plot as the trajectory crosses the *time*-axis gives the correct value of interest. For under-damped oscillatory case of gravity flow tank, there are multiple feasible solutions as the trajectory cuts the *time*-axis at multiple points (refer to Fig. 4.1 showing an oscillatory impulse response profile). But the tank will be empty when the trajectory cuts the *time*-axis at the very first value of time, so the least of these multiple values is taken as the solution. Also, starting at different initial levels in gravity-flow tank, values of $U(0^+)$ would be different. Different values of time-to-empty the tank are, thus, obtained using Eq. (4.27), which goes well with the physical fact. So, if the initial discontinuity in efflux velocity $U(0^+)$ was ignored (as in Eq. (4.26)), the calculations of time-to-empty for gravity-flow tank would result in same values irrespective of the initial level.

Now, consider the over-damped case of gravity-flow tank, calculation of the time-to-empty the tank from Route (b) gives $t \rightarrow \infty$ because the over-damped trajectory becomes asymptotic to the *time*-axis with the passage of time but never cuts the *time*-axis (as in Fig. 4.2 and 4.3). This value of time comes out to be the same irrespective of the initial level. But taking $H = 0.1$ (say) (i.e., a very small value as the empty tank condition), Eqs. (4.27) would yield different values of time-to-empty the flow-level tank for different initial levels. From Routes (a) or (b), this fact is analogously true for the first tank of a two interacting tank system (Eq. 3.34), non-interacting tanks system, or for a single tank system for that matter (as these tanks only behave over-damped). These flow-level tank systems are, thus, not affected by initial discontinuities as also shown in the sections above. For these systems, Routes (a) and (b) happened to be the same.

## 4.9 Outcomes Revisit

Some linear time-invariant numerator-dynamics systems and the corresponding nonlinear systems with terms containing differentials of the input, e.g., U-tube manometer, first tank of the interacting tanks, etc. are unaffected by the initial discontinuities, whereas, the

others, e.g., gravity-flow tank, constant holdup CSTR, etc. are affected by the initial discontinuities, as is studied above.

The results of Sections 4.4 through 4.8 substantially corroborate the indications of the preceding analysis carried out in Sections 4.1 through 4.3, anticipating the conformity and the closeness of the calculated solution profiles obtained through the initialization Route (b), to the physical facts of time-to-empty, and the experimental level response profiles of different flow-level tanks. The observations clearly substantiate the analysis that $u(0^-)$ can not be used in place of $u(0^+)$, and, hence, it is necessary to account for the initial discontinuities in the gravity-flow tank system for the case of impulse response. With the introduction of the impulse input, the level of the tank suddenly increases, and there is a resultant sudden increase in the efflux velocity in the pipe. This explains the findings of the numerical simulations that as the value of the initial condition for $u(0)$ is increased above $u(0^-)$, the calculated level profiles approach the experimental level profiles. So, as remarked earlier, Route (b), based on finding initial discontinuities through the application of physical balances to the initial effects, is the correct route for the initializations of the systems perturbed by the singular inputs. Route (b), thus, yields more accurate solutions than Route (a).

# 5 General Framework for Analysis and Initialization

The last chapter strongly indicated the significance of putting the theoretical analysis consistent with the physical principles, i.e., of material, energy, and momentum balances. These effects of initial discontinuities were revealed for systems essentially by matching the coefficients of input and output terms in the models. Having established these qualitative effects of initial discontinuities on the calculated solution profiles of the nonlinear systems, a simple, direct, and comprehensive framework in the time domain is now proposed. The framework is meant for the analysis and initialization of the lumped-parameter chemical engineering systems containing a set of first-order ODEs. The aim is to quantitatively describe their response to a singular (step or impulse), initial or input condition.

Effects of linearization will be discussed in the subsequent Section 5.12. Limitations of the symbolically transformed models shall be discussed in Section 5.13. The framework shall be applied to the linear time-invariant systems in Chapter 6 to address, reveal, and resolve the inconsistency in the Laplace transform treatment.

## 5.1 Framework of Discontinuity Analysis and Initialization

The analysis of initial discontinuities is carried out to expose the inconsistency in initial conditions, and to estimate the initial values of the discontinuous output variables. Mathematical models are used in conjunction with the physical principles of material, energy, and momentum balances. A schematic of the proposed methodological framework for singular inputs is presented in Fig. 5.1. The methodology is based on the fact that a physical balance must maintain equality at all times, and, in particular, must be balanced at the initial time that includes the singularity.

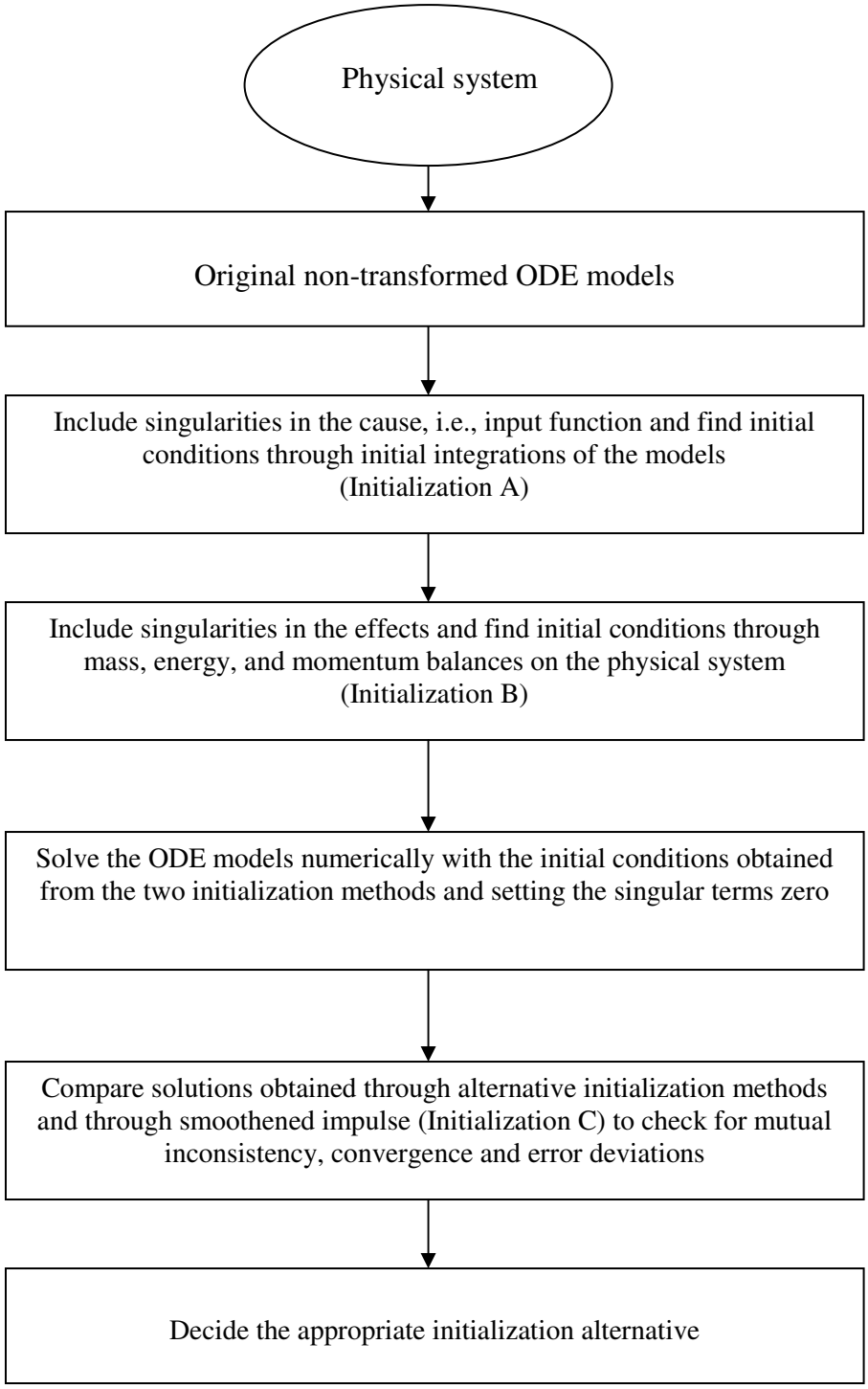


**Fig. 5.1** Framework of the proposed analysis and initialization methodology for the systems with singular inputs

Furthermore, since the derivatives of discontinuous functions contain singularity at the origin, the resultant magnitudes of the initial discontinuities can also be worked out by integrating the ODE at the initial time. These are explained further in the strategy that is adopted to address singularity and the inconsistency thus emanating. The analysis is carried out in two steps by including impulse first in the cause, and then, in the effect.

In the first step (Initialization A), impulse is included in the cause, i.e., the input function, and the magnitude of the initial discontinuities in the outputs is estimated from the time integration of the model within the limits of $0^-$ to $0^+$, and the sifting property of the impulse ($\delta$-Dirac) function is used to evaluate the singular terms. This integration is carried out, using its physical interpretation as the area under a curve within the limits of integration without following the generalized functions treatment. The applicability of this procedure is suggested in this study by its comparison with other approaches.

Consider a general physical process represented by the following set of first-order nonlinear ODE system, which has an input variable suffering a singular perturbation.

$$\dot{\mathbf{z}}(t) = F(t, \mathbf{z}(t), m(t)) \tag{5.1}$$

where $t$ is the independent variable (time), $m(t)$ is the input forcing function, and $\mathbf{z}(t) \in \Re^n$ are the dependent variables. As is remarked in the following sections, the original models, rather than the models obtained from symbolic differentiations and manipulations, must be used.

As described in Fig. 5.1, the discontinuity analysis for the system Eq. (5.1) is first carried out by including impulse in the input function. The system is initially at a particular state at time $t \rightarrow 0^-$. For impulse input at $t \rightarrow 0^+$, the forcing function $m$ changes from its pre-initial value $m(0^-)$ (steady or unsteady) to:

$$m(t) = m(0^-) + M\ \delta(t - t_o) \text{ with } t_o = 0^+ \tag{5.2}$$

where $M$ represents the magnitude of the impulse and $\delta$ represents the unit-impulse function. Since Eq. (5.1) must maintain equality at all times, each equation in (5.1) can be integrated at $0^+$ time by placing this value of the input function. This gives:

$$\int_{0^-}^{0^+} \dot{\mathbf{z}}(t)dt = \int_{0^-}^{0^+} F(t, \mathbf{z}(t), m(t))dt \tag{5.3}$$

The right side of this Eq. (5.3) is evaluated in the following way. The integrals of the terms with limited integrands vanish, i.e.:

$$\int_{0^-}^{0^+} m(0^-)dt = 0; \quad \int_{0^-}^{0^+} \mathbf{z}(t)dt = 0; \quad \int_{0^-}^{0^+} m(0^-).\mathbf{z}(t)dt = 0 \tag{5.4}$$

The integral of the term involving impulse function of magnitude *M*, equals *M*, as the integral of unit impulse equals one.

$$\int_{0^-}^{0^+} M\,\delta(t-t_o)dt = M\int_{0^-}^{0^+} \delta(t-t_o)dt = M \tag{5.5}$$

The integral of the terms involving the product of the dependent variable(s) with the impulse function are evaluated as:

$$\int_{0^-}^{0^+} \mathbf{z}(t).M\,\delta(t-t_o)dt = M\mathbf{z}(t_o) = M\mathbf{z}(0^+) \tag{5.6}$$

The last Eq. (5.6) follows from the sifting property of $\delta$-Dirac function. This property is applicable for continuous functions at $t_o$. Though $\mathbf{z}$ may have a discontinuity at $t_o$, it can be considered continuous from the right of $t_o$, i.e., $0^+$; thus, interpreting the integral as the area under the curve, which is 0 everywhere except at the point $t = t_o$, and at $t = t_o$, the area under the impulse, $M$, is scaled by the value of the function $\mathbf{z}$, i.e., $M\mathbf{z}(t_o)$, this leads to Eq. (5.6).

Evaluation of left side of Eq. (5.3) gives:

$$\int_{0^-}^{0^+} \dot{\mathbf{z}}(t)dt = \mathbf{z}(0^+) - \mathbf{z}(0^-) \tag{5.7}$$

Using Eqs. (5.2), (5.4), (5.5), (5.6), and (5.7), the set of Eq. (5.3) can be solved simultaneously to get the initial discontinuity in each variable of $\mathbf{z}$, i.e., $\mathbf{z}(0^+) - \mathbf{z}(0^-)$.

The procedure can be easily extended to a second-order linear time-invariant system containing a derivative of the input term, as illustrated in the next chapter. The proposed framework is also applicable to systems initially at steady or unsteady state, and, so, it is equally applicable to systems perturbed by an impulse train with impulses occurring at non-zero times.

In the second step of the analysis (Initialization B), the impulse is included in the effect, i.e., the effect of the introduction of impulse on the initial conditions of the system is quantified by the application of physical balances. Thus, the magnitudes of the initial discontinuities are obtained by applying the principles of mass, energy, and momentum balances on the physical system at the initial instant of the introduction of the input.

The applicability of the initialization A procedure is suggested in the next section. Its resultant initial values are identical with the definitely and apparently known initial values of several cases. Also, the initial values of initialization A are, invariably, identical with that of the elementary Laplace analysis of the linear cases (see Chapter 6).

As seen in the following sections, the initial values obtained from even the well established Laplace analysis may or mayn't be consistent with that obtained from initialization B. For many linear and nonlinear cases studied, it is found that the initialization A can be either consistent or inconsistent with initialization B. The initial discontinuities calculated from the physical principles, i.e., initialization B are found to be more accurate as compared to that calculated from a mathematical model of the physical system, i.e., initialization A, because of the inability of a model to completely represent the physical system affected by singularity at the origin. It can be shown that initializations A and B respectively reduce to routes (a) and (b) for the cases of Chapter 4. The analysis carried out in Chapter 4 for linear and nonlinear systems also showed that for some chemical engineering systems, an initial discontinuity in the output variable of the impulse response, identified on applying the physical principles, couldn't be accounted for on theoretical analysis of the model (Ahuja, 2010; 2011). This effect was corroborated by the finding that, the numerical solution profiles were closer to the experimental results, when this discontinuity was taken into account.

For carrying out the solution through initialization C, the unit impulse function is approximated with a continuous function of area equal to one, i.e., a Gauss pulse function

of a parameter $a$, that becomes sharper as the parameter $a$ decreases and approaches an impulse function as $a \to 0$. So, the input function, in general, is approximated as:

$$m(t) = m(0^-) + \frac{M}{a\sqrt{\pi}} e^{-t^2/a^2} \tag{5.8}$$

This equation is substituted in the system Eq. (5.1), which is solved numerically for each dependent variables **z**. Several numerical computations for decreasing value of the parameter $a$ should reveal the correct asymptotic behavior of the solution profiles. The sharpened Gauss pulse functions for several decreasing values of $a$ applied in the numerical integrations are plotted in Fig. 5.2. The plots for still lower applied values of $a$ couldn't be shown because of extreme sharpening.

Numerical results are discussed in the next section. To quantify the degree of accuracy of initialization A, the numerical solutions obtained through it are compared with that obtained through initialization B and the resulting error margins are noted. The models are then solved by interpreting an impulse function as the limit of Gaussian pulse (Initialization C), and the above error margins for initialization A are compared with the corresponding error margins for initialization C.

The error deviations of the solution profiles obtained through alternative initialization approaches A and C are presented as normalized root mean square deviations (NRMSD), and are expressed as percentage of the range of values of the dependent variable obtained through initialization B:

$$\text{NRMSD} = \frac{100}{b_{\max} - b_{\min}} \sqrt{\frac{\sum_{i=1}^{m} (b_i - y_i)^2}{m}} \tag{5.9}$$

where $b_{\max}$ and $b_{\min}$ represent the maximum and the minimum of $m$ values of the dependent variable $b_i$ obtained through initialization B, and $y_i$ represent the corresponding values obtained through an alternative approach.

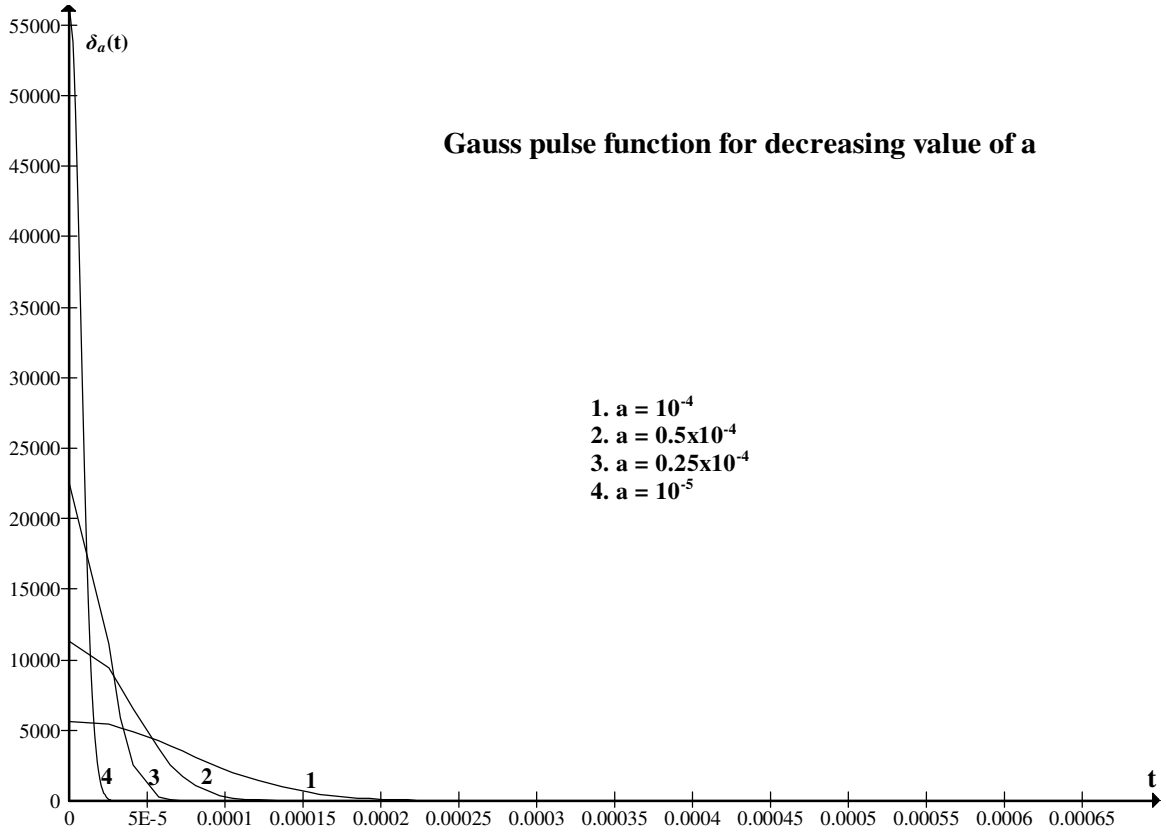


**Fig. 5.2** Approximation of unit impulse function ($\delta(t)$) with a continuous Gauss pulse function ($\delta_a(t)$) sharpened with decreasing value of parameter $a$

## 5.2 Applications

The proposed framework is illustrated in the following sections by using some examples from chemical engineering. Initial conditions were first evaluated from the direct methods proposed above, and the corresponding numerical results were computed. For the numerical integration of the systems using initializations A and B, the values of singular input terms in the equations were substituted equal to their initial values, since the effect of the impulse was already included in the model while calculating the initial conditions. The working of the proposed methodology is, in no way, limited to the establishment of an initial steady state, *a priori*, at $t \rightarrow 0^-$, still the pre-initial values were arbitrarily taken equal to the initial steady state values for the numerical solution and the convergence of the solution to these values was examined. The numerical integrations of the models were carried out using RKF45 from Polymath.

For convenience in comparison of alternative initializations A and B, the native models of Chapter 3 rather than the dimensionless forms were used. Nonlinear models involving mixing with chemical reaction, phase change, interaction of different capacities, and closed loop system with dead time, were considered, viz., non-isothermal CSTR, single component condenser, closed loop stirred tank heater with dead time, gravity-flow tank, and semi-batch reactor with a II order reaction. The cases discussed here are different in their physical and model structure, analysis, and effects of initial discontinuities. Relatively simple cases are treated first, followed by the intricate ones. The cumulative results and corresponding discussion follow each example sequentially.

## 5.3 Example 1

The non-isothermal CSTR model of Chapter 3 that has been used extensively to study nonlinear dynamics in the literature is first considered in this section. With changes in flow rate, material and thermal capacities are interacting. The constant density, jacketed, non-isothermal CSTR is carrying out a liquid-phase, first-order reaction $A \rightarrow R$. The feed contains only $A$. The symbols were defined in Chapter 3.

$$\frac{dV}{dt} = v_o - v \tag{5.10}$$

$$\frac{d(VC_A)}{dt} = v_o C_{Ao} - vC_A - kC_A V \tag{5.11}$$

$$\rho C_P \frac{d(VT)}{dt} = \rho C_P (v_o T_o - vT) + (-\Delta H_R) kC_A V + U_h A_h (T_j - T) \tag{5.12}$$

$$k = k_o e^{-E/RT} \tag{5.13}$$

For estimating exit flow rate $v$, various equations have been assumed in the literature, i.e., depending upon that based on linear resistance, weir or valve characteristics, controller equations, etc. (Coughanowr and LeBlanc, 2009; Luyben, 1996). It is worth noting that the magnitudes of the initial discontinuities obtained through the application of the above framework, and hence, the effects to be studied are independent of the choice of this equation because any selected equation—as can be seen in the treatment that follows—

would yield a limited integrand, whose integral would be zero according to Eq. (5.4) of the framework.

Two simple flow head relationships were assumed (and the head is proportional to the holdup volume), i.e.:

$$v = c_1 V \qquad (5.14); \qquad v = c_2\sqrt{V} \qquad (5.14')$$

These are applicable respectively to the cases of laminar and turbulent flow through pipes and valves. The constants of proportionality are based on the pre-initial conditions.

An impulse perturbation in exit flow rate $v$ is, first, considered. The variable holdup non-isothermal CSTR, which was at a particular state at the pre-initial time instant $t \to 0^-$, is perturbed at the post-initial time instant $t \to 0^+$ by an impulse in the exit volumetric flow rate $v$. This impulse input at $t \to 0^+$ in the exit flow can be realized by suddenly withdrawing $M$ ($m^3$) of the liquid directly from the tank suddenly, all in one go.

***Initialization A***

Following the initialization A procedure, let the impulse be included in the cause, first. So, $v$ has *two* components: one due to the perturbation, and the other due to the change in $V$ (since, $v = c_1 V$ ). So, $v$ becomes $v = c_1 V + M\,\delta(t - t_o)$ with $t_o = 0^+$ (Note that $c_1 V$ already includes $v(0^-)$). Placing this in Eqs. (5.10) through (5.14) gives the discontinuities in $V$, $C_A$, and $T$. For the case of laminar flow through the exit line, Eqs. (5.10) and (5.14) give:

$$\frac{dV}{dt} = v_o - (c_1 V + M\,\delta(t - t_o)) \qquad (5.15)$$

Upon time integration with in the limits $0^-$ to $0^+$, gives:

$$\int_{0^-}^{0^+} \frac{dV}{dt} dt = \int_{0^-}^{0^+} v_o\, dt \; - \int_{0^-}^{0^+} c_1 V dt - M \int_{0^-}^{0^+} \delta(t - t_o) dt \qquad (5.16)$$

The last term is evaluated by Eq. (5.5). The integrands in the second and the third terms are limited (though $V$ is discontinuous), and their integrals vanish (Eq. (5.4)). This gives:

$$V(0^+) - V(0^-) = -M \qquad (5.17)$$

Now, for evaluating the discontinuities in $C_A$ and $T$, integrating Eq. (5.11) gives:

$$\int_{0^-}^{0^+} \frac{d}{dt}(VC_A)dt = \int_{0^-}^{0^+} v_o C_{Ao} dt - \int_{0^-}^{0^+} \{c_1 V + M\delta(t-t_o)\}C_A dt - \int_{0^-}^{0^+} k_o e^{-E/RT} C_A dt \tag{5.18}$$

The third term in this equation is evaluated according to the sifting property of $\delta$-Dirac function, Eq. (5.6), and, thus, the integral evaluated at $t_o = 0^+$ is: $MC_A(t_o) = MC_A(0^+)$. Eq. (5.18) yields an implicit equation:

$$V(0^+)C_A(0^+) - V(0^-)C_A(0^-) = -MC_A(0^+) \tag{5.19}$$

Combining this with Eq. (5.17) and solving, gives the initial discontinuities in $C_A$ (and similarly $T$, see also Example 2):

$$C_A(0^+) - C_A(0^-) = 0\,;\;\; T(0^+) - T(0^-) = 0 \tag{5.20}$$

Thus, initialization A yields these initial discontinuities to be zero. Similarly, all these discontinuities in $V, C_A$, and $T$ are the same as well for the case of exit flow following the square-root relation Eq. (5.14'), these are used in the numerical solutions below.

**Remark 1** *A linear case:* It may be noted that Eq. (5.15) is linear, and its solution can be obtained by using the following elementary Laplace analysis. Eq. (5.15) is first subtracted from the same equation at $t \to 0^-$. This equation upon Laplace transformation and inverse transformation ($v_o$ is constant), gives ($s$ is the Laplace parameter):

$$s(V - V(0^-))(s) = (v_o - v_o(0^-))(s) - c_1(V - V(0^-))(s) - M\;; \tag{5.21}$$

$$(V - V(0^-))(s) = -\frac{M}{s + c_1}; \qquad V(t) - V(0^-) = -Me^{-c_1 t} \tag{5.22}$$

The initial discontinuity evaluated from this equation at $t \to 0^+$ turns out to be ($-M$), i.e., the same as given by Eq. (5.17). This also turns out to be the same from the physical balances (initialization B below).

***Initialization B***

Impulse is now included in the effect. Application of material and energy balances to the initial effect of impulse on conditions of the system also gives the same extent of the above initial discontinuities. The impulse in $v$ is realized by suddenly withdrawing $M$ ($m^3$) of liquid from the tank, all in one go. Thus, the holdup volume of tank decreases by an amount $M$, which is same as in Eq. (5.17) above.

Next, applying the component material balance on $A$ and energy balance lead to zero initial discontinuities in $C_A$ and $T$ respectively, since withdrawing $M$ ($m^3$) of liquid at the exit conditions $C_A(0^-)$ and $T(0^-)$ from the tank that is already at this state, will cause no initial change in the state of the tank. These definitely known results through initialization B conform to the results obtained through initialization A above.

**Remark 2** *A transformed model case:* However, in the above model, if Eq. (5.11) was transformed by applying differentiation rule of the product of variables $V$ and $C_A$ on the left hand side, and substituting material balance Eq. (5.10) for the differential of $V$, one would obtain (some studies use such an equation as in Example 2 below):

$$\frac{dC_A}{dt} = \frac{v_o}{V}(C_{Ao} - C_A) - kC_A$$

Finding the initial discontinuities from this equation (and similarly for $T$) through initialization A, as is done above, would yield:

$$C_A(0^+) - C_A(0^-) \neq 0; \;\; T(0^+) - T(0^-) \neq 0 \qquad (5.23)$$

which are obviously wrong. Hence, the original, mathematically non-transformed models must be used to obtain correct results from the procedure. Its relevance comes across further in later discussion.

***Perturbation in $T_j$***

Let $M$ (K)(s) be the magnitude of the impulse perturbation in the jacket temperature. The initial discontinuity in the tank temperature $T$ through initialization A on Eq. 5.12 comes out to be $U_h A_h M / V\rho C_p$ (K). This is same through initialization B as shown below.

***Initialization B*** The impulse perturbation of magnitude $M$ (K)(s) in $T_j$ is equivalent to introducing $U_hA_hM$ (Joules) of enthalpy directly into the tank, all in one go. This causes the same increase in the tank temperature $T$ of $U_hA_hM$ / $V\rho C_p$ (K) through the application of energy balance at the initial instant as:

Initial change in temperature in tank = Enthalpy change of $U_hA_hM$ (J) per unit thermal capacity of the tank liquid (J/K)

$$T(0^+) - T(0^-) = U_h A_h M \,/\, V\rho C_p \tag{5.24}$$

***Perturbation in $C_{Ao}$:*** A perturbation in $C_{Ao}$ makes Eq. (5.11) *linear*, it can also be verified that it would result in identical initial conditions for $C_A$ through initializations A, B, and the Laplace analysis. This case was considered in Section 4.2.4, wherein it was shown that the system exhibits same results for $C_A$ but different ones for the product concentration $C_R$ through the two alternative initialization routes (see also Chapter 6).

***Perturbation in $v_o$:*** Similarly, it can be shown that a perturbation in the volumetric feed rate $v_o$ results in the same initial discontinuities through initializations A & B, again if the original non-transformed models are used (as is shown in Example 2).

***Initialization C:*** For perturbation in $v$, the system was solved numerically with the Dirac function $\delta(t - t_o)$ in Eq. (5.15) replaced with the Gauss pulse term $\frac{1}{a\sqrt{\pi}} e^{-t^2/a^2}$.

### 5.3.1 Numerical results

To quantify the resultant effects of the initial conditions, the numerical solution of this model for impulse perturbation in exit flow rate $v$ was carried out using the above initializations A & B and the results were compared with the approach of smoothening of impulse (initialization C). For the numerical solution, Eqs. (5.10) and (5.12) were numerically integrated and the results of $V$ and the product $(V \times T)$ were obtained with

respect to time, respectively; the values of $T$ were obtained as: $T = (V \times T)/V$. The parameter values used are presented in Table 5.1. The magnitude of impulse input, $M$ = $3.40 \times 10^{-1}$ m$^3$ (25% of the initial holdup volume) was used.

**Table 5.1** Parameters for Non-isothermal CSTR

| | | |
|---|---|---|
| $V = 1.359$ m$^3$ | $C_{Ao} = 8.0$ kg mol/m$^3$ | $R = 8.314 \times 10^3$ J/kg mol-K |
| $A_h = 23.225$ m$^2$ | $\rho = 800.848$ kg/m$^3$ | $\Delta H_R = -6.978 \times 10^7$ J/kg mol |
| $T_j = 330.33$ K | $k_o = 1.967 \times 10^7$ /s | $E = 6.978 \times 10^7$ J/kg mol |
| $T_o = 294.44$ K | $v_o(0^-) = 3.147 \times 10^{-4}$ m$^3$/s | $U = 851.721$ W/m$^2$-K |
| $T(0^-) = 333.33$ K | $C_A(0^-) = 3.924$ kg mol/m$^3$ | $C_p = 3.140 \times 10^3$ J/kg-K |

The results for $V$ are presented in Fig. 5.3 for the square-root resistance, where the curves corresponding to initializations A, B, and C are plotted together. The results converge to the consistent steady state values. Initializations A and B yield identical curve, give the correct quantitative results, and exhibit the correct initial discontinuity of $3.40 \times 10^{-1}$ m$^3$. This value *must* be achieved as is seen even from the elementary Laplace analysis in Remark 1. However, it is observed that the smoothening approach yield highly inaccurate results, since it can't reveal the actual asymptotic behavior despite several decreasing value of the parameter $a$, as the curve for initialization C exhibit an initial discontinuity of only $1.59 \times 10^{-1}$ m$^3$, i.e., an error of 53%, and shows large deviations (NRMSD = 21%) from the correct curve obtained through initializations A & B.

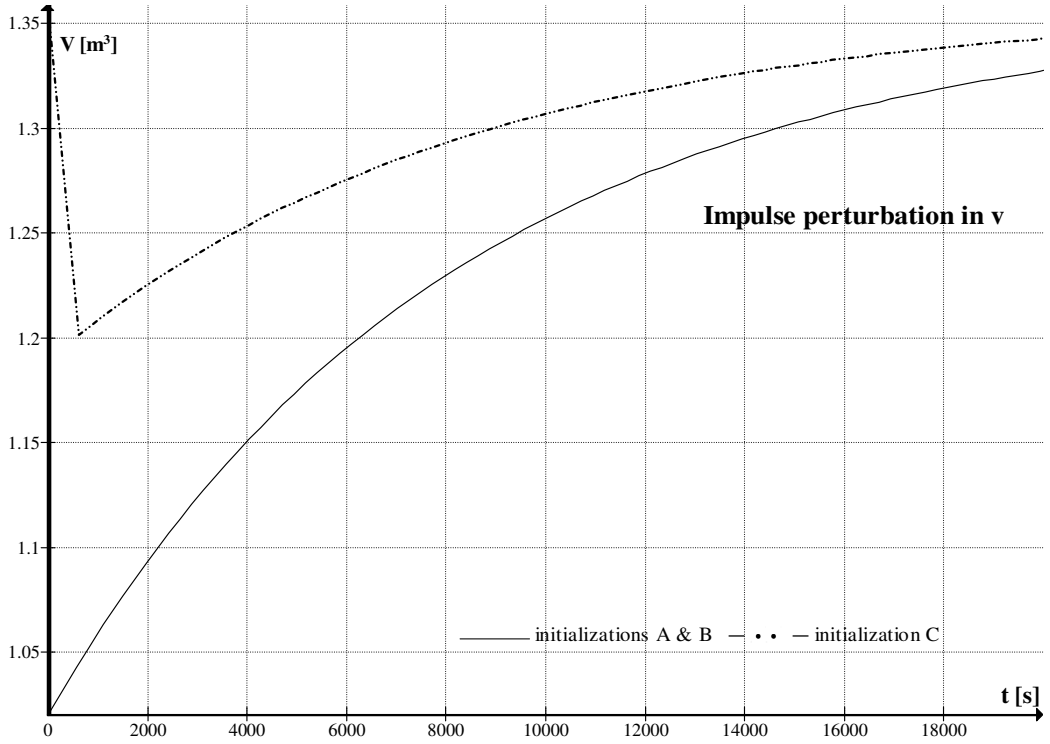


**Fig. 5.3** Comparison of alternative initialization approaches for impulse response of holdup volume of CSTR, to a perturbation in exit volumetric flow rate

The curves for $C_A$ and $T$ are plotted in Figs. 5.4 and 5.5. The response curves plotted through initialization C show large error deviations of 26% for $C_A$, and 12% for $T$, from the corresponding correct curves obtained using initializations A & B. For decreasing value of $a$, viz. $a = 10^{-4}$, $a = 10^{-5}$, and $a = 10^{-6}$, there is no improvement in the behavior of the curves for initialization C as these curves overlap. Exactly the same was observed for the linear resistance when the value of $a$ was decreased, as the curves practically overlapped even until the value of $a$, as low as $a = 10^{-150}$. Simulations failed below the respective lowest values mentioned for the square-root and the linear resistances.

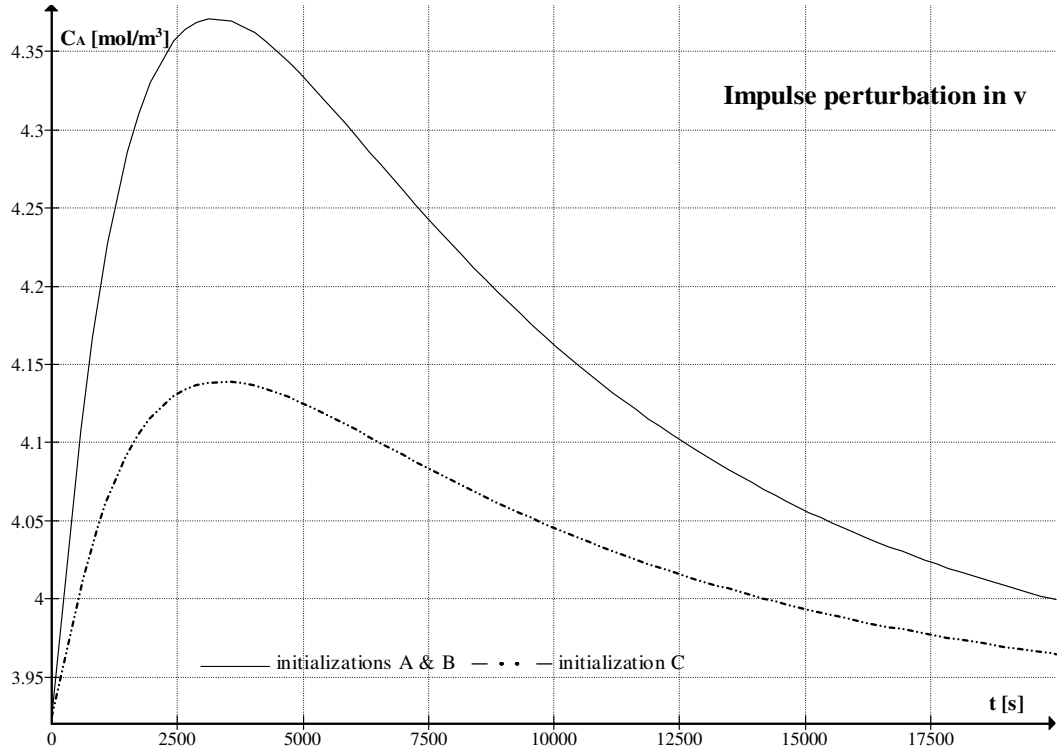


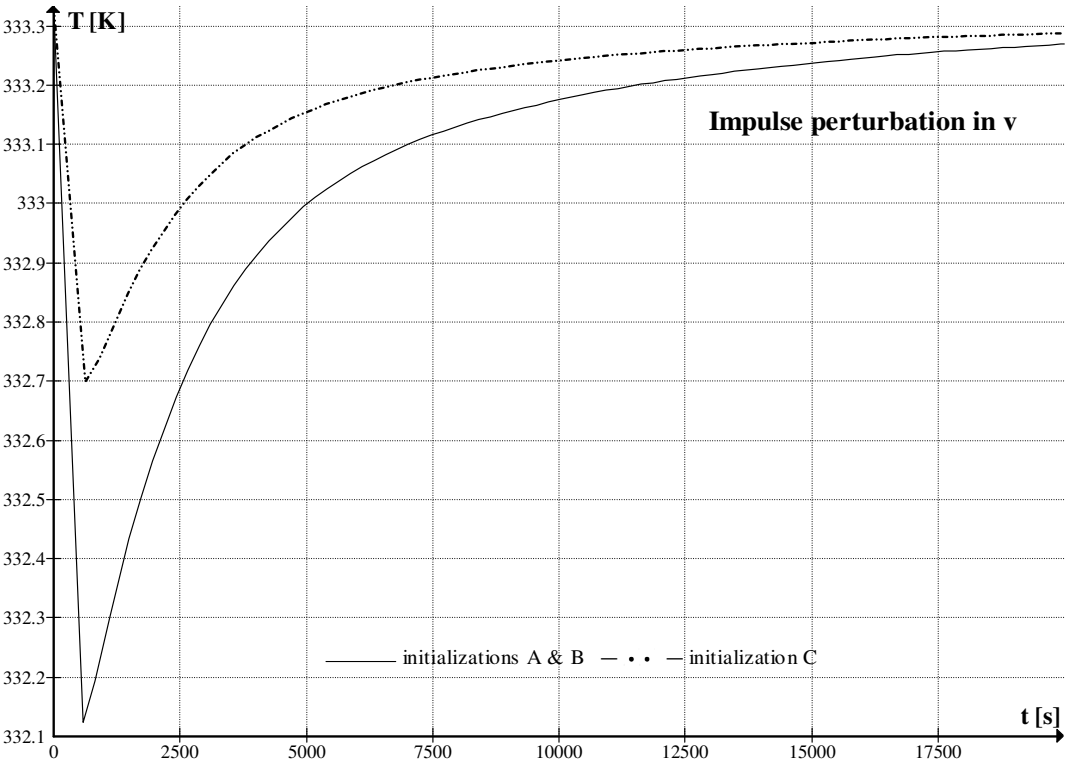


**Figs. 5.4 and 5.5** Comparison of alternative initialization approaches for impulse response of concentration and temperature, respectively in variable holdup CSTR, to a perturbation in exit volumetric flow rate

To observe these effects minutely and more accurately, the simulations for initializations C were repeated by focusing on the initial time duration of only 0.9 s. These curves are plotted together for $V$ in Fig. 5.6, for the square-root resistance, for several decreasing value of $a$, viz. $a = 10^{-4}$, $a = 0.5\times10^{-4}$, $a = 0.25\times10^{-4}$, $a = 10^{-5}$, $a = 10^{-6}$, and $a = 0.25\times10^{-6}$ below which the simulation failed. It can be observed from this figure that as the value of $a$ decreases, the value of the initial discontinuity in $V$ (occurring at $t$ ~ 0.02 s) is the same of $1.70 \times 10^{-1}$ m$^3$ (against the correct value of $3.40 \times 10^{-1}$ m$^3$), thus, exhibiting a very high error of 50 %. This value of initial discontinuity is the same in all these cases, and there is no improvement upon decreasing the value of $a$ below $a = 10^{-6}$, as the curves for $a = 10^{-6}$ and $a = 0.25\times10^{-6}$ practically overlap. The behavior couldn't be improved even on increasing the accuracy further by decreasing the focus of the time duration.

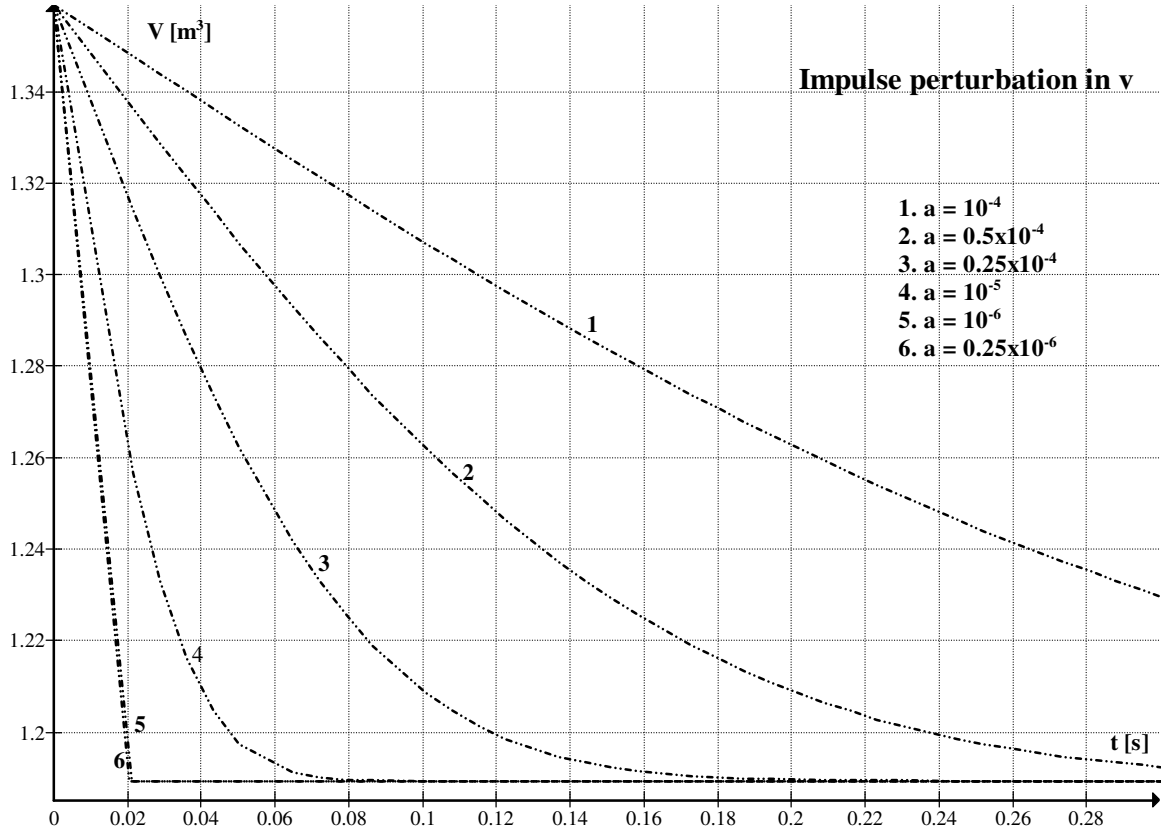


**Fig. 5.6** Comparison of the impulse response of holdup volume of variable holdup CSTR, to a perturbation in exit volumetric flow rate, for decreasing value of parameter $a$ of smoothened impulse function

### 5.3.2 Discussion

The above treatment of Example 1 substantiates the applicability of the proposed methodology as it predicts the correct and the same initial conditions as are obtained from an elementary physical balance or Laplace analysis. The initial discontinuities and solution profiles computed through initialization A exactly conform to the definitely known values of initial discontinuities and solution profiles for several cases, and these are computed equally well through Laplace analysis for the linear cases. Initialization A is, thus, adequate and found to be consistent with initialization B for the above cases.

However, despite extreme sharpening, the smoothened impulse (Gauss pulse) in initialization C is not able to catch up with the initial discontinuity. The solution profiles obtained through initialization C exhibit high magnitudes of error deviations from the correct solution profiles.

This indicates that the Gaussian pulse approximation can't reliably model the singularity of the $\delta$-Dirac function, which is accurately done through initialization A. The limitations of initialization procedure C further come across in the following cases.

## 5.4 Constant Holdup CSTR

The tank is, then, assumed closed and fully filled, so that, the holdup volume $V$ is taken constant. The constant density CSTR, which was at a particular state initially at $t \to 0^-$, is perturbed by an impulse in the volumetric flow rate of the feed $v_o$.

***Initialization A:*** Applying this procedure gives the following discontinuities in $C_A$ and $T$:

$$C_A(0^+) - C_A(0^-) = M\{C_{Ao} - C_A(0^-)\}/(M+V) \tag{5.25}$$

$$T(0^+) - T(0^-) = M\{T_o - T(0^-)\}/(M+V) \tag{5.26}$$

***Initialization B***

The impulse in $v_o$ is realized by plunging $M$ ($m^3$) of liquid feed into the tank, all in one go. Since the tank is closed and fully-filled, and the liquid is incompressible; this sudden introduction *will cause a sudden ejection* (*of an equal volume*) *of the already present tank*

*fluid at concentration* $C_A(0^-)$ *and temperature* $T(0^-)$. Applying material balance on *A*, to these effects of the impulse, gives:

Initial change in moles of *A* in tank = (Moles of *A* in the inserted *M* ($m^3$) of liquid that is at concentration $C_{Ao}$ (mol/$m^3$)) — (Moles of *A* in the ejected *M* ($m^3$) of liquid that is at concentration $C_A(0^-)$ (mol/$m^3$)), or:

$$VC_A(0^+) - VC_A(0^-) = MC_{Ao} - MC_A(0^-)$$

$$C_A(0^+) - C_A(0^-) = M\{C_{Ao} - C_A(0^-)\}/V \tag{5.27}$$

So, the corresponding discontinuities calculated from material balance on the effects are not the same as in the cause (Eq. (5.25)). On exactly same lines, energy balance gives:

Initial change in enthalpy in tank = (Enthalpy of the inserted *M* ($m^3$) of liquid that is at temperature $T_o$) — (Enthalpy of the ejected *M* ($m^3$) of liquid that is at temperature $T(0^-)$), or:

$$V\rho C_p T(0^+) - V\rho C_p T(0^-) = M\rho C_p T_o - M\rho C_p T(0^-)$$

$$T(0^+) - T(0^-) = M\{T_o - T(0^-)\}/V \tag{5.28}$$

Hence, unlike the previous case, the initial discontinuities calculated from model's considerations (initialization A) are not consistent with that calculated from the consideration of physical balances (initialization B).

### 5.4.1 Numerical results

The numerical results for the above impulse perturbation in feed rate $v_o$ are discussed. The parameter values are the same as presented in Table 5.1. A magnitude of perturbation, $-3.40 \times 10^{-1}$ $m^3$ (25% of the initial value), was, first, used for the three initializations A, B, and C. For initialization C, an extremely low value of *a*, i.e.,

$a = 10^{-150}$ was used. The results for $C_A$ and $T$ are presented in Figs. 5.7 and 5.8, respectively. *In all Figs. henceforth, the darkened segments along the y-axis mark the magnitude of initial discontinuities.* The results converge to the consistent steady state values. For $C_A$ and $T$ respectively, the profiles for initialization C show significant deviations of 20% and 10% from the solution profile for initialization B; whereas, the corresponding deviations in the solution profiles for initialization A are of much smaller magnitudes of 11% and 4%.

A lower magnitude of perturbation, $-1.13 \times 10^{-1}$ m$^3$ (8% of the initial value), was, then, used, and the above runs were repeated. The above deviations for initialization C remained nearly the same of 19% for $C_A$ (Fig. 5.9), and 10% for $T$ (Fig. 5.10). Thus, the deviations are significant as in the previous case, which reaffirm the non-applicability of the smoothening of impulse approach, irrespective of the magnitude of perturbation.

However, for initialization A, the deviations reduce to as low as 6% for $C_A$ (Fig. 5.9), and 2% for $T$ as the curves for initializations A and B practically overlap (Fig. 5.10), for this reduced magnitude of perturbation, $-1.13 \times 10^{-1}$ m$^3$. So, as the magnitude of the initial discontinuities decrease, the deviations become further smaller.

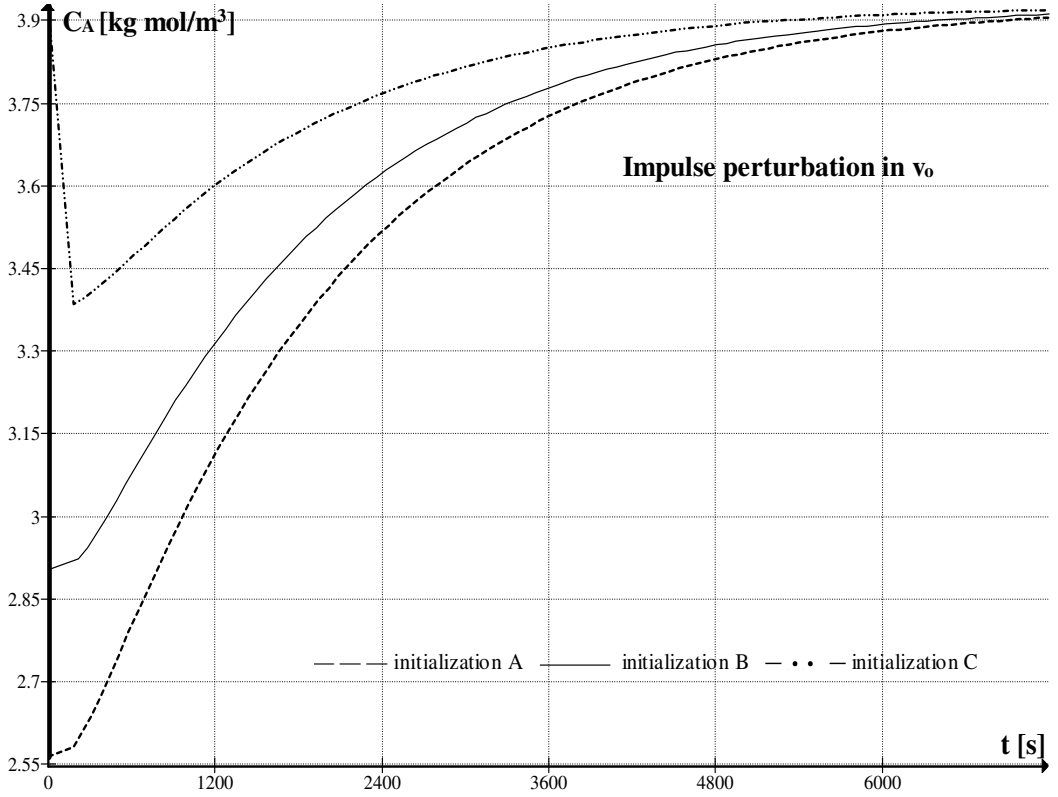


**Fig. 5.7** Comparison of alternative initialization approaches for concentration response of constant holdup CSTR to an impulse perturbation in volumetric feed rate

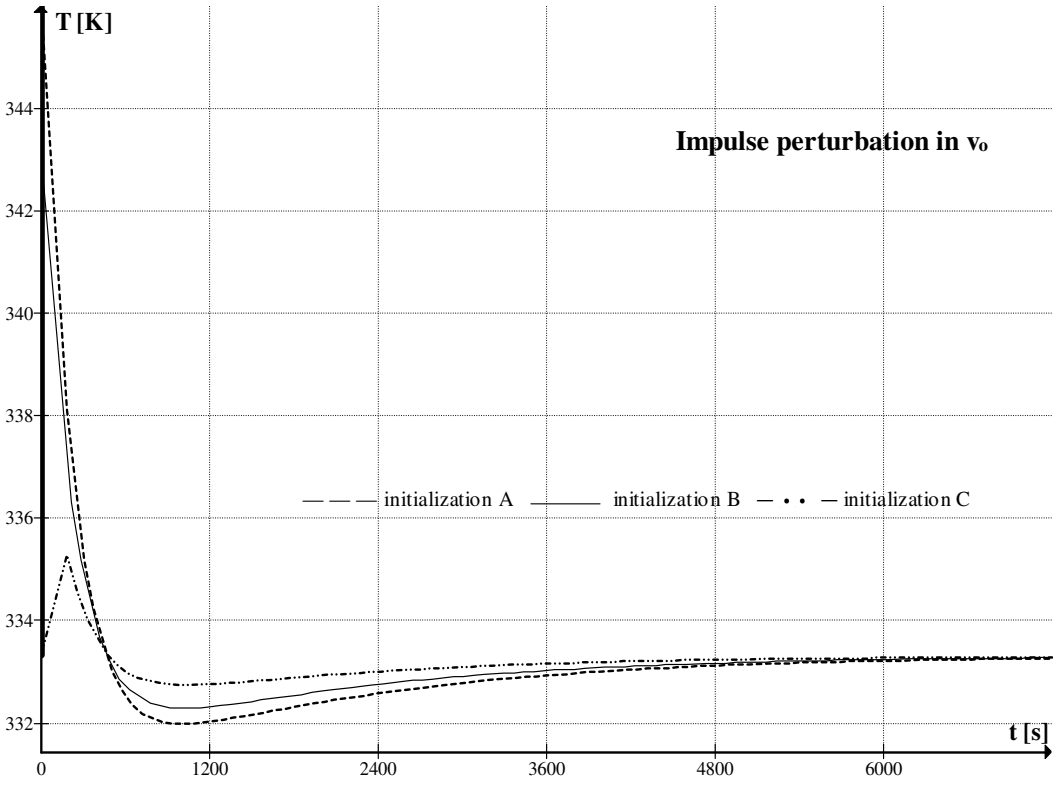


**Fig. 5.8** Comparison of alternative initialization approaches for temperature response of constant holdup CSTR to an impulse perturbation in volumetric feed rate

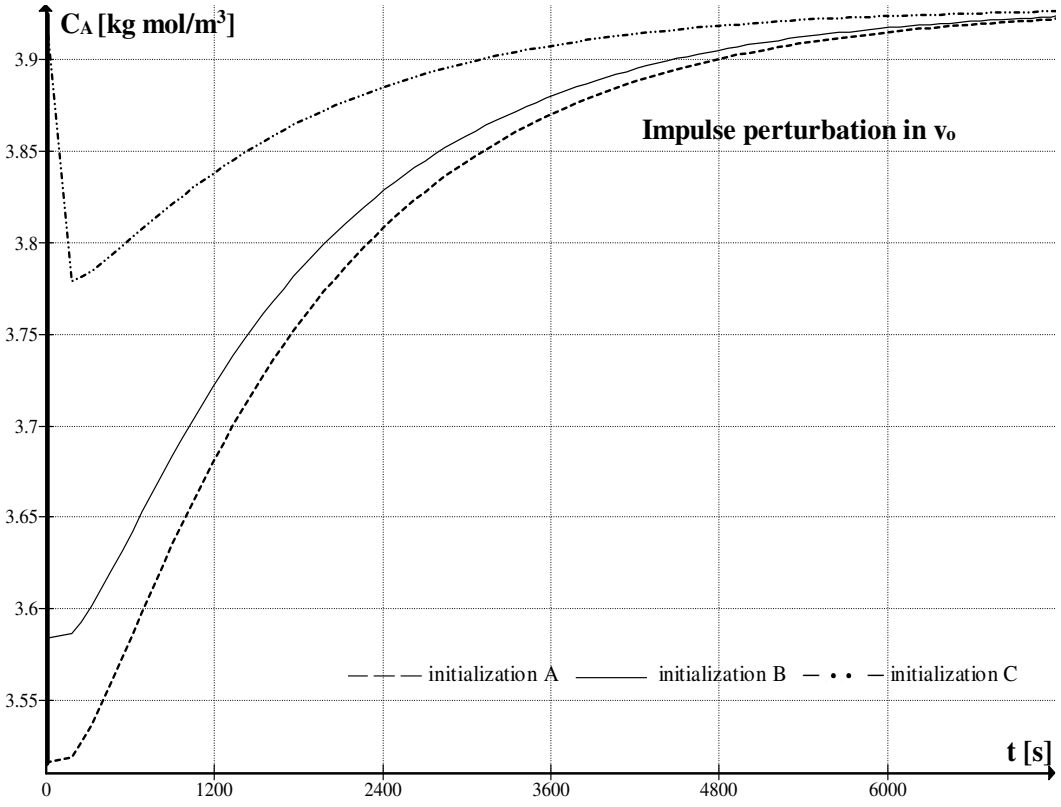


**Fig. 5.9** Comparison of alternative initialization approaches for concentration response of constant holdup CSTR to a lower magnitude of impulse perturbation in volumetric feed rate

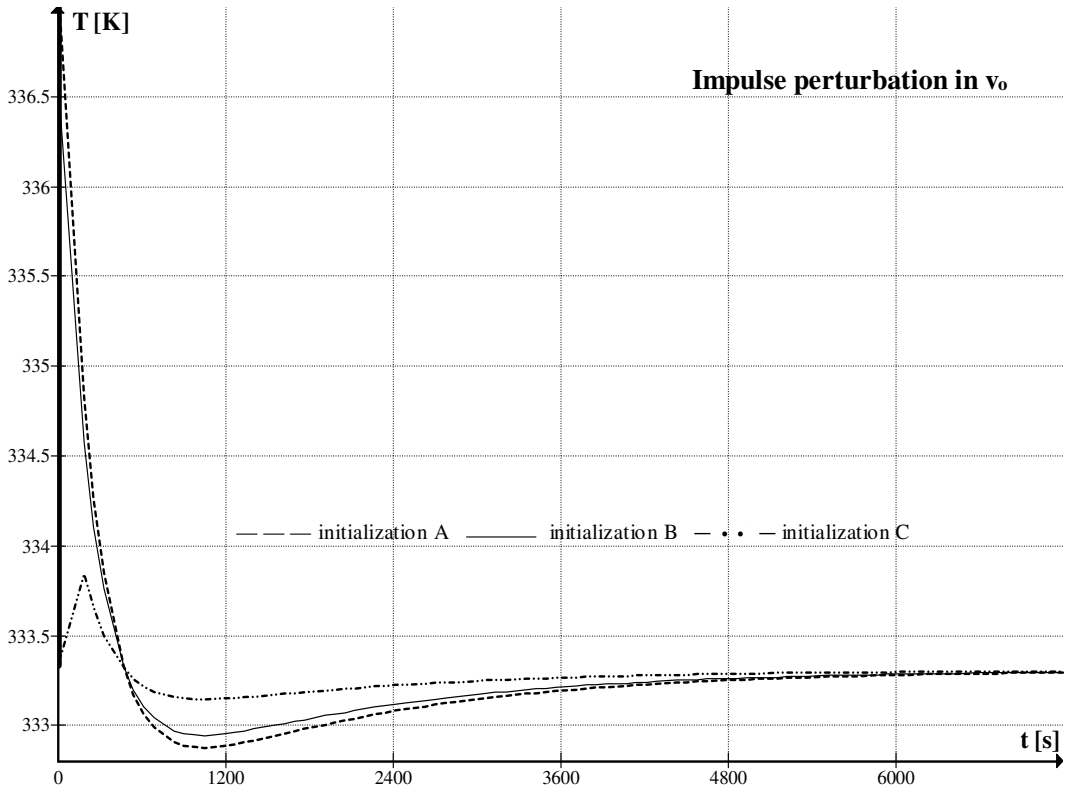


**Fig. 5.10** Comparison of alternative initialization approaches for temperature response of constant holdup CSTR to a lower magnitude of impulse perturbation in volumetric feed rate

### 5.4.2 Outcomes revisit

Initialization A can be adequately used for moderate magnitudes of perturbation, i.e., for the system not being operated very far away from its normal operating conditions, whereas, initialization C is found to be inadequate.

## 5.5 Example 2

Consider the vapor-phase dynamics, single component condenser system described in Sections 3.4, and 3.4.1. It assumes quasi-static conditions, so that, the specific rate of condensation is small and, thus, at any moment, the amount of vapor condensed is small in comparison to the amount of vapor present in the condenser. Hence, the time rate of accumulation of the material and energy in the liquid phase can be neglected. Therefore, this model neglects the dynamics of the liquid phase. It also assumes that vapor and

liquid are in equilibrium throughout and any sub-cooling of the liquid is, thus, neglected. So, the pressure of the vapor is replaced by the vapor pressure of the liquid.

$$\frac{dT}{dt} = \frac{F}{N}(T_o - T) + \frac{L\Delta H}{NC_p} + \frac{UA_h}{NC_p}(T_j - T) \tag{5.29}$$

$$C_p \frac{d(NT)}{dt} = FC_pT_o + UA_h(T_j - T) - L(C_pT - \Delta H) \tag{5.29'}$$

$$\frac{dN}{dt} = F - L \tag{5.30}$$

$$P^* = A\exp\left(-\frac{B}{T+C}\right) \tag{5.31}$$

$$V = \frac{NRT}{P^*} \tag{5.32}$$

Eq. (5.29) is energy balance on the vapor phase, Eq. (5.30) is the molar balance on the vapor phase, Eq. (5.31) is the Antoine's equation and Eq. (5.32) is the equation of state for vapor. For *L*, various equations have been assumed in the literature, i.e., the equations based on valve or weir characteristics, controller equations, etc. (Luyben, 1996; Unger et al., 1995). In the following treatment, the molar rate of condensation of vapors (also equal to exit molar flow rate of liquid *L* as there is no accumulation of liquid as per the vapor-phase dynamics assumptions) is taken proportional to the moles of vapor *N* at any time, this gives:

$$L = c'N \tag{5.33}$$

The constant of proportionality $c'$ is based on the pre-initial conditions. As remarked in Example 1, it re-emphasized here that the magnitudes of the initial discontinuities resulting through the framework, and hence, the effects to be studied are independent of the choice of this equation because any selected equation—as can be seen in the treatment that follows—would yield a limited integrand, whose integral would be zero according to Eq. (5.4) of the framework.

As noted in Section 3.4.1 of Chapter 3, Eq. (5.29) has been used in the literature and is obtained through symbolic manipulations and differentiation of the original energy balance Eq. (5.29'). This model works for the step input only, and not for the impulse input (as is also seen through Eqs. (5.23) and (5.24) in the CSTR case).

The original energy balance Eq. (5.29') was formulated in section 3.1.1. In this section, explicit model containing Eqs. (5.29') through (5.33) is considered. The numerical results obtained from this model are also plotted along with the corresponding results of mathematically transformed models approaches in Section 5.13, where several limitations of mathematical transformations are discussed.

***Perturbation in F***

For impulse perturbation in $F$, the initial discontinuity in $T$ is given by the following Eq. (5.34), obtained through initialization A.

***Initialization A:*** It is applied (presented in brief) on Eqs. (5.30) and (5.29'), respectively:

$$\int_{0^-}^{0^+} \frac{dN}{dt} dt = \int_{0^-}^{0^+} F(0^-) dt + M \int_{0^-}^{0^+} \delta(t - t_o) dt - \int_{0^-}^{0^+} L dt \tag{5.34.a}$$

$$N(0^+) - N(0^-) = M \tag{5.34.b}$$

$$C_p \int_{0^-}^{0^+} \frac{d}{dt}(NT) dt = \int_{0^-}^{0^+} FC_p T_o dt + \int_{0^-}^{0^+} UA_s (T_c - T) dt - \int_{0^-}^{0^+} L(C_p T - \Delta H) dt \tag{5.34.c}$$

$$C_p N(0^+) T(0^+) - C_p N(0^-) T(0^-) = C_p M T_o \tag{5.34.d}$$

$$T(0^+) - T(0^-) = \frac{M\{T_o - T(0^-)\}}{N(0^+)} \tag{5.34.e}$$

***Initialization B:*** Physical balances on the conditions of the system at the time of introduction of the input also give the same extent of discontinuities in both $N$ and $T$. The impulse in $F$ is introduced by plunging $M$ moles of vapor into the condenser at the feed temperature $T_o$, all in one go. So, the sudden rise in the energy of the vapor in the condenser (same as the left side of Eq. (5.34.d)), is equal to the enthalpy of $M$ moles of vapor added at temperature $T_o$ (same as the right side of Eq. (5.34.d)). Eq. (5.34) yields

mutually consistent results for the initialization procedures A and B of the framework, and the system, thus, remains unaffected by the initial discontinuities.

***Perturbation in L***

Consider, now, a perturbation in the exit liquid molar flow rate *L*. The condenser, which was at a particular state initially at $t \rightarrow 0^-$, suffers an impulse perturbation of magnitude *M* (moles) at $t \rightarrow 0^+$. Now, *L* has *two* components: one of the perturbation and the other of the initial discontinuity caused by the change in *N* (since, $L = c'N$). Therefore, the value of *L* is placed as: $L = c'N + M\delta(t - t_o)$ with $t_o = 0^+$ in the model (Note that $c'N$ already includes $L(0^-)$).

***Initialization A:*** Initialization A on Eqs. (5.30) and (5.29') as in Example 1 gives:

$$N(0^+) - N(0^-) = -M \tag{5.35}$$

$$T(0^+) - T(0^-) = \frac{M\Delta H / C_p}{N(0^-)} \tag{5.36}$$

***Initialization B***

The discontinuity for *N*, calculated from material balance is the same as that given by Eq. (5.35). However, the discontinuity for *T*, calculated from energy balance, is not equal to the discontinuity given by Eq. (5.36). As *M* moles of liquid are removed from the condenser, the initial change in the energy of the vapors in the condenser is equal to the enthalpy of *M* moles of condensed liquid leaving the condenser (including the enthalpy of condensation). And, the rate of condensation is equal to the rate of exit of liquid, as per the assumptions of the model. So:

$$N(0^+)C_pT(0^+) - N(0^-)C_pT(0^-) = -M(C_pT(0^-) - \Delta H) \tag{5.37}$$

Combining Eq. (5.37) with Eq. (5.35), and solving for the initial discontinuity in *T*, gives:

$$T(0^+) - T(0^-) = \frac{M\Delta H / C_p}{N(0^+)} \tag{5.38}$$

Hence, in this case, the initial discontinuity calculated from initialization A is not consistent with that calculated from initialization B. Therefore, the impulse response is affected by the discontinuities as seen from the following results of numerical solutions.

### 5.5.1 Numerical results

The parameter values used for the numerical solution are presented in Table 5.2. An impulse perturbation in $L$ is considered for the three initializations A, B, and C. For initialization C, an extremely low value of $a$, i.e., $a = 10^{-150}$ was used. The variables $P$ and $T$ exhibited high sensitivity to the initialization effects. Other variables exhibited little sensitivity. The results converge to the consistent steady state values. The results for $N$ are presented in Fig. 5.11 for a magnitude of impulse of 100 mol (27% of the initial mol of vapor).

**Table 5.2** Parameters for the Condenser Example

| For Example 2 | | | |
|---|---|---|---|
| $\Delta H = 5.0\times10^{3}$ J/mol | $F(0^-) = 50$ mol/s | $L(0^-) = 50$ mol/s | $A = 1.2\times10^{10}$ Pa |
| $UA_h = 2.0\times10^{3}$ W/K | $M = 100$ mol | $T(0^-) = 376.73$ K | $B = 3816$ K |
| $C_p = 3.35\times10^{2}$ J/mol-K | $V(0^-) = 10$ m$^3$ | $N(0^-) = 373.63$ mol | $C = -46$ K |
| $R = 8.314$ J/mol-K | $T_o = 373$ K | $T_j = 283$ K | $k = 1.338\times10^{-1}$ (mol/s)/mol |

Initializations A and B yield identical curve, give the correct quantitative results, and exhibit the correct initial discontinuity of 100 mol. Whereas, the initialization C curve exhibit an initial discontinuity of only 44.33 mol, and shows large deviations from the correct curve, thus, exhibiting the inadequacy of initialization C once again. The error deviation in the two curves is of 17%.

The results for $T$ are presented in Fig. 5.12. The initializations A and C curves respectively exhibit initial discontinuity values of 1.617 K and 3.99 K, against the value of 5.452 K exhibited by the initialization B curve based on the considerations of physical

balances. The deviation of the initialization C curve vis-à-vis the initialization B curve is a significant value of 13%; whereas, the corresponding deviation of the initialization A curve is only of 5%.

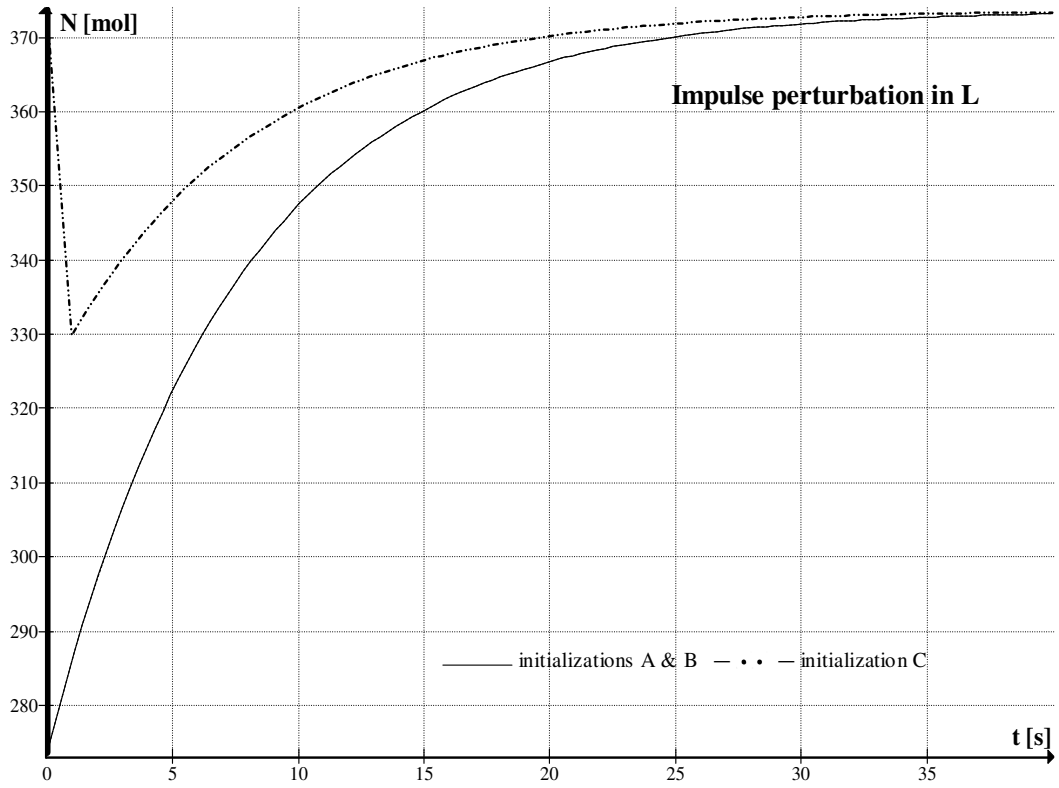


**Fig. 5.11** Comparison of alternative initialization approaches for impulse response of moles of vapor in condenser, to a perturbation in exit liquid molar flow rate

These runs were, then, repeated for a lower magnitude of impulse of magnitude, 30 mol (8% of the initial mol of vapor). The initialization C curve for *N*, presented in Fig. 5.13, shows the same magnitude of deviation, i.e., of 17%. The results for *T* are shown in Fig. 5.14, where again it is clearly seen that the initialization C curve still shows an error of 12%, thus, confirming our earlier observations of inadequacy of initialization C, in spite of the decreased magnitude of perturbation.

However, in same Fig. 5.14, the initialization A curve comes even closer to the initialization B curve, and the corresponding deviations become insignificant (2%) for this small magnitude of perturbation of 30 mol.

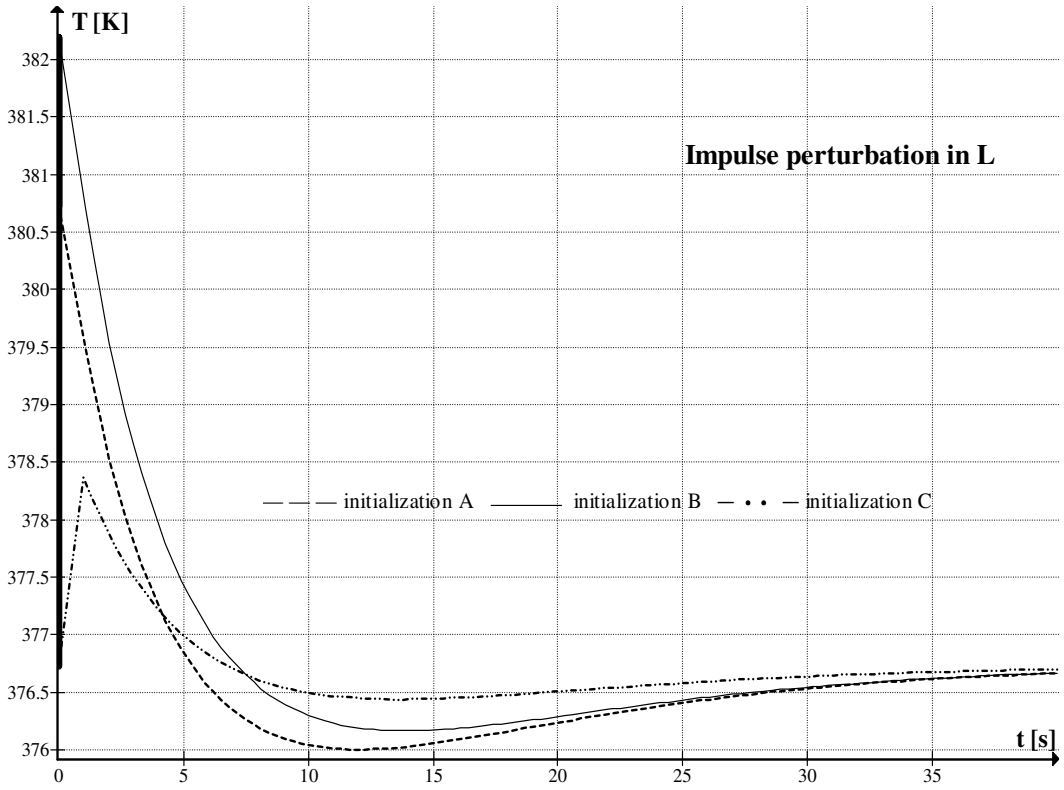


**Fig. 5.12** Comparison of alternative initialization approaches for impulse response of temperature in condenser to a perturbation in exit liquid molar flow rate

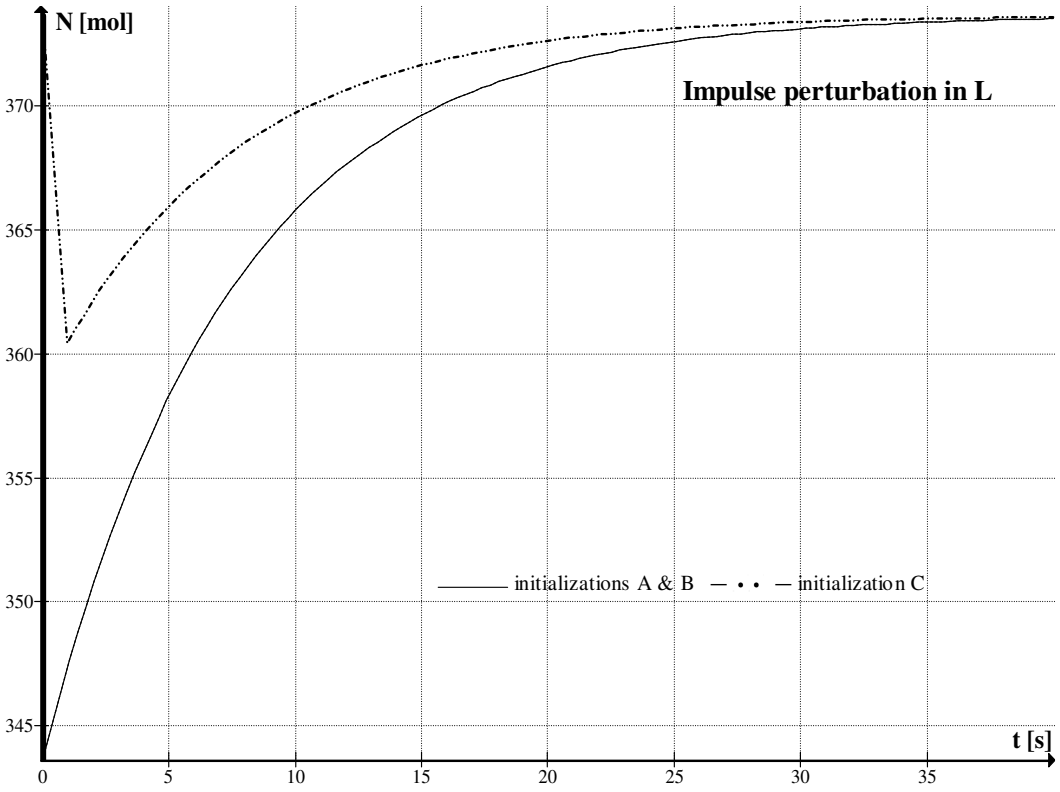


**Fig. 5.13** Comparison of alternative initialization approaches for impulse response of moles of vapor in condenser, to a lower magnitude of perturbation in exit liquid molar flow rate

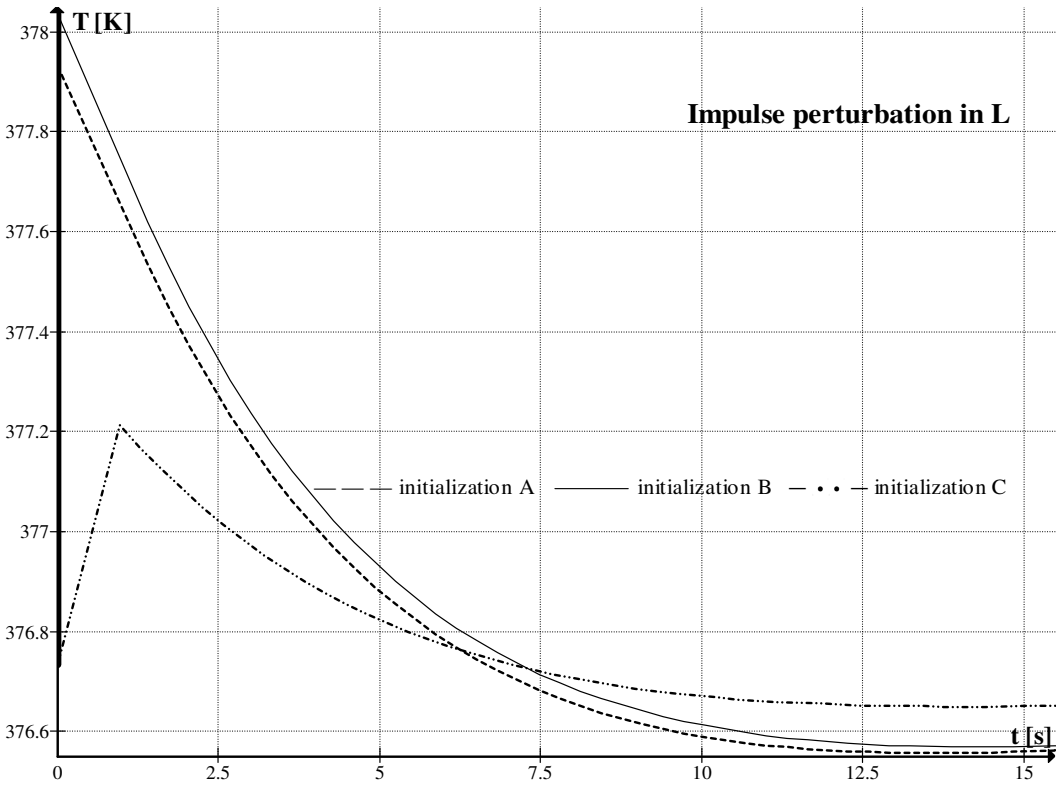


**Fig. 5.14** Comparison of alternative initialization approaches for impulse response of temperature in condenser, to a lower magnitude of perturbation in exit liquid molar flow

## 5.6 Discussion

Cumulative results are now discussed. For linear and nonlinear cases studied throughout this chapter (Examples 1 through 5), it is found that initialization A (or alternatively the Laplace analysis) is consistent with initialization B for many cases. However, it can also be inconsistent with initialization B for many other cases, which indicates the inherent inability of a model to exactly represent the physical system affected by singularity at the origin. Thus, the techniques of Laplace transformation of a model, and initialization A of integration of a model (interpreted as area under a curve) have inherent limitations of mathematical representation of singularity. The machinery of generalized functions also involves many complications and ad hoc interpretations when the Dirac function is multiplied with a discontinuous function, and, hence, some studies prefer to use the basic integral notion rather than the generalized integral notion (Grizzle, 2004; Makila, 2006). These remarks are more appropriate for the nonlinear systems for which the machinery

involves further mathematical technicalities (Pilipchuk, 1999). Thus, the model's considerations would inherently lead to less than exact solution profiles for some cases, which are, therefore, affected by the discontinuities.

Nevertheless, the numerical results exhibit that initialization A attains exact or close to exact initial values, while initialization C—despite extreme sharpening of the smoothened impulse—is far off from the correct initial values calculated from the application of the physical balances (initialization B) or Laplace analysis. Also, initialization A exhibits small deviations, while initialization C exhibits large deviations in their solution profiles. Furthermore, on decreasing the magnitudes of perturbation, the errors for initialization A decrease sharply and become negligible, while the percentage errors for initialization C remain nearly the same (though actual errors decreased marginally).

The outcomes of these examples, thus, show that the initialization procedure A that involves including the impulse in the cause, can be safely used for the systems operated not very far away from their normal operating conditions. Operations fairly close to the normal operating conditions are of significant practical importance if the plant variables are well controlled to remain close to the steady state. Hence, initialization A, based on ready-to-use initial integration of the model, can be a good substitute to the procedure of initialization B that requires additional effort of applying physical balances on the effects of singularity at the origin.

However, the same is not true for initialization C, based on the smoothening of impulse function, which is found to be highly inadequate in all the cases of above examples, and, so, is not discussed further. *Nevertheless, the trajectories for initializations A, B, and C of all the cases studied exhibited the same trend and so the plausibility of our results.*

## 5.7 Example 3

This example is selected to illustrate the effect of initial conditions on the closed-loop systems in the presence of dynamic lags. This is done by the comparison of the solution profiles of an open and closed loop system with dead time obtained through initializations A and B. Consider the stirred tank heater system of Section 3.7, Chapter 3:

$$\frac{dT_m}{dt} = K_1 Q(0^-) - K_1 K_c T_m(t-\tau_d) + K_1 K_c T_m(0^-) + K_3 v_o(t-\tau_d) - K_2 v_o(t-\tau_d) T_m$$
$$\text{where } K_1 = 1/\left(\rho C_p v_o\right),\ K_2 = 1/V,\ \text{and } K_3 = T_o/V \tag{5.39}$$

This DDE couldn't be solved through ordinary means; hence, an independent program was developed (algorithm is presented in Appendix II).

***Initialization A:*** If the impulse is included in the cause, $v_o = v_o(0^-) + M\,\delta(t-t_o)$, with $t_o = 0^+$. Thus, $v_o(t-\tau_d) = v_o(0^-) + M\,\delta(t-\tau_d)$. The discontinuities now occur at $t = \tau_d^{\ +}$ because of the dead time. Carrying out the initial integration procedure on Eq. (5.39), the discontinuity in this constant volume system becomes:

$$\int_{\tau_d^-}^{\tau_d^+} \frac{dT_m}{dt} dt = 0 - K_1 K_c \int_{\tau_d^-}^{\tau_d^+} T_m(t-\tau_d).dt + 0 + K_3 \int_{\tau_d^-}^{\tau_d^+} M\,\delta(t-\tau_d).dt - K_2 \int_{\tau_d^-}^{\tau_d^+} M\,\delta(t-\tau_d) T_m dt$$
$$T_m(\tau_d^+) - T_m(\tau_d^-) = \frac{M\{T_o - T_m(\tau_d^-)\}}{V+M} \tag{5.40}$$

***Initialization B:*** However, the corresponding discontinuities calculated from energy balance on the effect are not the same as these. Since the tank is closed and fully-filled, and, the liquid is incompressible; an introduction of $M$ ($m^3$) of liquid at temperature $T_o$ in the tank will cause an equal amount of the additional ejection of tank fluid at temperature $T_m(\tau_d^-)$. Carrying out initial energy accounting in the tank, gives:

$$V\rho C_p T_m(\tau_d^+) - V\rho C_p T_m(\tau_d^-) = M\rho C_p T_o - M\rho C_p T_m(\tau_d^-);$$
$$T_m(\tau_d^+) - T_m(\tau_d^-) = \frac{M\{T_o - T_m(\tau_d^-)\}}{V} \tag{5.41}$$

### 5.7.1 Numerical results

To see the effect of buildup of errors in the closed loop systems in the presence of dynamic lags in the loop, numerical solution of the above model was carried out. The parameter values used for the numerical solution of this model are presented in Table 5.3. Open and closed loop cases were solved almost immediately by the program.

**Table 5.3** Parameters for Closed Loop Stirred Tank Heater

| | | |
|---|---|---|
| $\rho C_p = 9.87\times10^3$ kJ/m$^3$-°C | $T_o = 34$ °C | $V = 5.0\times10^{-4}$ m$^3$ |
| $v_o(0^-) = 1.262\times10^{-5}$ m$^3$/s | $\tau_d = 21.4$ s | $M = 4.0\times10^{-4}$ m$^3$ |
| $K_3 = 6.8\times10^4$ °C/m$^3$ | $T(0^-) = 45$ °C | $K_2 = 2.0\times10^3$/m$^3$ |
| $K_1 = 2.027\times10^{-1}$ °C/kJ | $Q(0^-) = 1.37$ kW | $K_c = 0.35$ kW/°C |

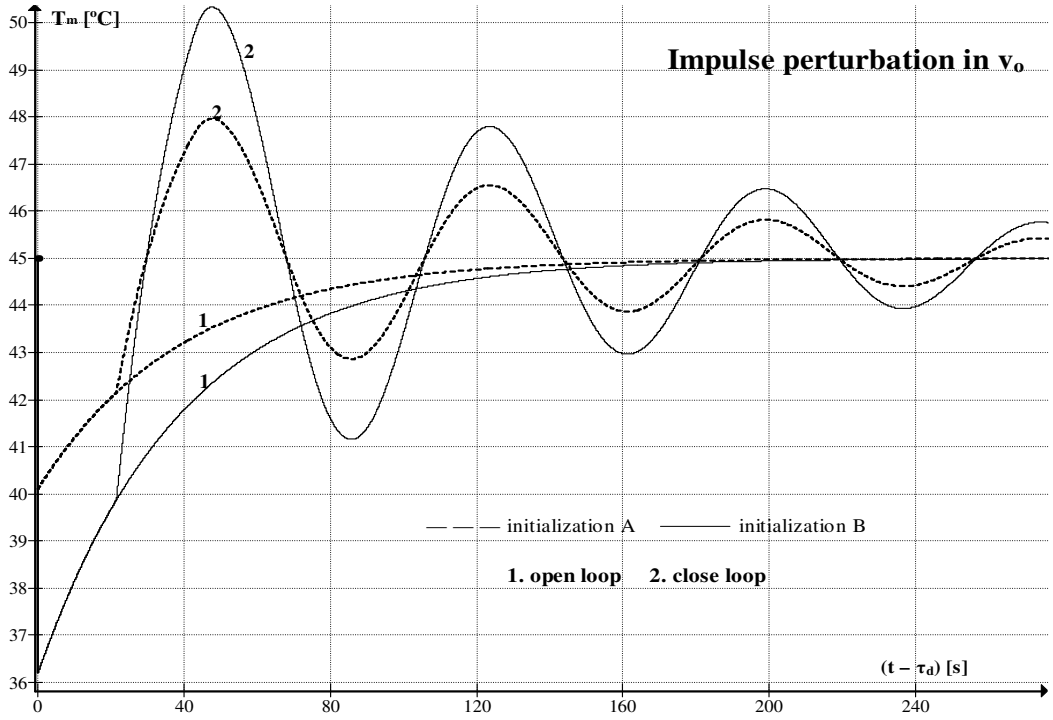


**Fig. 5.15** Comparison of open loop (1) and closed loop (2) cases—Impulse responses of stirred tank heater with dead time ($\tau_d$ = 21.4 s) through alternative initialization approaches

The results are presented in Fig. 5.15 for both the open and the closed loop cases. The systems remain at the steady state until the dead time ($\tau_d = 21.4$ s). The profiles start at one dead time and the discontinuities occur at this time, rather than at zero time. It is interesting to note that the corresponding solution profiles for the open and the closed loop cases are the same for the initial period until a further lapse of *one more* dead time. This is so, because the controller action signal takes one more dead time to reach the

output end. The solutions converge to the consistent steady state values. The deviation between the solution profiles of the two initialization procedures A and B is of 7% for the open loop case, and increases to 10% for the closed loop case. Thus, there are moderate errors involved in the initial integration procedure A for a high magnitude of perturbation of 0.0004 $m^3$.

## 5.8 Outcomes Revisit

The above Examples 1, 2, and 3 show that for relatively high magnitudes of perturbation there are moderate errors in the solution profiles obtained through initialization A, and, so, initialization B may be used in case a high degree of accuracy is the need. Nevertheless, for the systems, in which, initialization B doesn't seem handy, the initial conditions calculated through the initial integration, i.e., initialization A satisfactorily predict the system behavior with an error not more than 10% for moderate magnitudes of perturbations in the cases studied.

## 5.9 Example 4

The framework is applied to the gravity-flow tank system of Section 3.5 consisting of a tank with an inflow stream and a straight, horizontal outflow pipe at the bottom exit. It is unique in the respect that it has interacting material (tank) and mechanical energy (pipe) capacities. The system is at steady state at time $t \rightarrow 0^-$. Volumetric flow rate is perturbed by impulse at $t \rightarrow 0^+$. This is realized by plunging a measured amount of liquid into the tank, all in one go (with no change in inflow rate $q$); the magnitude of disturbance $M$ ($m^3$) equals the volume of liquid added. So, $q(t) = q(0^-) + M\ \delta(t - t_o)$ with $t_o = 0^+$ .

Application of initialization A to the model equations respectively yields the following initial discontinuities:

$$h(0^+) - h(0^-) = M\ /\ A_T \tag{5.42}$$

$$\dot{h}(0^+) - \dot{h}(0^-) = M\,\delta(t)\ /\ A_T \tag{5.43}$$

$$u_p(0^+) - u_p(0^-) = 0 \tag{5.44}$$

Eq. (5.43) exhibits singularity because of the initial jump discontinuity in the initial level in Eq. (5.42). From the initialization B approach, i.e., applying material balance on the effects of singularity, it is found that Eq. (5.42) is valid because the sudden level rise in the tank is equal to the $M$ ($m^3$) of the volume of liquid inserted per unit area of the tank. However, the last Eq. (5.44) is not true, as the impulse perturbation causes a sudden change in the initial level, and simultaneously in the initial velocity $u_p$ because of the instantaneous head change. Hence, the level impulse response exhibits inconsistency in the initialization A approach. A better value of this discontinuity can be evaluated by assuming quasi-static process and zeroing differentials, valid if $A_T$ is quite large compared to $A_p$ (or further approximate Bernoulli's Eq. be used):

$$u_p(0^+) - u_p(0^-) = \left(\frac{gD_p}{2fL}\right)^{1/2} \left(h^{1/2}(0^+) - h^{1/2}(0^-)\right) \tag{5.45}$$

This equation can be combined with the material balance Eq. (5.42) above and the two solved simultaneously to yield the initial discontinuity in velocity $u_p$.

## 5.10 Example 5

The model of semi-batch reactor presented in Section 3.3 is considered. It is carrying out a liquid-phase constant-density reaction $A + B \rightarrow R + S$ having second-order rate constant $k$. No outlet stream is there. $A$ is already in the reactor, and $B$ is being fed continuously at constant rate $v_o$. $M$ ($m^3$) of reactant $B$ is fed suddenly at $t \rightarrow 0^+$. This is equivalent to an impulse perturbation (in $B$) volumetric flow rate of feed $v_o$ at $t \rightarrow 0^+$. Holdup volume $V$ is *not* constant.

Following initialization A to the model, gives the discontinuities in $C_B$ and $C_A$.

$$C_B(0^+) - C_B(0^-) = M\{C_{Bo} - C_B(0^-)\} / \{V(0^-) + M\} \tag{5.46}$$

$$C_A(0^+) - C_A(0^-) = -MC_A(0^-) / \{V(0^-) + M\} \tag{5.47}$$

Here, these initial discontinuities are *consistent* with that obtained from initialization B. Hence, the impulse response remains unaffected by initial discontinuities.

## 5.11 Fundamental Limitation of the Laplace Transformed Models

The resolution of inconsistency inherent in the Laplace domain dynamics is discussed in detail in Chapter 6. The two initializations A and B happen to be mutually consistent for some linear cases. However, this is not true of the linear systems, in general; especially, it is not true for the impulse responses of the non-trivial chemical engineering systems involving phase changes, mixing with reaction, and interacting capacities of material, thermal, and mechanical engineering capacities mentioned in introduction (see the next section on linearized systems).

Hence, for such systems the Laplace transform approach that uses pre-initial values of dependent variable ($0^-$ values), would be less accurate as it would yield post-initial values ($0^+$ values) that are inconsistent with physical principles (Chapter 6).

## 5.12 Fundamental and Practical Limitations of the Linearized Models

Effect of the transformation of the models through linearization (using Taylor's series expansion, with the system assumed in the vicinity of the initial state), on the evaluation of initial discontinuities through alternative approaches, is now discussed. The condenser Example 2 exhibited identical initial discontinuities via approaches A & B for impulse in $F$ (Eq. (5.34.e)). However, if the model is linearized (Section 3.4.3), the initial discontinuity in $T$, calculated via initialization A, would be:

$$T(0^+) - T(0^-) = \frac{M\{T_o - T(0^-)\}}{N(0^-)} \tag{5.48}$$

which is not equal to the one estimated from initialization B (Eq. (5.34.e)). Hence, the system that is unaffected by initial discontinuities originally, would be affected by it upon linearization. However, for impulse in $L$, approach A exhibits the same initial discontinuities upon linearization as that calculated from the maiden nonlinear model (Eq. 5.36):

$$T(0^+) - T(0^-) = \frac{M\Delta H / C_p}{N(0^-)} \tag{5.36}$$

This was not equal to the one estimated from initialization B (Eq. (5.38)). Hence, this system that is affected by discontinuities originally would remain affected by it upon linearization. The same is true for the gravity-flow tank and isothermal CSTR systems.

However, if the closed loop stirred tank heater of Example 3 is linearized, the initial discontinuity, via initialization A, would turn out to be the same as that calculated from initialization B (Eq. (5.41)). Hence, this system that is affected by discontinuities originally, interestingly, would be unaffected by it upon linearization. Exactly the same happens for the constant holdup CSTR.

The variable-volume non-isothermal CSTR of Example 1 perturbed by impulse in the exit flow rate remains unaffected by discontinuities before and after linearization (Eq. (5.20)). Many systems were analyzed, i.e., gas phase pressurized CSTR, semi batch reactor, bimolecular reaction CSTR, two phase CSTR, flash distillation, interacting and coupled systems, etc. It was found that many systems are affected by the discontinuities. And, only a very few of them, get rid of this effect upon linearization. However, many other systems remained unaffected in their maiden nonlinear form. And, among them, some cases showed the effect of discontinuities upon linearization. Single component condenser and variable-volume CSTR for feed rate change presented here, are such examples. Thus, all the above four possibilities of appearance/disappearance of the effect, exist for the chemical engineering systems. Various linearized models are presented in Chapter 3.

So, if a system is affected/unaffected by an initial discontinuity in the linearized form, in general, nothing can be said about the effect/non effect of the discontinuity on the corresponding nonlinear system. This is an important result, because linearized systems generally behave in the same manner as the maiden nonlinear systems for near normal operations, and the practical linear control systems are designed on this basis of the operations in the neighborhood of the normal operation. However, as shown above, in particular, the initial discontinuous response of a linearized model can be significantly different from the initial response of the actual system and can deviate significantly from the normal operation. These facts elicit the limitations of using the linearized transformed models instead of the native models for initialization A for singular inputs.

Furthermore, the Laplace transformation approach that uses pre-initial values would be less accurate in treating those linearized cases, which were affected by the discontinuities under the impulse inputs. These limitations of the Laplace transformation were stated at the end of the preceding sub-section and would be discussed in detail in Chapter 6. Limitations of the models transformed through symbolic differentiations and manipulations are discussed in Section 5.13.

### 5.12.1 Special cases

Some systems also undergo order reduction and reduction to standard systems (i.e., not containing derivative of input) upon linearization. These are discussed here.

Consider the non-isothermal CSTR of Section 3.1 and assume constant holdup volume. Through the above analysis, it is seen that the temperature response of this system is affected by discontinuities for an impulse perturbation in the feed stream concentration $C_{Ao}$. Upon linearization, the temperature response of this system reduces to a standard second-order system for feed concentration perturbation. However, it remains affected by initial discontinuities.

The concentration response of the same system (Section 3.1.1) is found to be affected by discontinuities for impulse perturbation in the jacket temperature $T_j$. Upon linearization, this system too, reduces to a standard second-order one (Eq. 3.5) and remains affected by discontinuities.

Consider the linear isothermal constant holdup CSTR under feed concentration perturbation of Section 3.2. This model was a standard second-order system (i.e., not containing the derivative of input) and was not affected by initial discontinuities for step perturbation. However, for the impulse perturbation in Section 4.2.4, it is found to behave as a second-order system with numerator-dynamics and is affected by the discontinuities (as given by Eq. (4.13)).

A few systems also undergo simultaneous order-reduction upon linearization due to pole-zero cancellation (Ahuja, 2010; 2011). These are: temperature response of a constant volume non-isothermal CSTR for zero reaction enthalpy under jacket temperature perturbation (as shown through Eq. 3.77), the same system under feed flow rate perturbation, and the variable volume stirred tank heater under feed rate perturbation

(as shown in Section 3.7.1 through Eq. 3.40), which reduced to standard first-order systems. The first one is affected by initial discontinuities in its maiden nonlinear form but is unaffected by them upon linearization. The remaining two are not affected by initial discontinuities in nonlinear, as well as, linearized adaptations.

## 5.13 Limitations of the Symbolically Transformed Models

In this section, several models obtained from mathematical transformations of the condenser model are considered, and upon inconsistent initialization, their numerical results are plotted simultaneously with the results of the original mathematically non-transformed explicit ODE model Eqs. (5.29') through (5.33) used above in Example 2 (non-transformed model). The transformed models considered are: (a) model of symbolic differentiations and manipulations of Eqs. (5.29) through (5.32) for index reduction (transformed model I) (Vieira and Biscaia Jr, 2001); (b) Explicit ODE model consisting of Eqs. (3.15), (3.16), (3.17), (3.22), and (3.23) (transformed model II, of Section 3.4.2), obtained through symbolic differentiations and manipulations of the condenser model; and (c) Explicit ODE model consisting of Eqs. (5.29) through (5.33) (transformed model III), which uses mathematically transformed Eq. (5.29) instead of Eq. (5.29') of the non-transformed model. Narrowing down of the working ranges of inconsistent initial conditions for these transformed models is also discussed. The inconsistent initialization problems for the step and the impulse perturbations arising from the mathematical transformations are thoroughly explained next.

### 5.13.1 Inconsistency in the symbolically transformed models

This inconsistency was discussed at length in the literature review Section 2.3.1. To illustrate the inconsistency arising out of symbolic manipulations and differentiations, consider a perturbation in the molar feed rate $F$ introduced into the single component condenser model of Section 3.4.2 (transformed model II). In the two alternative explicit models of Section 3.4.2, $L$ was calculated from the equation derived after symbolic manipulations, i.e., Eq. (3.23) (at constant volume). The discontinuities analysis exposing their inconsistency is presented below, and the numerical results are discussed subsequently.

***Step perturbation in F***

Inconsistency, during numerical solutions, is anticipated due to the following two reasons:

- The numerical integration of the set of Eqs. (3.15), (3.16), (3.17), (3.22), and (3.23) require initializations of $N$ and $T$. However, if these values are either chosen quite different from their initial steady state values, or *any* combination of the values of $N$ and $T$ is chosen arbitrarily; *those* values of $N$ and $T$ would be mutually inconsistent. This would happen because they don't satisfy the algebraic Eqs. (3.17) and (3.18). Hence, Eq. (3.23), derived from them, would yield a wrong value of $L$, initially and afterwards. This will lead to gross errors and wrong or no convergence at all.
- It is clear that if one starts with mutually consistent or initial steady state conditions (as explained above) for all the other variables except $F$ ($F$ suffers a discontinuous step input from $t \rightarrow 0^-$ to $t \rightarrow 0^+$), the value of $L$ at $t \rightarrow 0^+$ should remain at its original value at $t \rightarrow 0^-$ (from a physical observation, the dynamic lag in the condenser would prevent a discontinuity in $L$). However, the new initial value of $F$, i.e., $F(0^+)$ is substituted in Eq. (3.23) during the numerical integration, which gives a wrong initial value of $L(0^+)$. Thus, this wrong value would be used for $L$ at $t \rightarrow 0^+$ and, hence, subsequently. The original value $L(0^-)$ would have been obtained only if the initial value $F(0^-)$ was substituted into Eq. (3.23). This would lead to a completely wrong initialization of $L$. This initial discontinuity in $L$ would cause a discrepancy in the system, even if, one starts with the consistent or initial steady state conditions for all the other variables except $F$. The problems will be compounded during numerical integration, in case, one starts with inconsistent initialization pointed above (results for such a case are discussed in Section 5.13.2 below).

***Impulse perturbation in F***

Nevertheless, for impulse input, the second problem does not come in, since the input variable $F$ doesn't change in a stepwise manner. If, in the symbolically manipulated explicit model of Section 3.4.2, one starts with a mutually consistent set of initial conditions, the results would converge to the consistent values. However, the impulse input will cause initial jump discontinuities in the dependent variables whose magnitude

will depend upon the magnitude of the input. So, these variables jump to mutually inconsistent post-initial conditions, even if they started with consistent pre-initial or steady state values (consistent by default). This leads to the first problem mentioned above. The same is true for other DAE approaches that use symbolic manipulations for index reduction.

### 5.13.2 Numerical Results

***Step perturbation in F with singular initial conditions***

In the models transformed through symbolic differentiations and manipulations, the presence of initial discontinuities involves singular initial conditions even for step inputs, and, thus, they have inconsistent initial conditions. To illustrate the resultant effects and limitations of the mathematical transformation of models, the numerical results of the non-transformed model of condenser, are plotted together with those of mathematically transformed model I. A numerical integration *must* converge to the consistent final steady state values, irrespective of whether the integration is started with a consistent or an inconsistent set of values. The computations are done, keeping this objective in mind, to get a plausible solution set. However, it is seen below that the transformed models don't converge to the consistent steady state values.

The literature study for the step perturbation to the index-2 model of single component condenser ((Eqs. (5.29) through (5.32)) assumed constant volume, and applied symbolic manipulation and differentiation of these equations to convert the model to index-1 DAE model (transformed model I) in order to employ the integration code DASSL. Since the results were not converging with the discontinuous step function, consistent initialization was achieved based on the fact that initial steady state can be used as a consistent set of initial conditions. Hence, the system was assumed to be at the initial steady state at $0^-$ time, then, at $0^+$ time, the system was rapidly initialized to the actual $0^+$ state of Table 5.4 and the discontinuous step perturbation was approximated by a smoothed function; smoothing was based on the response to a step perturbation into the first tank of the $n$ tanks-in-series model of total time constant $\tau$ (Vieira and Biscaia Jr, 2001). To draw a clear conclusion, the parameter values, magnitude of the input and the

**Table 5.4** Parameters for the Condenser Example

| For Section 5.13 | | | |
|---|---|---|---|
| $\Delta H = 4.5\times10^{3}$ J/mol | $F(0^-) = 50$ mol/s | $L(0^-) = 50$ mol/s | $A = 1.2\times10^{10}$ Pa |
| $UA_h = 1.0$ W/K | $F(0^+) = 30$ mol/s | $T(0^+) = 488.63$ K | $B = 3816$ K |
| $C_p = 3.35\times10^{1}$ J/mol-K | $T_j = 283$ K | $N(0^+) = 532.43$ mol | $C = -46$ K |
| $R = 8.314$ J/mol-K | $T_o = 373$ K | $k = 6.89\times10^{-2}$ (mol/s)/mol | $n = 1$ $\tau = 10^{-6}$ |

initial conditions were kept the same as in the reference study as given in Table 5.4. A case of a step perturbation in $F$ from 50 mol/s to 30 mol/s was considered. The consistent initial steady state values were calculated in the present study corresponding to the constant parameters given in Table 5.4 by zeroing the derivatives in Eqs. (5.29) and (5.30) and, using (5.31), and (5.32). These are: $L(0^-)$ = 50 mol/s, $N(0^-)$ = 725.725 mol, $T(0^-)$ = 507.195 K. Similarly, the final steady state values assuming constant volume are calculated: $L(\infty)$ = 30 mol/s, $N(\infty)$ = 725.039 mol, $T(\infty)$ = 507.135 K. If the volume is allowed to vary, the initial steady state set remains the same, and the final steady values can still be calculated by including Eq. (5.33) for the non-transformed model. The final steady state values of $L(\infty)$ and $T(\infty)$ remain the same as that for the constant volume case, but $N(\infty)$ = 435.414 mol.

The results of the non-transformed and transformed model I are plotted together in Figs. 5.16, 5.17, and 5.18. However, as seen from these figures, the reference study profiles converge to neither of the two sets of the final steady state values; this is due to the fact that mathematically transformed models were used in this study. According to the initial conditions in Table 5.4, $N$ and $T$ were initialized at values that were inconsistent with their initial steady state values (singular initial conditions due to initial discontinuities). Thus, there must be initial discontinuities in $L$ and $P$ as seen physically.

This initial discontinuity for $L$ is seen in Fig. 5.16 for the non-transformed model curve. However, the reference study curve only exhibits a discontinuity of 5%, and its behavior is sharper. In Fig. 5.17, $N$ shows a monotonic decrease for the non-transformed

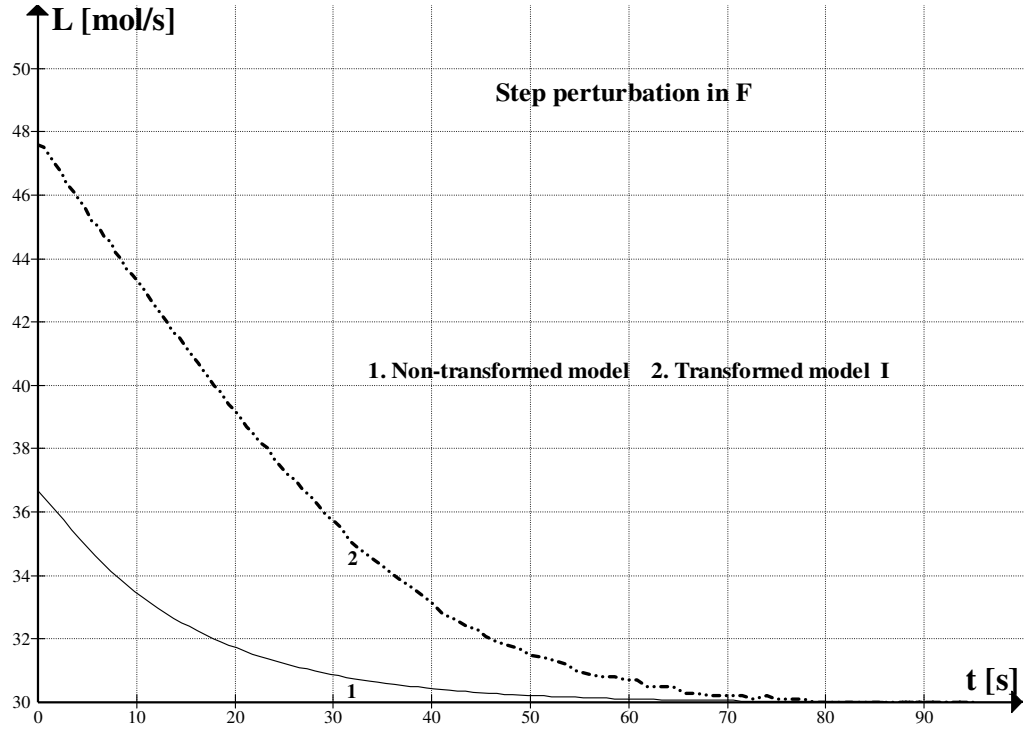


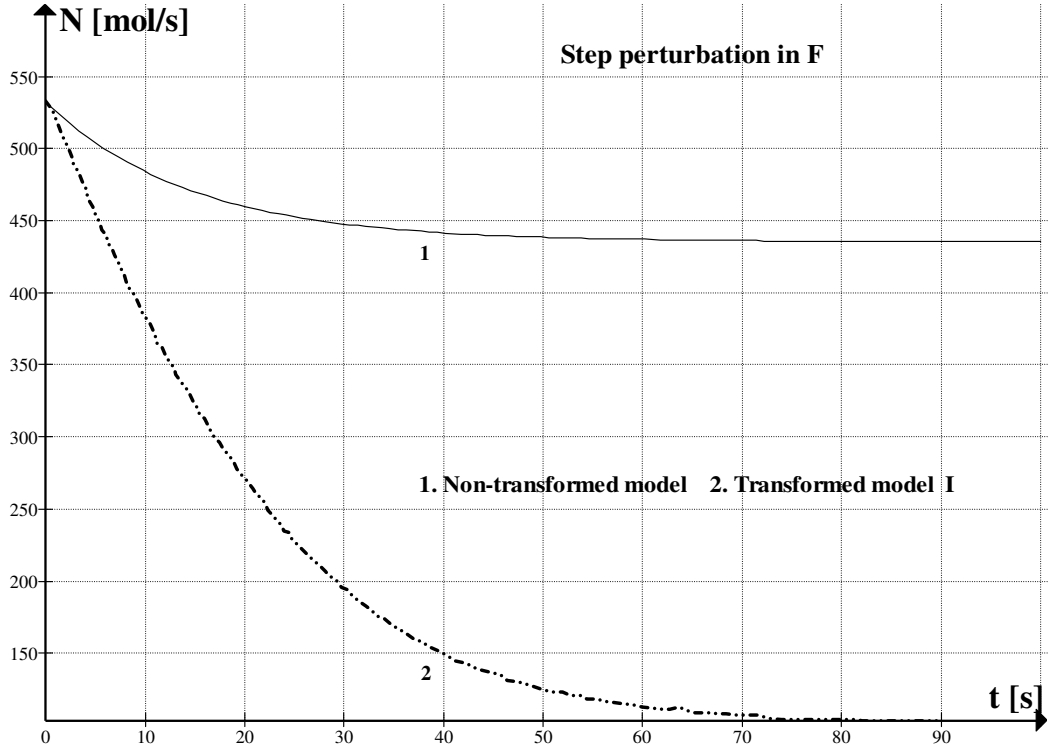


**Figs. 5.16 and 5.17** Numerical solutions of non-transformed and transformed models—Step response respectively of liquid exit flow rate ($L$), and moles ($N$) of vapor in condenser to perturbation in molar feed rate ($F$) 2. Vieira & Biscaia Jr, 2001

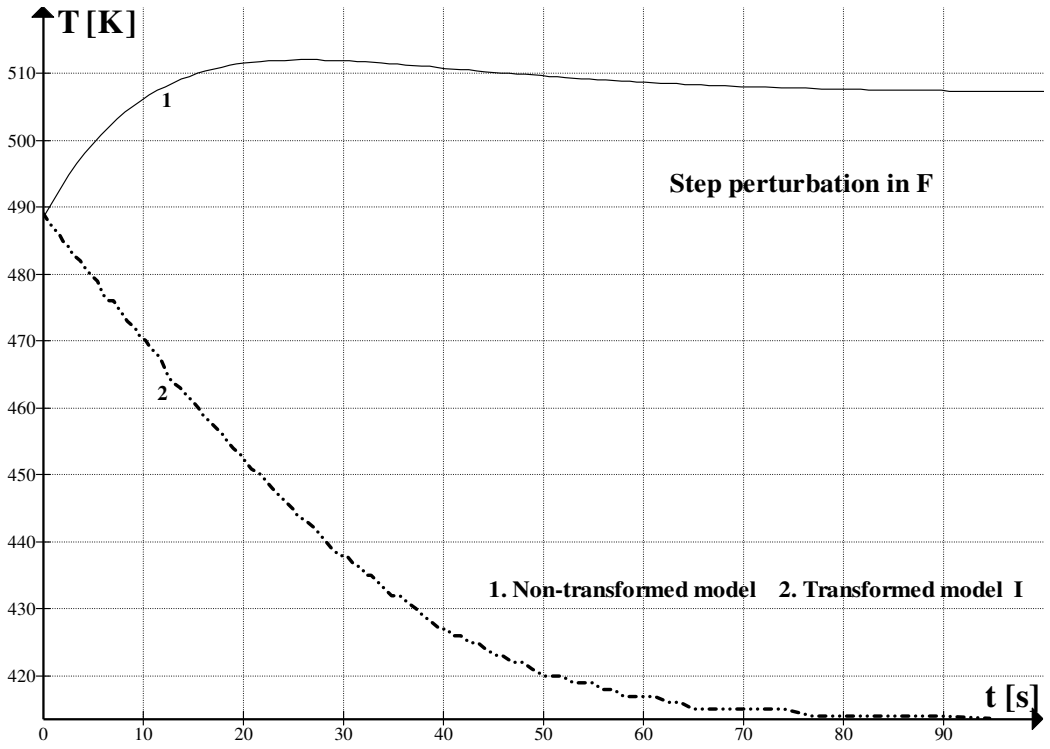


**Fig. 5.18** Numerical solutions of non-transformed and transformed models—Step response of temperature ($T$) of vapor to perturbation in molar feed rate
2. Vieira & Biscaia, 2001

model before converging to the consistent value of 435.414 mol. The reference study curve also exhibits a monotonic decrease in $N$ but converges to an inconsistent value of 100.930 mol, thus exhibiting erroneous solution profile. Also, $T$ in Fig. 5.18 for the reference study decreases and converges to a value of 413.663 K instead of 507.105 K, whereas the non-transformed model curve rises and converges correctly to 507.105 K.

***Impulse perturbation in F***

Result of non-transformed model for the condenser (that uses Eq. (5.29') for energy balance) is plotted along with the result of transformed model III (that uses Eq. (5.29) instead). The rest of Eqs. (5.30) through (5.33) were kept common in both these cases. The transformed model III would exhibit wrong numerical integrations because Eq. (5.29') was obtained from the differentiation and manipulation of the original equations. These two single component condenser models, were solved for impulse perturbation in $F$. Initial conditions $T(0^+)$ and $N(0^+)$ were obtained by including impulse in the cause and

carrying out the integration at initial time (initialization A). Since, the energy balances in the two cases were different, different initial conditions were obtained in the two cases presented. The initial discontinuity for perturbation in $F$ to the non-transformed model was given by Eq. (5.34). This initial discontinuity happened to be the same from the initialization procedures A and B of the framework. The value of initial discontinuity using the transformed model III is calculated through initialization A as:

$$T(0^+) - T(0^-) = \frac{M\{T_o - T(0^+)\}}{N(0^+)} \tag{5.49}$$

A magnitude of the impulse perturbation of –100 mol (13% of initial steady-state $N$) was considered. The results converge to the initial steady-state values. The same parameter values of Table 5.4 as in the above case of step perturbation (except $T(0^+)$ and $N(0^+)$) were applied. The results are presented in Fig. 5.19 for $T$.

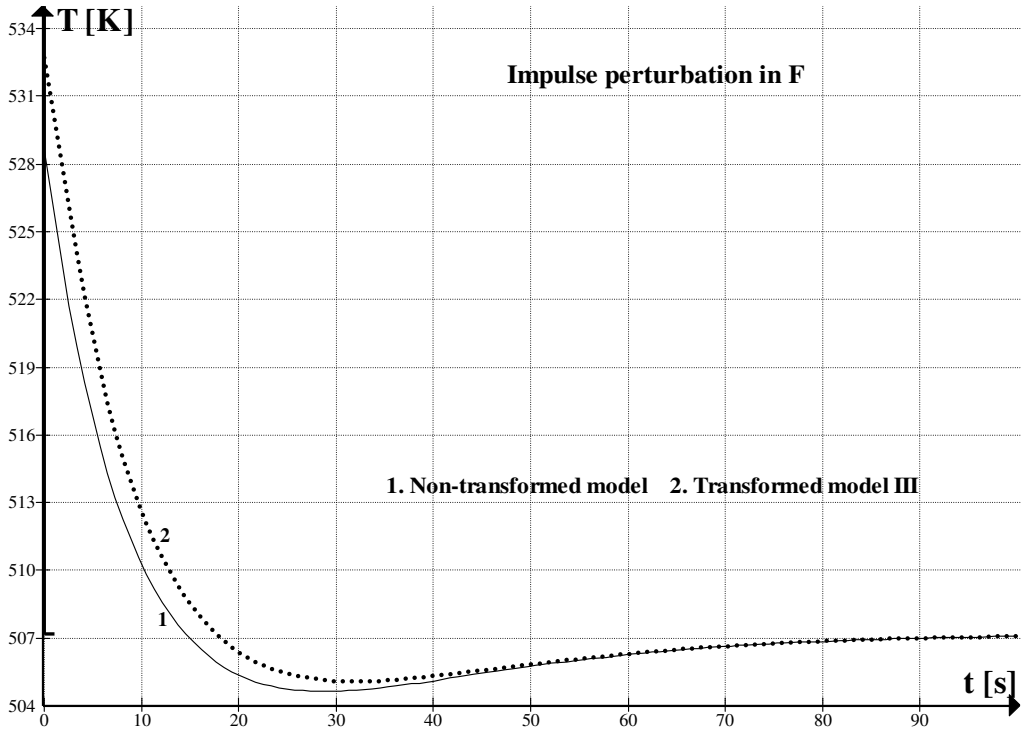


**Fig. 5.19** Numerical solutions of non-transformed and transformed models—Impulse response of temperature of vapor in condenser to a perturbation in feed molar flow rate of magnitude of −100 mol

The curve for the transformed model III exhibits a significant error of 10%. So, the first principles model Eq. (5.29'), rather than Eq. (5.29), obtained after differentiation and manipulations should be used for the condenser system. Transformed model II converged to 731.562 mol against the correct value of 725.039 mol (not shown in Figs.).

However, the non-transformed model curves in Figs. 5.16-5.19 are converging to the consistent final steady state values for all the variables $T$, $P$, $L$ and $N$ (not shown on the Figs. for some). Hence, this model provides accurate solutions, that converge to the right values even for a wide range of inconsistent initial conditions, in addition to being simple (no symbolic manipulations needed), direct, and computationally efficient.

The results of this section clearly signify that the results of the transformed models I and II are inaccurate, and the errors increase at inconsistent initializations. These errors are attributed to the symbolic manipulations and differentiations as elicited in Section 5.13.1; with initial discontinuities, the differentiations of the original equations cause singularity and the resultant singular and inconsistent initial conditions in the output. This fact is also appropriate for the case of impulse inputs that put the systems far off from their consistent initial steady state.

***Working range of inconsistent initial conditions***

Since impulse inputs put the system decently far from the consistent initial steady state, the range of the applicability of the solvers needs to be specified, especially, if the system is relatively stiff. The working range of initial discontinuities was tested by increasing/decreasing a variable from its consistent initial value (keeping others fixed) until the solvers gave an error message. The computations were performed on a PC with Intel Core 2 CPU, 1.66 GHz and 0.5 GB of RAM. The numerical integrations were carried out using the ODE solvers, RKF45, BS, STIFF, etc. from Polymath. The range (of positive values) are expressed as percentage of the consistent value (of Tables 5.1 and 5.2), and the CPU times correspond to the extreme value of this range.

The constant holdup CSTR of Section 5.4 was a stiff system of slow and fast dynamics combined, as $T$ changed very slowly compared to $C_A$. STIFFBS, generally meant for the stiff systems, was very slow outside the range of $T(0^+)$ of 133%, and took 30.09 s of CPU time. The BS solver that works for the non-stiff problems, worked in the

range of 251%, took around 10.35 s; RKF45 (took 4.63 s) and RKF56 (took 5.79 s) worked faster in the range of 333% and 384%, respectively. However, STIFF was the best with a tremendous working range of (0 K – $2.0 \times 10^7$ K), i.e., 60,060%, taking only 3.47 s.

The non-transformed condenser model was immediately solved with all the solvers in the range of 717% except STIFFBS, which worked in the range of 60% and took 45 s. All the above results converged to the consistent steady state values.

For the condenser transformed model II, the working ranges of all the solvers was similar and was only of (50 K – 400 K), i.e., 72%. All the solvers solved immediately except STIFFBS, which took 31.25 s at 50 K. So, the working range of this transformed model is very narrow as compared to the above non-transformed models.

The error messages flashed by the solvers were: (a) BS: Internal Error Trapped ODEINT_BS: Too many steps in routine odeint; (b) STIFF & STIFFBS: Internal Error Trapped ODEINT_ST & ODEINT_BSST: Too many steps in routine odeint; (b) STIFFBS: Internal Error Trapped: Step size underflow; (c) STIFF: Division by zero; and, (d) Overflow error in all the solvers.

The working deviations of various for transformed battery model simulations are cited (Wu and White, 2001) for comparison: for positive values, these are, 0% (MAPLE®), 14.2% (DASSL), 544% (DAEIS); and, reported as 871% (Soares and Secchi, 2005), and 5,053% (with JACOBIAN®) (Methekar *et al.*, 2011). Thus, they depend very strongly on the solver used, whereas, the solvers for non-transformed ODE models worked over wider inconsistencies.

It is emphasized that the working of the proposed methodology is, in no way, limited to the establishment of an initial steady state, *a priori*, at $t \rightarrow 0^-$. The steady states are included here, only to check the convergence and the plausibility of our results.

## 5.14 Outcomes Revisit

To wind up the discussion, it is concluded that the two ways of initializations (A and B), in general, are mutually inconsistent. However, initialization A accurately models the singularity and the initially discontinuous systems for operations not too far away from the normal operating conditions.

Step responses of the original, un-manipulated models, however, are not affected by initial discontinuities, even though they can exhibit initial discontinuities and singularity due to the derivatives of inputs.

The numerical solutions, obtained using the symbolically transformed models I, II, and III, including that based on the smoothening of the inputs, exhibited incorrect values. Nevertheless, non-transformed explicit ODE model of single-component condenser exhibits (formulated in Section 3.4.1) consistent convergence and accounts for changes in volume. Furthermore, the solutions for the non-transformed models for all the systems presented in Chapter 3 can be obtained quite efficiently using an ODE solver that works over a wide range of the mutually inconsistent initial values of the output variables.

The post-initial conditions, calculated via the inclusion of impulse in the cause (initialization A), satisfactorily predict the system behavior within an error of the order of 10% for small magnitude of the inputs. Initialization C is, however, inadequate. These effects are illustrated by computer simulation of the nonlinear models of single-component condenser, non-isothermal CSTR and closed-loop stirred tank heater systems, in this chapter. The closeness of initialization A to initialization B is quantified in these examples. The superiority of initialization B was discussed in the last chapter, and was substantiated there through computer simulations of the nonlinear models of gravity-flow tank and interacting two-tank systems and the calculations of time-to-empty these flow-level tanks.

First, the post-initial conditions are obtained from the direct methods A and B proposed; these are used subsequently for the numerical solutions using an ODE solver through the framework proposed (Fig. 5.1). However, for the numerical solutions of the impulse responses, the values of the impulse input terms in the equations must be substituted equal to *zero*, since the magnitude of these terms have already been included in the model while calculating the initial conditions. Thus, for the impulse response, this framework corresponds to route (b) of the preliminary analysis presented in Fig. 4.1, and followed in Sections 4.2 through 4.8 of the last chapter; wherein, all the initial conditions of output variables are used at $t \rightarrow 0^+$ with the input variable equated to zero, i.e., the initial discontinuities are accounted for in the initial conditions of the output variables.

# 6 Framework Applied to the Linear System Analysis

The framework of analysis and initialization proposed for singular inputs in the last chapter consisted of the comparison of two direct initialization approaches of finding the post-initial conditions, *a priori*, viz. (A) including singularities in the cause, i.e., the input function, and carrying out the time integration of the model with in the limits of $0^-$ to $0^+$; and (B) including singularities in the effect, i.e., applying physical balances to the conditions of the system at time zero. Subsequently, the model is solved by using these two sets of initial conditions, and setting the singular terms zero. This framework is applied to the linear time-invariant systems to handle the inconsistency in the Laplace domain dynamics.

## 6.1 Inconsistency in the Laplace Transform Treatment

In the literature review Section 2.1, the inconsistency in the Laplace transform treatment was discussed at length. It is briefed here and commented upon. The source of the inconsistencies was the fine point of the use of $0^+$ and $0^-$ in the definition of the Laplace transform and the corresponding derivative rule:

$$f(s) = \mathcal{L}\{f(t) = \int_0^\infty f(t)e^{-st}dt\,; \qquad \mathcal{L}\{f'(t) = sf(s) - f(0) \tag{6.1}$$

For systems perturbed by singular inputs, there are initial jump discontinuities in the output functions and/or their derivatives. Due to the discrepancy in the unilateral Laplace transform treatment, the initial values calculated from the derived responses (post-initial values $f(0^+)$) are inconsistent with the original initial conditions chosen for deriving these responses (pre-initial conditions $f(0^-)$). The $\mathcal{L}_-$ Laplace transform approach uses $0^-$ while the $\mathcal{L}_+$ Laplace transform approach uses $0^+$ in the above equation. The $\mathcal{L}_+$ Laplace transform of the $\delta$-Dirac function becomes zero from the derivative rule:

$$\mathcal{L}_+\{\delta(t)\} = su(s) - u(0^+) = s\frac{1}{s} - 1 = 0 \tag{6.2}$$

Many studies advocate the $\mathcal{L}_-$ approach, but the resultant $0^+$ values are inconsistent with the $0^-$ values. The $\mathcal{L}_+$ approach requires additional effort of applying physical principles to calculate the $0^+$ values, *a priori*. Nevertheless, subsequent solution through the $\mathcal{L}_+$ approach yields the same $0^+$ values. Thus, the $\mathcal{L}_+$ form resolves the inconsistency. However, the $\mathcal{L}_+$ transform of the $\delta$-Dirac function becomes zero, i.e., $\mathcal{L}_+\{\delta(t)\}=0$ (Eq. (6.2)). Many studies use the $\mathcal{L}_+$ form, while retaining $\mathcal{L}_+\{\delta(t)\}=1$. Bilateral and double-sided forms were also suggested. Makila (2006), on the other hand, reported the futility of the $\mathcal{L}_-$ and $\mathcal{L}_+$ forms and limitations of the bilateral and double-sided forms. However, it used a convoluted strategy by transforming the ODE into a form consisting of differentials of the integrals that don't suffer from singularity. We clearly represent this strategy in Appendix I. However, there we show that this strategy works for the step perturbation only, and not for the impulse.

As seen above, there is inconsistency prevailing on this issue. More relevantly, the inconsistency for the chemical engineering systems, which are further complicated by mixing with chemical reactions, phase changes, and the interaction of material, thermal, and mechanical energy (inertia) cap!cities, e.g., CSTRs, gravity-flow tanks, condensers, etc., rema)n to be thoroughly investigated.

Initialization studies reported on the linear time-invariant systems frequently consider systems with terms containing differentials of the input function as they contain a singularity due to the derivative of *step* input term (Brigola & Singer, 2009; Grizzle, 2004; Makila, 2006; Lundberg *et al.*, 2007). Several linear and linearized chemical engineering systems also exhibit such models (Ahuja, 2010; 2011). The application of the proposed framework is illustrated below through an example of U-tube manometer system used in chemical engineering science. These results are also compared with that of an analogous system considered in Section 2.2.2 (Lundberg *et al.*, 2007). Unlike the literature studies, *impulse* input is also considered. So, the system also contains a singular term of the derivative of the impulse input function.

## 6.2 Example

Consider the U-tube manometer model of Section 3.8.1:

$$\begin{aligned} &m\ddot{u} = -a\dot{u} - bu + A(\Delta\dot{\bar{P}}) \\ &\text{where} \quad a = 8\pi\mu LA, \quad b = 2\rho gA \end{aligned} \tag{6.3}$$

***Step input***

A step input in $\Delta P$ of magnitude $(\Delta P(0^+) - \Delta P(0^-))$ is first considered. Since Eq. (6.3) must maintain equality at all times, it can be integrated within $0^-$ and $t$ limits of time using the initialization A procedure of the proposed framework:

$$\int_{0^-}^{t} m\ddot{u}dt = -\int_{0^-}^{t} a\dot{u}.dt - \int_{0^-}^{t} bu.dt + \int_{0^-}^{t} A\Delta\dot{\bar{P}}dt \tag{6.4}$$

$$m\{\dot{u}(t) - \dot{u}(0^-)\} = -a\{u(t) - u(0^-)\} - \int_{0^-}^{t} bu(t)dt + A\{\Delta P(t) - \Delta P(0^-)\} \tag{6.5}$$

The above equation applied at $0^+$ value of time gives the expression for the post-initial condition for the acceleration of the column. The integrand in the third term of Eq. (6.5) is limited and the integral vanishes. So, it gives:

$$m\{\dot{u}(0^+) - \dot{u}(0^-)\} = -a\{u(0^+) - u(0^-)\} - 0 + A\{\Delta P(0^+) - \Delta P(0^-)\} \tag{6.6}$$

Similarly, re-integrating Eq. (6.5) within $0^-$ and $0^+$ limits of time gives the value of the post-initial condition of the velocity:

$$m\{\int_{0^-}^{0^+} \dot{u}(t)dt - \int_{0^-}^{0^+} \dot{u}(0^-)dt\} = -a\{\int_{0^-}^{0^+} u(t)dt - \int_{0^-}^{0^+} u(0^-)dt\} - \int_{0^-}^{0^+}\int_{0^-}^{t} bu(t)dt\,dt + \int_{0^-}^{0^+} A\{\Delta P(t) - \Delta P(0^-)\}dt \tag{6.7}$$

$$m\{u(0^+) - u(0^-) - 0\} = a\{0 - 0\} + 0 + 0 = 0 \tag{6.8}$$

All the terms on the R.H.S. of Eq. (6.7) vanish as the integrands are limited. Thus, there is no discontinuity in $u$. Using this in Eq. (6.6), gives the following discontinuity in $\dot{u}$:

$$m\{\dot{u}(0^+) - \dot{u}(0^-)\} = A\{\Delta P(0^+) - \Delta P(0^-)\} \quad (6.9)$$

The initial conditions obtained from initialization B, i.e., the momentum balance considerations also happen to be the same. Since, imposing a step change in the pressure causes no change in the initial velocity because of the inertia of the column, the same is given by Eq. (6.8). However, this change of pressure causes a simultaneous change in the initial acceleration of the liquid column that is equal to the force applied $A\{\Delta P(0^+) - \Delta P(0^-)\}$ per unit mass $m$ of the column, and the same is given by Eq. (6.9).

### *Impulse input*

On similar lines, it can be verified that the proposed methodology gives correct initial conditions for the impulse input. For the treatment of this case via initialization A, in the above equations, the impulse is included in the cause, i.e., the input function. The system is initially at a particular state at time $t \rightarrow 0^-$. For an impulse input at $t \rightarrow 0^+$, the forcing function $\Delta P$ changes from its pre-initial value $\Delta P(0^-)$ (steady or unsteady) to the following equation. This equation is, then, placed in the above equations.

$$\Delta P(t) = \Delta P(0^-) + M\ \delta(t - t_o) \text{ with } t_o = 0^+ \quad (6.10)$$

where $M$ represents the magnitude of the impulse and $\delta$ represents the unit-impulse function. Noting that the integral of the unit impulse, i.e., the $\delta$-Dirac function is one, application of the initialization A procedure to Eq. (6.7), gives the discontinuity in $u$:

$$m\{u(0^+) - u(0^-) = A.M \quad (6.11)$$

This is the same as obtained by applying initialization B. $A$ times the magnitude of the applied impulse equals the simultaneous change in the initial momentum of the column.

Again, Eq. (6.6) of initialization A yields the initial discontinuity in acceleration:

$$m\{\dot{u}(0^+) - \dot{u}(0^-)\} = -a\{u(0^+) - u(0^-)\} - 0 + A\{M\,\delta(t - t_o)\} = -aAM\ / m + AM\,\delta(t - t_o) \quad (6.12$$

which happens to be the same from initialization B (momentum balance). $m$ times the discontinuity in the initial acceleration of the liquid column is equal to $A$ times the

magnitude of the applied impulse $M$ minus the initial frictional force offered due to the sudden change in initial velocity. The restoring force term (zero term) is zero as the initial discontinuity in the displacement is zero. Eq. (6.12) exhibits a singularity in the initial acceleration because of the jump discontinuity in the initial velocity in Eq. (6.11).

Thus, the two initializations A and B yield consistent post-initial conditions, and it can be verified that the $\mathcal{L}_-$ Laplace transform approach also yields the same values.

***$\mathcal{L}_+$ approach*:** In this approach, post-initial conditions obtained above are subsequently used to solve the system Eq. (6.3). For this, Eq. (6.3) is first subtracted from the same equation at $0^-$ time; the resultant equation is $\mathcal{L}_+$ Laplace transformed to give the following equation:

$$m[s^2U(s)-sU(0^+)-\dot{U}(0^+)]+a[sU(s)-U(0^+)]\ +bU\left(s\right)\ =sA\Delta\bar{P}(s)-A\Delta\bar{P}(0^+) \quad (6.13)$$

where $U(t)=u(t)-u(0^-)$, and $\Delta\bar{P}(t)=\Delta P(t)-\Delta P(0^-)=M\ \ \delta(t-t_o)$ with $t_o=0^+$ (6.14)

Now, for an impulse perturbation in Eq. (6.13), $\Delta\bar{P}(s)=0$ from Eq. (6.2). Also, the last term of Eq. (6.13) is singular, as:

$$A\Delta\bar{P}(0^+)=AM\,\delta(t-t_o) \quad (6.15)$$

Eq. (6.15) is obtained from Eqs. (6.10) and (6.14). $\dot{U}(0^+)$ on the left of Eq. (6.13) has the same singular term (from the last term of Eq. (6.12)). Thus all the singular terms in Eq. (6.13) cancel spontaneously and its time-domain solution is feasible through inversion.

An analogous system, i.e., a car-wheel suspension is considered in Section 2.2.2, wherein the relevant details of Lundberg *et al.* (2007) are also given for ready reference. Applying the framework, it was seen that the post-initial values computed from initialization A were identical with that obtained using the $\mathcal{L}_-$ approach for three different pre-initial sets of conditions of the non-zero values, unsteady values, and values yielding immediate convergence to the final value of the response. This result is true in general.

***Outcomes revisit***

- Invariably, the post-initial conditions obtained through initialization A conform to the post-initial conditions computed through the $\mathcal{L}_-$ approach, and both these approaches include singularities in the *cause*. The $\mathcal{L}_-$ approach is, however, a one-step procedure.
- The $\mathcal{L}_+$ approach (a two-step procedure) is analogous to the initialization B approach, in case, the post-initial conditions are obtained in the first step by applying physical principles to the effects of singularities. Both these approaches include singularities in the *effect*. Again, in the $\mathcal{L}_+$ approach, the solution is obtained in the second step while all the singular input terms cancel/vanish spontaneously. The same happens in initialization B as the singular terms are set zero while carrying out the solution subsequently.
- In the above case, yet not true in general, the $\mathcal{L}_-$ and initialization A approaches are found to be consistent with the $\mathcal{L}_+$ and initialization B approaches.

## 6.3 Discussion: $\mathcal{L}_-$ *vs.* $\mathcal{L}_+$ Approach

The contributions in the literature have carried out the analysis for the step inputs to the simple cases as above. Thus, the $\mathcal{L}_-$ approach seems to be satisfactory, and reportedly yields post-initial conditions consistent with that of the $\mathcal{L}_+$ approach invariably (see Section 2.1, Lundberg *et al.*, 2007; Makila, 2006). However, the $\mathcal{L}_-$ approach is inexact and inconsistent for the cases of impulse inputs to the complex processes involving mixing with reactions, phase changes, and the interaction of various capacities.

In Sections 4.1, 4.2, 4.8, 5.11, and 5.12 dealing with linear and linearized cases of nontrivial cases of chemical engineering in the preceding chapters, it was discussed that the post-initial conditions computed through the model's considerations, viz., initialization route (a) of Chapter 4, and initialization A of Chapter 5, were inconsistent with that obtained from initialization B. Hence, impulse must be included in the effect rather than the cause as proposed in the $\mathcal{L}_+$ and initialization B approaches. However, the $\mathcal{L}_-$ and initialization A approaches include impulse in the cause. In the nontrivial cases of

chemical engineering systems, the $\mathcal{L}_-$ approach works for the step inputs only, and gives incorrect results for the impulse inputs, and, hence, the $\mathcal{L}_-$ and $\mathcal{L}_+$ approaches don't provide the same solutions always.

Therefore, in such cases, the post-initial values calculated from the $\mathcal{L}_-$ approach and from the initial integration of the model, i.e., initialization A are inconsistent with the ones estimated from a physical balance at the initial time, i.e., initialization B, as the model can't account for the initial discontinuities. This result is analogous to our previous findings on several cases of chemical engineering systems, viz., isothermal and non-isothermal CSTRs, condenser, flow-level tanks, etc., which indicates the inherent limitation of the model to completely represent the system affected by singularities. Nevertheless, particularly for such cases, the solution based on the $\mathcal{L}_+$ approach, but with the initial conditions estimated from a physical balance, rather than from the initial integration procedure A, should be used for more accurate results. The post-initial conditions for several such cases were worked out through the physical balance considerations in the last chapter.

### 6.3.1 Resolving the inconsistency further

Further inconsistencies are now considered. The discrepancies discussed at length in Chapter 2 can be easily handled by the uniform use of the proposed methodology. Many studies report that the $\mathcal{L}_-$ approach is better than the $\mathcal{L}_+$ approach that requires the additional effort of applying physical balances to calculate the post-initial conditions, and involves the inconsistency of Laplace transform of the impulse function being zero. However, it is argued here that the $\mathcal{L}_-$ approach involves several inconsistencies. The $\mathcal{L}_+$ approach is better and the application of the additional effort can be circumvented for the simple cases as the post-initial conditions can be conveniently obtained through initialization A (Section 6.2). Subsequently, the solution can be obtained from the $\mathcal{L}_+$ approach as the impulse input or singular terms automatically vanish from the model as they did in the U-tube manometer case above.

Since, the singular part of the response has already been included while calculating its post-initial conditions, *a priori*; the effect of the impulse (or singular input

terms) has been accounted for in the post-initial conditions of the output functions. As the impulse input (or the singular input terms) occurs only for the post-initial, i.e., the $0^+$ time, and has been included in the effect, it would be erroneous to re-include it in the cause, i.e., in the input singular term. This argument also justifies the $\mathcal{L}_+$ Laplace transform of the $\delta$-Dirac function becoming zero in Eq. (6.2). As seen in the above Example 6.2, all the singular terms cancel/vanish spontaneously in the differential equation while calculating the solution profile subsequently. Thus, the $\mathcal{L}_+$ approach avoids taking the Laplace transform or the inversion of the singular input terms in the differential equation. So, as reasoned out, the $\mathcal{L}_+$ approach doesn't involve discrepancies in Eq. (6.2) that have been reported in the literature. Eq. (6.2) takes $\delta$-Dirac as the derivative of the discontinuous unit step function $u(t)$ and uses the derivative rule.

Extending the above argument for the derivative of other discontinuous functions yields interesting results. In fact, the $\mathcal{L}_+$ Laplace transform of the *differential of an initially discontinuous function is not inconsistent with that computed from the derivative rule*. For, if the above logic is applied to other initially discontinuous functions $f(t)$, which are the product of a function $g(t)$ with the unit step function $u(t)$, one gets consistent results for the $\mathcal{L}_+$ transform, while inconsistent ones for the $\mathcal{L}_-$ transform. There is inherent inconsistency in the $\mathcal{L}_-$ approach due to the discrepancy in the pre- and post-initial conditions. This is shown by considering the following three Cases for $g(t)$: (a) $g(t)$ is a smooth function, e.g., cos$t$; (b) $g(t)$ is continuous, but has a derivative discontinuity, e.g., modulus function $|t|$; and (c) $g(t)$ has a jump discontinuity at the origin, e.g., $u(t)$.

$$f(t) = g(t)u(t)$$

**a.** $g(t) = \cos t$

So, $g(t)$ is a smooth function, yet $f(t)$ has an initial jump discontinuity from 0 to 1, since:

$$f(t) = \cos t.u(t) \tag{6.16}$$

The $\mathcal{L}_+$ Laplace transform of $f'(t)$ from the derivative rule becomes:

$$\mathcal{L}_+\{f'(t)\} = s\,\mathcal{L}\{f(t)\} - f(0^+) = s\frac{s}{s^2+1} - 1 = -\frac{1}{s^2+1} \tag{6.17}$$

Again, since the derivative of Eq. (6.16) from the product rule is:

$$f'(t) = \cos t.\delta(t) - \sin t.u(t) = \delta(t) - \sin t.u(t) \tag{6.18}$$

The singular term in Eq. (6.18) is evaluated using the property:

$$g(t)\delta(t-a) = g(a)\delta(t-a) \qquad \text{(as } g(t) \text{ is smooth)} \tag{6.19}$$

The $\mathcal{L}_+$ transform of $f'(t)$ obtained through Eq. (6.18) turns out to be the same as given by Eq. (6.17), because the $\mathcal{L}_+$ transform of the singular part $\delta(t)$ vanishes, and if compared with the above derivative rule, Eq. (6.17), it has already been included in the post-initial condition $f(0^+)$ of the derivative rule.

Anyways, the $\mathcal{L}_-$ transform of $f'(t)$ also happens to be the same through the above two ways as $g(t)$ is smooth at the origin:

$$\mathcal{L}_-\{f'(t)\} = s^2/(s^2+1) \tag{6.20}$$

However, the $\mathcal{L}_-$ transform doesn't always yield consistent results from the above two ways as seen by applying the above treatment for Cases (b) and (c).

**b.** $g(t) = |t|$

which has a derivative discontinuity at origin. So, $f(t)$ also has a derivative discontinuity (see Figs. 6.1 & 6.2 for $g(t)$ & $f(t)$, respectively), since:

$$f(t) = |t|.u(t) \tag{6.21}$$

By referring to Fig. 6.2 ($f(t)$ is effectively $tu(t)$), the $\mathcal{L}_+$ Laplace transform of $f'(t)$ from the derivative rule is:

$$\mathcal{L}_+\{f'(t)\} = s\,\mathcal{L}\{f(t)\} - f(0^+) = s\frac{1}{s^2} - 0 = \frac{1}{s} \tag{6.22}$$

Again, since the derivative of Eq. (6.21) from the product rule is:

$$f'(t) = |t|\,\delta(t) + 1.u(t) = t\delta(t) + u(t) = 0 + u(t) \tag{6.23}$$

Eq. (6.23) is obtained using Eq. (6.19), as $g(t) = |t| = t$ can be considered smooth from the right, for $t \geq 0^+$ ( $\delta(t)$ is taken $\delta(t - 0^+)$ in $\mathcal{L}_+$ approach above). The $\mathcal{L}_+$ transform of $f'(t)$ obtained through the last Eq. (6.23) turns out to be the same as the above Eq. (6.22).

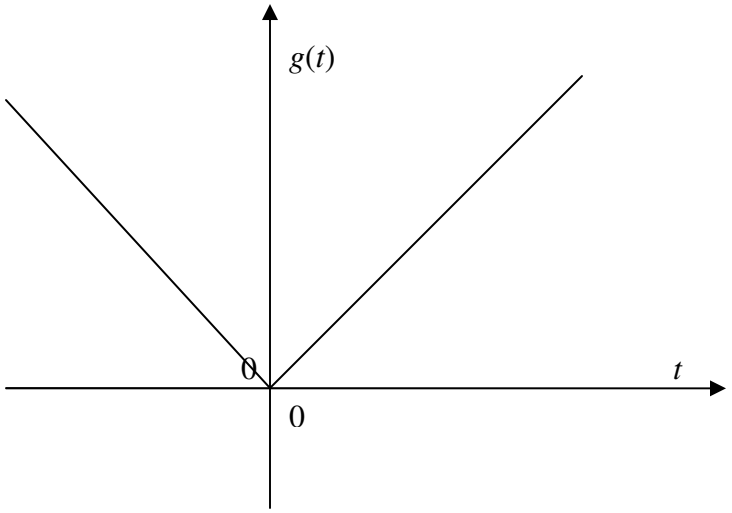


**Fig. 6.1** Graph of $g(t) = |t|$ the modulus function that has a derivative discontinuity at the origin

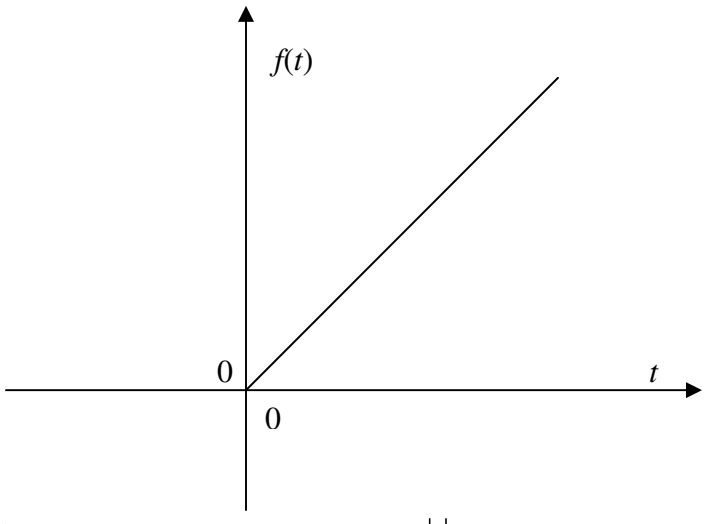


**Fig. 6.2** Graph of $f(t) = g(t)u(t) = |t|\,u(t)$ that has a derivative discontinuity at the origin

Now, for the $\mathcal{L}_-$ approach, the transform of $f'(t)$ from the derivative rule is the same as given by Eq. (6.22). However, the derivative $f'(t)$ and, hence, the $\mathcal{L}_-$ transform from the product rule becomes undefined in the domain $[0^-, \infty)$ as shown below:

$$\begin{aligned} &f'(t) = |t|\,\delta(t) \pm 1.u(t) = \text{undefined} \pm u(t) \\ &(\text{as } g(t) = |t| = \pm t \text{ is not smooth at origin}) \end{aligned} \tag{6.24}$$

So, the two ways don't give the same results for the $\mathcal{L}_-$ transform.

**c.** $g(t) = u(t)$

which has an initial jump discontinuity. So, $f(t)$ also has an initial jump discontinuity from 0 to 1, since:

$$f(t) = g(t).u(t) \tag{6.25}$$

For the $\mathcal{L}_+$ Laplace approach, the transform of $f'(t)$ from the derivative rule becomes (as $f(t)$ is effectively $u(t)$ only):

$$\mathcal{L}_+\{f'(t)\} = s\,\mathcal{L}\{f(t)\} - f(0^+) = s\frac{1}{s} - 1 = 0 \tag{6.26}$$

Again, since the derivative of Eq. (6.25) from the product rule is:

$$f'(t) = u(t)\delta(t) + u(t)\delta(t) = \delta(t) + \delta(t) \tag{6.27}$$

Eq. (6.27) is obtained using Eq. (6.19), as $g(t) = u(t)$ can be considered smooth from the right, for $t \geq 0^+$ ($\delta(t)$ is taken $\delta(t - 0^+)$ in $\mathcal{L}_+$ approach above). The $\mathcal{L}_+$ transform of $f'(t)$ obtained through the last Eq. (6.27) also turns out to be zero from Eq. (6.2).

Now, for the $\mathcal{L}_-$ approach, the transform of $f'(t)$ from the derivative rule is:

$$\mathcal{L}_-\{f'(t)\} = s\,\mathcal{L}\{f(t)\} - f(0^+) = s\frac{1}{s} - 0 = 1 \tag{6.28}$$

However, the derivative $f'(t)$ and, hence, the $\mathcal{L}_-$ transform from the product rule becomes undefined in the domain $[0^-, \infty)$ as shown below:

$$f'(t) = u(t)\delta(t) + u(t)\delta(t) = \text{undefined}$$
$$(\text{as } g(t) = u(t) \text{ is non-smooth at origin}) \tag{6.29}$$

So, the two ways don't always give the same results for the $\mathcal{L}_-$ transform. Also, in Case (b), the function $|t|.u(t)$ is the same as $t.u(t)$, and, so, the two possess the same $\mathcal{L}_+$ Laplace transform of their derivatives. However, this is not true of the $\mathcal{L}_-$ Laplace transform. The same happens for Case (c). Hence, it is seen that the $\mathcal{L}_-$ transform depends not only upon $f(t)$ but also upon $g(t)$, i.e., on how the initial state has been achieved, whereas, the $\mathcal{L}_+$ approach is straight forward and only depends on $f(t)$ and not on its history past the origin. Hence, the $\mathcal{L}_-$ approach suffers from the inherent inconsistency for the systems involving initial jump discontinuities marked at the outset of Section 6.1.

### 6.3.2 Initial value theorem ($\mathcal{L}_+$ approach)

The present study further examines whether the logic of the $\mathcal{L}_+$ transform of the singular input terms becoming zero presented above is valid for the application of the initial value theorem based on the $\mathcal{L}_+$ approach for the step response, in general. The initial value theorem based on the $\mathcal{L}_+$ approach for the output variables $y$ and $\dot{y}$ becomes:

$$y(0^+) = \lim_{s\to\infty} sy(s) \quad \& \quad \dot{y}(0^+) = \lim_{s\to\infty} s\{\mathcal{L}_+ \dot{y}(t)\} = \lim_{s\to\infty} s\{sy(s) - y(0^+)\} \tag{6.30}$$

Note the appearance of $y(0^+)$ term here. If the U-tube manometer of Section 6.2 or the system considered in Section 2.2.2 are $\mathcal{L}_+$ Laplace transformed by setting the transform of the derivative of the step input, i.e., $\mathcal{L}_+\{\dot{x}(t)\} = 0$ according to Eq. (6.2), it can be easily verified that Eqs. (6.30) are satisfied. Application of these works out (details not shown for brevity) to the identities:

$$y(0^+) = y(0^+), \text{ and } \dot{y}(0^+) = \dot{y}(0^+) \tag{6.31}$$

Hence, it is seen that the initial value theorem using the $\mathcal{L}_+$ approach is satisfied. So, the $\mathcal{L}_+$ approach is again consistent.

### 6.3.3 Further discussion

Some more fallacies and confusion present in the literature are discussed. Consider a system equation that is analogous to the U-tube manometer example, i.e., Eqs. (6.3) (Grizzle, 2004):

$$1.\ddot{y} = -1.\dot{y} - 1.y + 1(\dot{x}) \tag{6.32}$$

Advocating in favor of the $\mathcal{L}_-$ approach in his article, this study has reported that since for a step input in $x$, the $\mathcal{L}_+$ Laplace transform of $\dot{x}$ through Eq. (6.2) is zero; the solution of the system Eq. (6.32) from the $\mathcal{L}_+$ approach is identically zero as long as the initial values of the output and its derivative are zero. On this very basis, it has advocated against the use of $\mathcal{L}_+$ form of the Laplace transform. This is examined here.

A physical system representing the system equation is that of a U-tube manometer (*but*, *now, y* becomes the column *velocity* and *x* the *pressure applied*). On comparison with the U-tube manometer, the zero pre-initial values would mean initial rest conditions as *y* is analogous to velocity, so, $y(0^-) = 0$ and $\dot{y}(0^-) = 0$. Nevertheless, even for these pre-initial rest conditions, the discontinuity analysis of initialization A for the step input above shows that the post-initial condition $\dot{y}(0^+) \neq 0$ from Eq. (6.9), whose right hand side is not zero because of the step input. On subsequent solution through the $\mathcal{L}_+$ approach, this non-zero post initial condition wouldn't yield identically zero dynamic solution as has been claimed by the study in question. This would have happened only if, hypothetically, $\dot{y}(0^+) = 0$, which is, in fact, not so. The reason for this confusion may be the failure to keep a physical analogy in mind. This can be very easily verified from the following preliminary physical reasoning. If one starts from rest, and introduce a step input by applying pressure, then initial acceleration can't be zero, i.e., $\dot{y}(0^+) \neq 0$.

Still though, if one considers the hypothesis of the post-initial acceleration becoming zero then the column doesn't move at all (it was at rest at $t \rightarrow 0^-$), and, then,

again, the $\mathcal{L}_+$ approach would predict the right "identically zero" solution. The same argument applies to an *analogous* RLC series circuit, with current *I* analogous to the velocity and applied voltage *E* to the applied pressure. If a voltage is applied, the voltage drop across the inductor element can't be zero, so, $\dot{I}(0^+) \neq 0$. Hence, yet again the $\mathcal{L}_+$ approach wouldn't yield the "identically zero" solution as has been claimed by the study in question.

Lundberg *et al.* (2007), also, advocates the use of the $\mathcal{L}_-$ approach. It affirms that, *in general*, the $\mathcal{L}_+$ approach is cumbersome as the determination of the post-initial conditions either requires applications of physical balances, or the technique of impulse matching (see Section 2.1). However, for the cases studied in the literature, it is shown above that the post-initial conditions can be easily and rightly calculated from the initialization A procedure of the proposed methodology. Having obtained the post-initial conditions, the correct solution is subsequently obtained from the $\mathcal{L}_+$ approach; thus, avoiding the inconsistencies and inaccuracy inherent in the $\mathcal{L}_-$ approach (these inconsistencies are marked at the outset and are discussed in Section 6.3). Furthermore, there is no real need for carrying out the analysis presented in the recent contributions based on the demanding and complicated framework of generalized functions. Additionally, the convoluted approaches such as that of mathematical transformations of equations to eliminate the singular terms presented by Makila (2006) (see Appendix I) are also not needed.

## 6.4 Outcomes Revisit

It is shown that the post-initial conditions obtained through initialization A are invariably the same as those obtained through the $\mathcal{L}_-$ approach. The subsequent solutions resulting through these post-initial conditions are consistent with that obtained through the $\mathcal{L}_+$ or initialization B approach for the step inputs, and for the simple cases under impulse inputs. However, the $\mathcal{L}_-$ and initialization A approaches are inconsistent and less exact, especially, for the nontrivial cases under impulse inputs.

Nevertheless, the $\mathcal{L}_+$ approach provides consistent results and satisfies the initial value theorem even in the presence of the non-zero pre-initial values, the non steady state pre-initial conditions, the input functions containing singularities, and more relevantly for the nontrivial chemical engineering systems containing interacting material, thermal, and mechanical energy capacities under impulse inputs. So, without requiring the convoluted approaches, and the demanding machinery of generalized functions, the application of our proposed framework finds a workable solution to the problem of $0^-$ and $0^+$ in the initial conditions of the responses from a direct approach perspective. Further, it reveals the inconsistencies inherent in the $\mathcal{L}_-$ approach for the nontrivial chemical engineering cases under impulse inputs. The treatment proposed, thus, addresses a fallacy reported in systems engineering by many authors (Grizzle, 2004; Lundberg *et al*., 2007; Stefani *et al*., 2002).

The methods proposed in this thesis are direct, avoid the complicated framework of generalized functions, address the singularities, and account for the inconsistencies in initial conditions. Further, they are general, and are equally applicable to the nonlinear and linear systems for the step and impulse inputs. The conformity of the framework of the methodology presented here to the established approaches for the linear systems once again demonstrates its validity. The same happened in Sections 5.3 and 5.4 of Chapter 5, wherein the post-initial conditions obtained from the proposed framework conformed to the definitely known post-initial conditions of the nonlinear cases.

# 7 Conclusions and Recommendations

## 7.1 Conclusions

A methodological framework for the analysis of initial discontinuities and the estimation of the initial conditions for the lumped-parameter chemical engineering systems for the singular inputs is proposed. The following conclusions can be drawn from this study:

- Lumped-parameter chemical engineering systems contain derivative of the input terms in their models when solved for one of the output variables, and, thus, exhibit numerator dynamics behavior upon linearization. These physical systems and their models present themselves with initial discontinuities for the singular inputs. Their range of assorted solution profiles and the corresponding characteristic conditions are obtained for negative real part poles and represented concisely on the real axis. These exhibit different behavior than the standard systems; the profiles exhibiting maximum/minimum are also important from design perspective.
- The inclusions of singularity via the cause (initialization A) and the effects (initialization B) give the same solutions for many systems, but mutually inconsistent solutions for many others as their models are affected by singularity. Initial conditions via initialization A are obtained by the integration of the models between $0^-$ and $0^+$ times, prior to carrying out the analytical or numerical solution. These initial conditions satisfactorily predict the system behavior within an error of the order of 10% vis-à-vis initialization B for operations not very far away from the normal operating conditions. Operations fairly close to the normal operating conditions are of significant practical importance if the plant variables are well controlled to remain close to the steady state. The applicability of initialization A procedure was suggested by its conformity to the definitely known cases, and to the Laplace transform treatment for linear systems.
- The solutions obtained by including singularity in the effects and the applications of physical balances (initialization B) have been found to be more accurate and conform to the physical facts than the ones calculated solely from a theoretical perspective (initialization A). This effect is substantiated by carrying out numerical experiments

and comparing the results with the experimental results of flow-level tanks. Further evidence to this effect is provided by carrying out the analysis of the calculations of time required for emptying the flow-level tanks.

- The approach of using a continuous function for an impulse can't reveal the true asymptotic behavior as it can't catch up with the correct initial conditions. The symbolically transformed models and the linearized models, also, can't predict the correct initial conditions, and, thus, lead to erroneous solution profiles and inconsistent convergence. In general, the non-transformed models work for operations over a wider range of the mutually inconsistent initial values of the output variables, as compared to the symbolically transformed models.
- For *linear* systems, it is revealed that the post-initial conditions obtained through initialization A and $\mathcal{L}_-$ approach are invariably the same. The $\mathcal{L}_+$ approach that uses the post-initial conditions obtained through physical balances on the effects is more exact and resolves several inconsistencies vis-à-vis the $\mathcal{L}_-$ approach, especially for complex chemical engineering cases under an impulse.

## 7.2 Recommendations for future work

- The present models can be extended further to deal with the problem of discontinuity/inconsistency in initial/boundary condition specifications in distributed-parameter systems, for example how to handle the situation when Dirichlet's boundary conditions are used and there is a discrepancy between the initial condition inside the domain and the value at the boundary.
- Future work can explore direct methods for other complex models and see how the computational effort scales with the model complexity and the way the algorithms are implemented, for example it would be challenging to treat discontinuity in fractional order ODE/PDE models, Volterra-Laguerre models, empirical models, etc.

## Notations

| | |
|---|---|
| $A$ | Antoine's constant [Pa]; Cross-sectional area of the U-tube manometer column [$m^2$] |
| $A_h$ | Surface area for heat transfer [$m^2$] |
| $A_T$, $A_P$ | Cross-section area of tank and pipe in gravity-flow tank, respectively [$m^2$] |
| $A_1$, $A_2$ | Cross-section area of the first and the second tank of the interacting liquid-level tanks, respectively [$m^2$] |
| $B$ | Antoine's constant [K] |
| $b$ | Damping coefficient in suspension system $\left[\frac{\text{N-s}}{\text{m}}\right]$ |
| $C$ | Antoine's constant [K] |
| $C_p$ | Specific heat $\left[\frac{\text{J}}{\text{mol-K}}\right]$ |
| $C_{Ao}$, $C_A$, $C_R$ | Concentration of $A$ in feed, $A$ in tank and $R$ in tank, resp. for a CSTR $\left[\frac{\text{mol}}{\text{m}^3}\right]$ |
| $D_p$ | Diameter of the pipe in gravity-flow tank [m] |
| $E$ | Reaction activation energy $\left[\frac{\text{J}}{\text{mol}}\right]$ |
| $f$ | Fanning friction factor [-] |
| $F$ | Molar feed rate to a condenser $\left[\frac{\text{mol}}{\text{s}}\right]$ |
| $g$ | Acceleration due to gravity $\left[\frac{\text{m}}{\text{s}^2}\right]$ |
| $h$ | Level of liquid in gravity-flow tank [m] |
| $h_1$,$h_2$,$H_1$,$H_2$ | Level in first and second tanks in interacting tanks and corresponding deviation variables, respectively [m] |
| $h$, $H$ | Level of liquid in gravity-flow tank and the corresponding deviation variable, respectively [m] |
| $\Delta H$ | Heat of condensation of vapor in condenser $\left[\frac{\text{J}}{\text{mol}}\right]$ |
| $\Delta H_R$ | Reaction enthalpy at the reaction temperature $\left[\frac{\text{J}}{\text{mol}}\right]$ |

| | |
|---|---|
| $k$, $k_o$ | Constant of proportionality for condenser $\left[\frac{\text{mol/s}}{\text{mol}}\right]$; First-order rate constant of reaction A → B and the same at a very high temperature, respectively $\left[\frac{1}{\text{s}}\right]$ |
| $k_s$ | Spring constant of suspension system $\left[\frac{\text{N}}{\text{m}}\right]$ |
| $K$, $K'$ | Steady-state gains of the transfer functions |
| $L$ | Condenser liquid exit molar flow rate $\left[\frac{\text{mol}}{\text{s}}\right]$; Length of pipe in gravity-flow tank [m]; Total length of the U-tube manometer column [m] |
| $\mathcal{L}$ | Laplace operator |
| $M$ | Magnitude of impulse (general) |
| $M_A$, $M_R$, $M_I$ | Molecular weights of $A$, $R$ and inert in a CSTR |
| $m$ | Mass of the car body [kg]; Mass of the U-tube manometer liquid column [kg] |
| $N$ | Moles of vapor in condenser [mol] |
| $P^*$ | Vapor pressure [Pa] |
| $\Delta P$ | Pressure difference applied to the U-tube manometer column [Pa] |
| $Q$ | Heat transfer rate [W] |
| $q$, $Q$ | Inflow rate to gravity-flow tank (or first tank of interacting system) and corresponding deviation variable $\left[\frac{\text{m}^3}{\text{s}}\right]$ |
| $q_{21}$,$q_2$,$Q_{21}$,$Q_2$ | Inflow and outflow of the second tank of interacting tank system and corresponding deviations, respectively $\left[\frac{\text{m}^3}{\text{s}}\right]$ |
| $R$ | Universal gas constant $\left[\frac{\text{J}}{\text{mol-K}}\right]$ |
| $s$ | Laplace parameter |
| $t$ | Time [s] |
| $T$, $T_o$, $T_J$ | Temperatures in the tank, in feed, and in jacket, respectively [K] |
| $u$,$U$ | Velocity of U-tube manometer liquid column, and its deviation from the pre-initial state $\left[\frac{\text{m}}{\text{s}}\right]$ |
| $u_p$,$U_p$ | Velocity in the pipe of gravity-flow tank and corresponding deviation variable, respectively $\left[\frac{\text{m}}{\text{s}}\right]$ |

| | |
|---|---|
| $U_h$ | Overall heat transfer coefficient $\left[\frac{\text{W}}{\text{m}^2\text{-K}}\right]$ |
| $u(t)$ | Unit step input (general) |
| $v_o$, $v$ | Inlet and outlet volumetric flow rate through a tank $\left[\frac{\text{m}^3}{\text{s}}\right]$ |
| $V$ | Volume of vapor in condenser, fluid in CSTR & stirred-tank-heater [$\text{m}^3$] |
| $x$ | Displacement of the wheel in car wheel suspension example [m] |
| $y$ | Displacement of the car body in car wheel suspension example [m] |
| $z$ | $(n^2 + m^2 + nm) / (n + m)$, a characteristic parameter for a numerator-dynamics system, where $n$ & $m$ are system constants |

***Greek letters***

| | |
|---|---|
| $\rho$ | Density $\left[\frac{\text{kg}}{\text{m}^3}\right]$ |
| $\mu$ | Viscosity [Pa-s] |
| $\tau_d$ | Dead time in stirred tank heater [s] |
| $\delta(t)$ | Unit impulse function (Dirac function) |
| $\tau_1$, $\tau_2$ | Time constants for the first tank and the second tank of the two interacting tanks system [s] |
| $\zeta$ | Damping coefficient |

***Subscripts and superscripts***

| | |
|---|---|
| *imp* | Impulse |
| *i* | Inflection |
| *max* | Maximum |
| *min* | Minimum |
| *s* | Initial steady states |
| *st* | Step |
| – | Over-bar, deviation from initial steady state |
| ' | First differential |
| ″ | Second differential |
| *n* | $n^{\text{th}}$ differential |
| *–n* | $n^{\text{th}}$ integral |

***Abbreviations***

| | |
|---|---|
| CSTR | Continuous flow stirred tank reactor |
| DAE | Differential and algebraic equations |
| DDE | Delay differential equation |
| FOPDT | First order plus dead time |
| NRMSD | Normalized root mean square deviation |
| ODE | Ordinary differential equation |
| PID | Proportional integral derivative control |
| RMSD | Root mean square deviation |

## References


Ahuja, S., 2010. Second-order numerator-dynamics systems: Effects of initial discontinuities. *Teoreticheskie Osnovy Khimicheskoi Tekhnologii* (Theoretical Foundations of Chemical Engineering), 44, 300-308.

Ahuja, S., 2011. Effects of initial discontinuities on nonlinear systems represented by differential equations with terms containing differentials of the input function. Chem. Eng. Commun. 198, 760-782.

Ahuja, S., 2012. Initialization of lumped-parameter systems for singular inputs (communicated to Chem. Eng. Commun.).

Al-Hayani, W., Casasús, L., 2006. On the applicability of the Adomian method to initial value problems with discontinuities. Applied Mathematics Letters 19, 22-31.

Alopaeus, V., Lavi, H., Aitamaa, J., 2008. A dynamic model for plug flow reactor state profiles. Computers and Chemical Engineering 32, 1494–1506.

Arbogast, J., Cooper, D., Rice, R., 2007. Graphical technique for modeling integrating (non-self-regulating) processes without steady-state process data. Chem. Eng. Commun. 194, 1566–1578.

Bachmann, R., Brull, L., Mrzigold, Th., Pallaske, U., 1990. On methods for reducing the index of differential algebraic equations. Computers and Chemical Engineering 14, 1271-1273.

Bansal, A., Wanchoo, R.K., Sharma, S.K., 2007. Modeling of trickle bed reactors involving beds of different configurations under low and high interaction regimes. Ind. Eng. Chem. Res. 46, 677-683.

Bansal, A., Wanchoo, R.K., Sharma, S.K., 2007. Transition from trickle to pulse regime in trickle bed reactors. International Conference on Gas-Liquid and Gas-liquid-solid Reactor Engineering, New Delhi.

Banu, U., Uma, G., 2008. Fuzzy gain scheduled CSTR with GA-based PID. Chem. Eng. Commun. 195, 1213–1226.

Bequette, B.W., 2002. Process Control: Modeling, Design and Simulation. Upper Saddle River, New Jersey, Prentice Hall PTR.

Bernstein, D.S., 2005. Matrix Mathematics. Princeton, NJ: Princeton Univ. Press.

Bhargava, R., Khanam, S., Mohanty, B., Ray, A.K., 2008. Simulation of flat falling film evaporator system for concentration of black liquor. Computers & Chemical Engineering, 32,3213-3223.

Botchwey, C., Dalai, A. Adjaye, J., 2006. Simulation of a two-stage micro trickle-bed hydrotreating reactor using athabasca bitumen-derived heavy gas oil over commercial NiMo/Al2O3 catalyst. Int. Journal of Chemical Reactor Engineering, 4(A20), 1-7.

Brenan, K.E., Campbell, S.L., Petzold, L.R., 1989. Numerical Solution of Initial Value Problems in Differential-algebraic Equations (I-Ed.) N.Y.: Elsevier.

Brigola, R., Singer, P., 2009. On initial conditions, generalized functions and Laplace transform. Electr. Eng. 91, 9-13.

Brouckaert, C.J., Botha, C.J., Baddock, L.A., Buckley, C.A., 1995. Impulse: A PC program for the determination of residence time distributions of biological and chemical reactors. Water Supply 13, 305-308.

Casasús, L., Al-Hayani, W., 2002. The decomposition method for ordinary differential equations with discontinuities. Applied Mathematics and Computation, 131, 245-251.

Čermáková, J., Siyakatshana, N., Silar, F., Kudrna, V., Jahoda, M., Machon, V., 2003. Comparison of residence time distributions of liquid for different types of input signal using a stimulus-response technique. Chemical Papers 57, 2003, 427-431.

Chauhan, S., Srivastava, V.K., 2008. Modeling exhaust gas pollution abatement: Part I — single hydrocarbon propylene. Computers and Mathematics with Applications, 55, 319–330.

Chauhan, S., Srivastava, V.K., 2009. Modeling catalytic converter for oxidation of hydrocarbon in the exhaust gas. Environmental and Computer Science, International Conference on, 236-239.

Chauhan, S., Kumar, D., Srivastava, V. K., 2009. Modeling catalytic combustion of methane during the warm-up period of the converter. Chemical Product and Process Modeling, 4, 144.

Chaves, M., Sontag, E.D., Dinerstein, R.J., 2004. Optimal length and signal amplification in weakly activated signal transduction cascades. J. Phys. Chem. B 108, 15311-15320.

Chowdhry, S, Krendl, H, Linninger, A., 2004. A symbolic numeric index analysis algorithm for differential algebraic equations. *Ind. Eng. Chem. Res.* 43: 3886-3894.

Corinthios, M.J., 2005. The complex-variable distribution theory for Laplace and z transforms. IEEE Proceedings-Vision Image and Signal Processing 152, 97-106.

Corinthios, M.J., 2007. New Laplace, z, and Fourier transforms. Proceedings of the Royal Society A-Mathematical Physical and Engineering Sciences 463, 1179-1198.

Coughanowr, D.R.; LeBlanc, S.E., 2009. Process Systems Analysis and Control, New York, McGraw-Hill.

Dasila, P.K., Choudhury, I., Saraf, D., Chopra, S., Dalai, A.K., 2012. Parametric sensitivity studies in a commercial FCC unit. Advances in Chemical Engineering and Science, 2, 136-149.

Dones, I., Manenti, F., Presig, H.A., Buzzi-Ferraris, G., 2010. Nonlinear model predictive control: a self adaptive approach. Ind. Eng. Chem. Res. 49, 4782-4791.

Dua, V., 2011. A decomposition approach for parameter estimation of system of ordinary differential equations. Computers and Chemical Engineering, 35, 545-553.

deSilva, C. W., 2009. Modeling and Control of Engineering Systems. CRC Press.

Engin, S.N., Kuvulmaz, J., Ömürlü, V.E., 2004. Modeling of a coupled industrial tank system with ANFIS. International Conference on Artificial Intelligence; Mexico City.

Evangelista, F., 2009. Dynamics of steam heated shell and tube heat exchangers: New insights and time domain solutions. Chemical Engineering Transactions 17, 1215-1220.

Fogler, H.S., 2005. Elements of Chemical Reaction Engineering, Prentice-Hall, Inc., Englewood Cliffs, New Jersey.

Gatzke, E.P., Meadows, E.S., Wang, C., Doyle III, F.J., 2000. Model based control of a four-tank system. Computers and Chemical Engineering 24, 1503-1509. 7th International Symposium on Process Systems Engineering; Keystone, CO, USA.

Gerald, C.F., Wheatley, P.O., 2004. Applied Numerical Analysis. 7th Ed. Pearson Education, Inc.

Gezici, S., Kobayashi, H., Poor, H. V, Molisch, A. F., 2005. Performance evaluation of impulse radio UWB system with pulse-based polarity randomization. IEEE Transactions on Signal Processing 53, 37-2549.

Girard, A, 2005. Linear time-invariant systems, Martin Schetzen. Automatica, 41, 2011 – 2017.

Gopal, V., Biegler L.T. 1988. A successive linear programming approach for initialization and reinitialization after discontinuities of differential-algebraic equations. SIAM J. Sci. Comput., 20, 447-467.

Goswami, D.Y., Hseih, C.K., Jotshi, C.K., Klausner, J.F., 1997. Contact resistance regulated storage heater for fluids. US Patent No. 5,694,515.

Graf, U., 2004. Applications of Laplace Transforms and Z-Transforms for Scientists and Engineers. Berkhäuser Verlag, Germany.

Grizzle, J.W., 2004. Linear time-invariant systems, Martin Schetzen. IEEE Control Syst. Mag., 24(3), 87-89.

Gupta, R.K., Kumar, V., Srivastava V.K., 2010. Modeling of fluid catalytic cracking unit riser reactor: a review. Int. J. Chem. React. Eng., 8, R6.

Harriott, P., 1972. Process Control. McGraw Hill: New York.

Hogarth, W.L., Noye, B.J., Stagnitti, J., Parlange, J.Y., Bolt, G., 1990. A comparative study of finite difference methods for solving the one-dimensional transport equation with an initial-boundary value discontinuity. Computers and Mathematics with Applications 20, 67-82.

Inamdar, S.R., Karim, I.A., Purulekar, S.J., Kulkarni, B.D., 2011. A sharp cut algorithm for optimization. Comp. Chem. Eng. 35, 2716-2728.

Jena, J., Sharma, V. D., 2008. Interaction of a characteristic shock with a weak discontinuity in a relaxing gas. J. Eng. Math. 60, 43–53.

Jotshi, C.K., Goswami, D.Y., Klausner, J.F., Malakar, S., 2001. A water heater using very high temperature storage and variable thermal contact resistance. Int. J. Energy Res. 25, 891-898.

Juneja, P.K., Ray, A.K., Mitra, R., 2009. Modeling dead time in consistency process dynamics in a paper mill. Advances in Chemical Engineering. McMillan Advanced Research Series, India, 201-205.

Kailath, T., 1980. Linear systems, Prentice-Hall, Englewood Cliffs, NJ., 10-11.

Kanagaraj, N., Kumar, N. R., and Sivashanmugam, P., 2009. A robust intelligent PID-type fuzzy control structure for pressure control. Chem. Eng. Commun. 196, 291–304.

Karelsky, K.V., Petrosyan, A.S., 2006. Particular solutions and Riemann problem for modified shallow water equations. Fluid Dynamics Research, 38, 339-358.

Kaya, I., 2004. Tuning PI controllers for stable process with specifications on gain and phase margins, ISA Trans., 43, 297–304.

Kelevedjiev, P., Seman, J., 2004. Existence of solutions to initial value problems for first-order differential equations, Nonlinear Analysis, 57, 879-889.

Khuri, S.A., Sayfy, A., 2009. Spline collocation approach for the numerical solution of a generalized system of second-order boundary-value problems. Applied Mathematical Sciences, 3, 2227-2239.

Kossik, J., 2000. Draining time for unpumped tanks. Chem. Eng. 107, 115-119.

Kröner, A., Marquardt, W., Gilles, E. D., 1992. Computing consistent initial conditions for differential–algebraic equations. In European symposium on computer aided process engineering —1, Computers and Chemical Engineering 16 (Suppl.), S131.

Kröner, A., Marquardt, W., Gilles, E. D., 1997. Getting around consistent initialization of DAE systems. Computers and Chemical Engineering 21(2), 145–158.

Kumar, V, Pandey, R.N., Upadhyay, S.N., 2000. Exact solution of convective mass transfer for calcium response of endothelium. Mathematical Problems in Engineering, 5, 1713-1724.

Kumar, V, Upadhyay, S.N., 2008. Convective-diffusive mass transfer of agonist and the intra-cellular calcium response of endothelial cell. Biotechnology and Bioengineering, 101, 843-849.

Kuo, B.C.,Golnaraghi, F., 2003. Automatic Control Systems, 8th ed. Hoboken: Wiley.

Lee, P.J., Vítkovský, J.P., Lambert, M.F., Simpson, A.R., Liggett, J, 2007. Leak Location in pipe lines using the impulse response function. Journal of Hydraulic Research 45(5) 643–652.

Leimkuler, B., Petzold, L. R., Gear, C. W., 1992. Approximation methods for the consistent initialization of differential–algebraic equations. SIAM Journal of Numerical Analysis, 28(1), 205–226.

Lemoine-Nava, R., Flores-Tlacuahuac, A., Saldivar-Guerra, E., 2006. Non-linear bifurcation analysis of the living nitroxide-meditated radical polymerization of styrene in a CSTR. Chem. Eng. Sci. 61, 370-387.

Levenspiel, O., 2004. Chemical Reaction Engineering. Wiley-Intersci., New York.

Lima, N.M.N., Manenti, F, Filho, R.M., Embiruc¸u, M., Maciel, M.R.W., 2009. Fuzzy model-based predictive hybrid control of polymerization processes. Ind. Eng. Chem. Res. 48, 8542–8550.

Liu, X., Ballinger, G., 2004. Continuous dependence on initial values for impulsive delay differential equations. Applied Mathematics Letters, 17, 483-490.

Loiacono, N.J., 1987, Time to drain a tank with piping. Chem. Eng., 94, 164-166.

Lundberg, K.H. Miller, H.R., Trumper, R.L., 2007. Initial conditions, generalized functions, and the Laplace transform. IEEE Control Syst. Mag., 27(1), 22-35.

Luyben, W. L., 1996. Process Modeling, Simulation and Control for Chemical Engineers. 2nd. Ed. Chemical Engineering Series; McGraw-Hill: New York.

Majer, C., Marquadt, W., Gilles, E.D., 1995. Reinitialization of DAE's after discontinuities. Computers and Chemical Engineering 19 (Suppl.), S507-S512.

Makila, P. M., 2006. A note on the Laplace transform method for initial value problems. Int. J. Control, 79, 36-41.

Maneneti, M., Rovaglio, M., 2008. Integrated multilevel optimization in large scale PETP plants. Industrial and Engineering Chemistry Research 47, 92-104.

Manenti, M., Dones, I, Buzzi-Ferraris, G, Presig, H.A., 2009. Efficient numerical solver of partially structured DAE systems. Ind. Eng. Chem. Res. 48, 9979-9984.

Maneneti, M., Sieri, S. Restelli, M., 2011. Considerations on the steady state modeling of methanol synthesis fixed-bed reactor.Chemical Engineering Science 66, 152-162.

Mao, G., Petzold, L.R., 2002. Efficient integration over discontinuities for differential-algebraic systems. Computers and Mathematics with Applications 43, 65-79.

Methekar, R. N., Ramadesigan, V., Pirkle Jr., Subramanian, V. R., 2011. A perturbation approach of index-1 differential-algebraic equations arising from battery model simulations. Comp. Chem. Eng. 35, 2227-2234.

McCoy, B.J., 1987. Approximate polynomial expansion method for inverting Laplace transforms of impulse responses. Chem. Eng. Comm. 52, 93-103.

Mickley, S.M., Sherwood, T.S., Reed, C.E., 1975. Applied Mathematics in Chemical Engineering, New Delhi, Tata McGraw-Hill Edition.

Moudgalya, K.M., Jaguste, S, 2001. A class of discontinuous dynamical systems II. An industrial slurry high density polyethylene reactor. Chemical Engineering Science 56 (11), 3611-3621.

Murata, V. V., Biscaia, E. C. Jr., 1997. Structural and symbolic techniques for automatic characterization of differential–algebraic equations. Computers and Chemical Engineering, 21(Suppl.), 829–834.

Nauman, E. B., 2008. Residence time theory, Ind. Eng. Chem. Res. 47, 3752-3766.

Ogata, K., 2004. System Dynamics, 4th ed. Englewood Cliffs: Prentice-Hall.

Oh, S.C., Yeo, Y.K., 1996. On-line identification of interacting two-tank system. Korean Journal of Chemical Engineering 13, 422-426.

Pantelides, C. C., Gritisis, D., Morsion, K. R., Sargent, R. W. H., 1988. The mathematical modeling of transient systems using differential-algebraic equations. Computers and Chemical Engineering, 12, 449-454.

Papadopoulos, K.D., 2001. Simple uses of Laplace Transforms in transient transport problems. Chemical Engineering Education**,** 35, 238-242.

Pareek, V.K., Adesina, A.A., Srivastava, A., Sharma, R., 2003. Modeling of a non-isothermal FCC riser. Chemical Engineering Journal, 92, 101-109.

Patel, R.S., Singh, K., Pareek, V.K., Tade, M.O., 2007. Dynamic simulation of reactive batch distillation column for ethyl acetate synthesis. Chemical Product and Process Modeling, 2, 1-18.

Patranbis, D., 1996. Principles of Process Control. McGraw-Hill.

Pederson, H., Tanoff, M., 1982. Spline collocation method for solving parabolic partial differential equations with initial discontinuities: application to mixing with reaction. Computers and Chemical Engineering, 6, 197-207.

Pilipchuk, V. N., Vakakis, A. F., Azeez, M. A. F., 1997. Study of a class of subharmonic motions using a non-smooth temporal transformation. Physica D 100, 145–164.

Pilipchuk, V. N., Vakakis, A. F., 1998. Study of the oscillations of a nonlinearly supported string using a non-smooth transformation. Journal of Vibration and Acoustics 120(2), 434–440.

Pilipchuk, V. N., 1999. Application of special non-smooth temporal transformations to linear and nonlinear systems under discontinuous and impulsive excitation. Nonlinear Dynamics 18, 203-234.

Phillips, C., Parr, J., Riskin, E., 2003. Signals, Systems and Transforms, 3rd Ed. Englewood Cliffs, NJ: Prentice Hall, 2003.

Pour, N. D., Huang, B. Shah, S. L., 2010. Subspace approach to identification of step-response model from closed-loop data, Ind. Eng. Chem. Res. 49, 8558–8567.

Powers, D. L., 2010. Boundary Value Problems and Partial Differential Equations, 5th Ed. Elsevier, Academic Press.

Prasad, V., Bequette B.W., 2003. Nonlinear system identification and model reduction using artificial neural networks. Computers & Chemical Engineering, 27, 1741-1754.

Prasad, V., Schley, M., Russo, L.P., Bequette, B. W., 2002. Multi-rate nonlinear model predictive control of a styrene polymerization reactor. J. Process Control, 12(3), 353-372.

Rabier, P. J., Rheinboldt W. C., 1996. Time-dependent linear DAEs with discontinuous inputs. Linear Algebra and its Applications, 247, 1-29.

Ramasamy, M. Sundaramoorthy, S., 2008. PID controller tuning for desired closed-loop responses for SISO systems using impulse response. Computers and Chemical Engineering, 32(8), 1773-1788.

Ray, Ajay K, 1995. Performance improvement of a chemical reactor by non-linear natural oscillations. The Chemical Engineering Journal, 59(2), 169-175.

Reissig, G., Boche, H., Barton, P.I., 2002. On inconsistent initial conditions for linear time-invariant differential-algebraic equations. IEEE Transactions on Circuits and Systems-I: Fundamental Theory and Applications, 49, 1646-1648.

Roy, C.U., 2003. Process Instrumentation, Dynamics and Control for Chemical Engineers, Asian Books, India.

Salehi, S., Shahrokhi, M., 2008. Two observer-based nonlinear control approaches for temperature control of a class of continuous stirred tank reactors. Chemical Engineering Science 63 (2), 395-403.

Sangal, V.K., Kumar, V., Mishra, I.M., 2012. Divided wall distillation column: rationalization of degree of freedom analysis. Theoretical Foundations of Chemical Engineering, 46(4), 375-385.

Saranen, J., Wendland, W., 1987. On convergence of the spline collocation with discontinuous data. Mathematical Methods in Applied Sciences, 9, 59-75.

Schetzen, M., 2003. Linear Time Invariant Systems. IEEE Wiley Inter-Science.

Siebert, W.M., 1986. Circuits, Signals, and Systems. Cambridge: MIT Press.

Shoaei, M., Sommerfeld, J.T., 1989. Draining tanks: How long does it really take? Chem. Eng., 96, 154-155.

Silva R., Sbarbaro D., Barra, B. A. L., 2006. Closed-Loop process identification under PI control: A time domain approach. Ind. Eng. Chem. Res. 45, 4678.

Sincovec, R. F, Erisman, A. M., Yip, E. L., Epton, M. A., 1981. Analysis of descriptor systems using numerical algorithms. IEEE Trans. on Automatic Control, 26, 139-146.

Skogestad, S., 2004. Simple analytic rules for model reduction and PID controller tuning, Model. Identif. Control, 25(2), 85–120.

Soares, R.P., Secchi, A.R., 2005. Direct initialization and solution of high-index DAE systems. Computer-Aided Chemical Engineering 20, 157-162. European Symposium on Computer-Aided Process Engineering-15, 38th European Symposium of the Working Party on Computer Aided Process Engineering.

Sommerfeld, J.T., Stallybrass, M.P., 1992. Integral solutions for drainage of horizontal cylindrical vessels with pipe friction. Ind. Eng. Chem. Res., 31, 743-745.

Souza, D.F.S., Vieira, R.C., Biscaia Jr. E.C., 2005. Strategies for numerical integration of discontinuous DAE models. Computer-Aided Chemical Engineering 20, 151-156. European Symposium on Computer-Aided Process Engineering-15, 38th European Symposium of the Working Party on Computer Aided Process Engineering.

Srivastava, V. C., Prasad, B., Mishra, I. M., Mall, I. D., Swamy, M. M, 2008. Prediction of breakthrough curves for sorptive removal of phenol by bagasse fly ash packed bed. Industrial & Engineering Chemistry Research, 47(5) 1603-1613.

Stefani, R.T., Shahian, B; Savant, C.J., Hostetter, G.H., 2002. Design of Feedback Control Systems, 4th Ed. New York: Oxford University Press.

Sundaram, S., Radhakrishnan, T.K., 2003. Process Dynamics and Control. Ahuja Publishers, N. Delhi.

Tanaka, S., 1989. Linear system theory of a heat conduction calorimeter part 1: some properties of a linear system with zero initial conditions. Thermochimica Acta 141, 181-193.

Thakkar, P. R., Gaikwad, R. W. 2005. Modeling and control of non-interacting level tanks in series. Chemical Engineering World, 40, 81-85.

Tondeur, D., Kabir, H., Luo, L. A., Granger, J., 1996. Multicomponent adsorbtion equllibria from impulse response chromatography. Chemical Engineering Science, 51, 3781- 3799.

Toscano, R., 2005. A simple PI/PID controller design method via numerical optimization approach, J. Process Control, 15, 81–88.

Unger, J., Kroner, A., Marquardt, W., 1995. Structural analysis of differential–algebraic equations systems — theory and applications. Comp. Chem. Eng., 19(8), 867–882.

Vakakis, A. F., Manevitch, L. I., Mikhlin, Yu. V., Pilipchuk, V. N., Zevin, A. A., 1996. Normal modes and localization in non-linear systems. Wiley-Intersci., New York.

Vieira, R. C., Biscaia, E. C. Jr., 2000. An overview of initialization approaches for differential–algebraic equations. Latin American Applied Research, 30(4), 303–313.

Vieira, R. C., Bascaia, E.C. Jr., 2001. Direct methods for consistent initialization of DAE systems. Computers and Chemical Engineering, 25, 145–158.

Vilanova, R., Pedret, C., 2010. Optimality Characteristics of PI/PID Controllers: A Combined Min-Max/ISE Interpretation, Chem. Eng. Commun. 197(9), 1240-1260.

Wanchoo, R.K., Kaur, N, Bansal, A, Thakur, A., 2007. RTD in trickle bed reactors: Experimental study. Chem. Eng. Commun. 194(11), 1503-1515.

Watt, S. D., Sidhu, H. S., Nelson, M. I., Ray, Ajay K., 2010. Analysis of a model for ethanol production through continuous fermentation in multiple tanks. International Journal of Chemical Reactor Engineering, 8, A52.

Wu, B., White, R.E., 2001. An initialization subroutine for DAEs solvers. Computers and Chemical Engineering 25, 301–311.

Wu, C, Al-Dahhan, M.A., Prakash, A, 2007. Heat transfer coefficients in a high-pressure bubble column. Chemical Engineering Science, 62, 140-147.

Yan, Z., 2008. Consistent-inconsistent decomposition to initial value problem of descriptor linear systems. ZAMM · Z. Angew. Math. Mech. 88, No. 7, 552–555.

Zhang, W., Ou, L. Gu, D., 2006. Algebraic solution to $H_2$ control problems. Ind. Eng. Chem. Res. 45, 7151-7162.

Zhang, X., Elgamel, M., Bayoumi, M. A., 2010. Gaussian pulse approximation using standard CMOS and its application for sub G-Hz UWB radio. International Journal of Circuit Theory and Applications 38, 383-407.

Zheng, O., Zafiriou, E., 2004. Volterra-Laguerre models for nonlinear process identification with application to a fluid catalytic cracking unit. Ind. Eng. Chem. Res. 43, 340-348.

# Appendix I

## Comments on Makila, P. M. (2006)

His strategy can be understood in the following way. Consider a *step* input to a lumped-parameter; linear second-order system having two poles and one zero that is represented mathematically by a linear, ordinary differential equation having constant coefficients *A* through *E* as:

$$A\frac{d^2Y}{dt^2}+B\frac{dY}{dt}+CY=D\frac{dX}{dt}+EX \tag{A1}$$

It contains a singularity due to the derivative of the step input term. The system Eq. (A1) can be rearranged to give the following equation, where $Y^{(-n)}$ represents the $n^{\text{th}}$ integral of $Y$. Thus, for $n=1$, $Y^{(-1)}=\int_0^t Y(t)dt$.

$$\frac{d^3}{dt^3}\left[AY^{(-1)}+BY^{(-2)}+CY^{(-3)}-DX^{(-2)}-EX^{(-3)}\right]=0 \tag{A2}$$

$$\text{Let, } W(t)=AY^{(-1)}+BY^{(-2)}+CY^{(-3)}-DX^{(-2)}-EX^{(-3)} \tag{A3}$$

$$\text{So, } \quad W'''(t)=0 \tag{A4}$$

Taking the Laplace transform of Eq. (A4), we get,

$$s^3W(s)-s^2W(0)-sW'(0)-W''(0)=0 \tag{A5}$$

$$\text{Let, } Z(t)=Y^{(-1)}(t) \text{ and } V(t)=X^{(-1)}(t) \tag{A6}$$

Substituting Eq. (A6) into Eq. (A3) and taking the Laplace transform, we get,

$$W(s)=AZ(s)+B\frac{Z(s)}{s}+C\frac{Z(s)}{s^2}-D\frac{V(s)}{s}-E\frac{V(s)}{s^2} \tag{A7}$$

Now Eq. (A7) can be inserted into Eq. (A5) to get the Laplace transform *Y*(*s*). Note that *Z*(*t*) and *V*(*t*) are continuous functions satisfying *Z*(0) = 0 and *V*(0) = 0. So, these

continuous functions don't suffer from the inconsistencies contained in the term $f(0)$ of the derivative rule. Hence, $sZ(s) = Y(s)$ and $sV(s) = X(s)$. Also note that $W(0) = 0$, because all integrals in Eq. (A3) are zero at zero time. These are shown below.

$V(0)$ is zero because $V(t)$ is a ramp for the step input. The other integrals are zero at zero time because of the nature of the solution $Y$, which is limited.

And $Z(0)$ becomes,

$$Z(0) = \int_{0-}^{0+} Y(t)dt = 0 \tag{A8}$$

So, $Z(0) = 0$, because the integrand is limited. Similarly, all the further integrals of $Y$ are zero at zero time.

Hence, finally we get,

$$Y(s) = \frac{sW'(0) + W''(0) + Ds + E}{As^2 + Bs + C} \tag{A9}$$

Thus, the solution can be obtained by putting either $0^-$ or $0^+$ in the above equation and taking the inverse Laplace transform. This method does not involve singularity contained in the derivative of discontinuous input.

However, in the following paragraph, it is shown that the above strategy works only for the step perturbation and *does not work for the impulse perturbation*, $X(t) = \delta(t)$. For the impulse inputs, the new function for the integral of the input (Eq. (A6)) contains an initial discontinuity (and, hence, inconsistency), since the integral of the impulse is a step. If one tries to circumvent this by redefining the new function as the double integral of input, one again ends up in a discontinuity (due to the appearance of the initial value of the derivative of the input function) in the Laplace transform of the new function. The Laplace transform of the new function of Eq. (A6) is required in Eq. (A7). This is shown below:

Since, then:

$$X(t) = V''(t) \tag{A10}$$

$$X(s) = s^2V(s) - sV(0) - V'(0) \tag{A11}$$

$$X(s) = s^2V(s) - V'(0) \tag{A12}$$

Even though $V(0)$ would then be 0, there would be discontinuity in $V'(0)$ as $V'(t) = X^{(-1)}(t)$ would be a step and hence,

$$V'(0) \neq 0 \tag{A13}$$

So, the inconsistency can't be avoided for the impulse input (i.e., for singular term of its derivative).

# Appendix II

### *Algorithm for the solution of the DDE of closed-loop stirred tank heater*

The presence of dead time in the model requires the program to retrieve the data obtained $\tau_d$ seconds earlier. This requires the data of the iterations to be stored in an array. However, the array can not store a data beyond its upper bound space *U*. For this purpose, the data of iterations are stored up to *U* number of spaces, and the next data is overwritten in the first data space of the same array. Similarly, each subsequent data is stored in the second, third…, etc. space. The cycle is repeated, after every *U*, 2*U*, 3*U*..., etc. numbers of values are filled. This is done in the *Result* (results of $dT / dt$ ) statement of the algorithm, where [(*X*) % *U*] means the remainder *R* obtained after dividing *X* by *U*. So, the data shall be stored in the $R^{th}$ space. In this statement, *U* is chosen in such a way that, in the subsequent cycle, the un-retrieved value of the array is not overwritten, i.e., $U > \tau_d / dt$ , where $dt$ is the step size of the Runge-Kutta integration algorithm.

*Y* stands for the array for temperature, *U* for the dimension of the array, *dt* for the step size of time, *derivative* for the derivative of *Y*, *toud* for dead time, *Y_at_time* for *Y* at a particular instant of time, *i* for the count of iteration number at a particular instant of time; $k_1$, $k_2$, $k_3$ & $k_4$ for the parameters of Runge-Kutta, and *N* for the total number of iterations. $F = v_o(t - \tau_d)$ and $Q_s = Q(0^-)$ in the main text. Other symbols are defined in Section 3.7 of the main text.

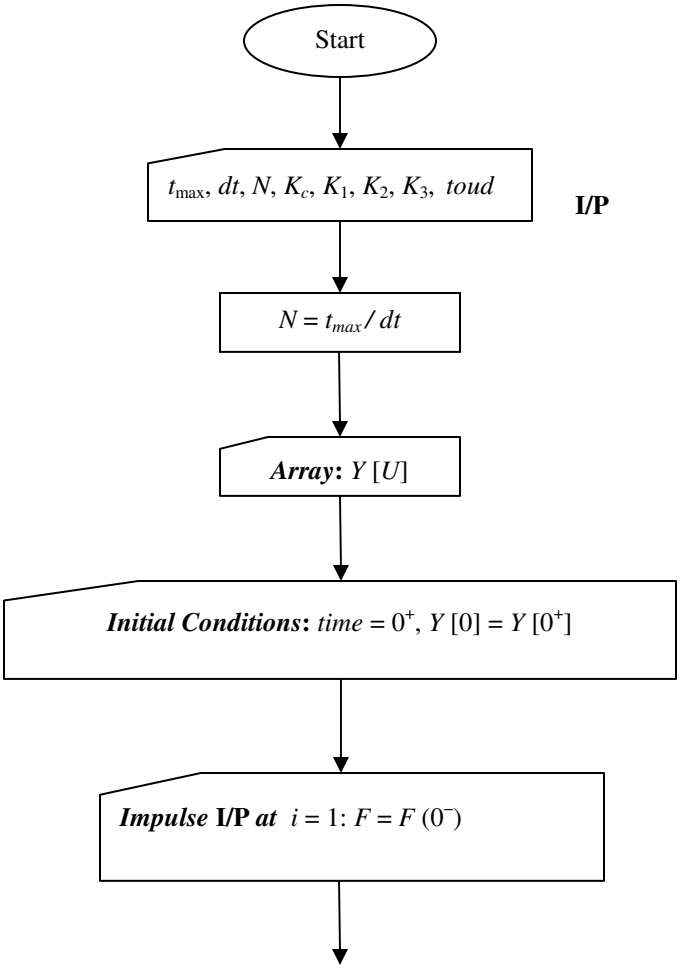

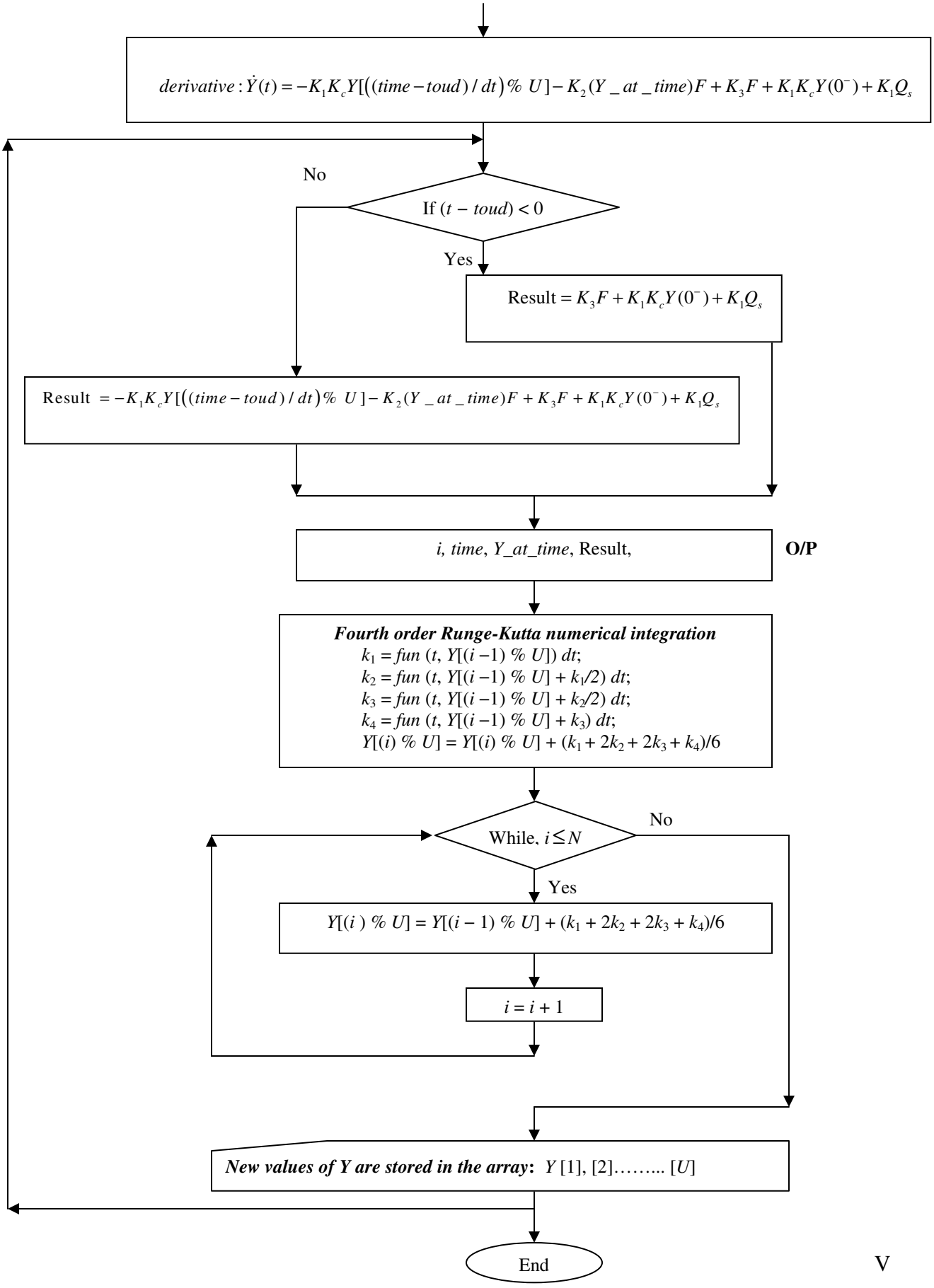
derivative : $\dot{Y}(t) = -K_1K_cY[((time-toud)/dt)\%\ U] - K_2(Y\_at\_time)F + K_3F + K_1K_cY(0^-) + K_1Q_s$
No
If $(t - toud) < 0$
Yes
Result $= K_3F + K_1K_cY(0^-) + K_1Q_s$
Result $= -K_1K_cY[((time-toud)/dt)\%\ U] - K_2(Y\_at\_time)F + K_3F + K_1K_cY(0^-) + K_1Q_s$
*i, time*, *Y_at_time*, Result,
O/P
***Fourth order Runge-Kutta numerical integration***
$k_1 = fun\ (t, Y[(i-1)\ \%\ U])\ dt$;
$k_2 = fun\ (t, Y[(i-1)\ \%\ U] + k_1/2)\ dt$;
$k_3 = fun\ (t, Y[(i-1)\ \%\ U] + k_2/2)\ dt$;
$k_4 = fun\ (t, Y[(i-1)\ \%\ U] + k_3)\ dt$;
$Y[(i)\ \%\ U] = Y[(i)\ \%\ U] + (k_1 + 2k_2 + 2k_3 + k_4)/6$
While, $i \le N$
No
Yes
$Y[(i)\ \%\ U] = Y[(i-1)\ \%\ U] + (k_1 + 2k_2 + 2k_3 + k_4)/6$
$i = i + 1$
***New values of Y are stored in the array*: $Y$ [1], [2]…….. [$U$]**
End

V